12-2010

The Immune Inhibitor A1 Protease of *Bacillus anthracis*

Kathryn Pflughoeft

The Immune Inhibitor A1 protease of *Bacillus anthracis*

by

Kathryn J. Pflughoeft, B.A.

Approved:

_____

Supervisory Professor

Theresa M. Koehler Ph.D.

_____

Jeffrey K. Actor Ph.D.

_____

David A. Engler, Ph.D.

_____

Magnus Höök, Ph.D.

_____

William Margolin, Ph.D.

Approved:

_____

Dean, The University of Texas

Health Science Center at Houston

Graduate School of Biomedical Sciences

THE IMMUNE INHIBITOR A1 PROTEASE OF *BACILLUS ANTHRACIS*

A

Dissertation

Presented to the Faculty of

The University of Texas

Health Science Center at Houston

and

The University of Texas

M. D. Anderson Cancer Center

Graduate School of Biomedical Sciences

In Partial Fulfillment

of the Requirements

for the Degree of

DOCTOR OF PHILOSOPHY

by

Kathryn J. Pflughoeft, B.A.

Houston, TX

December, 2010

Acknowledgments

The most important lessons that I have learned in graduate school is that science is a team endeavor and the importance of collaboration. Therein, I would like to first and foremost thank my many collaborators, David Engler, Rise Matsunami, Hye Jeong Yeo, Yi Xu, Rick Lyons, Julie Lovchik, Halli Miller, Gregory Shipley, Paul Sumby, and Richard Cook without whom this work would not have been possible. Similarly, I would like to thank Colin Harwood, Adam Driks, and Jeffrey Actor for providing strains and reagents for this project. I would also like to cite the helpful work and insightful conversations of the people with whom I have spent the last five years, Maria Hadjifrangiskou, Cana Ross, Wade Williams, Kerrie Thomason, Amy Courtney, Troy Hammerstrom, Jennifer Dale, Jason Rall, Jung H. Roh, and Maureen Ty.

I have been lucky to have had amazing mentors who have provided exceptional advice throughout my developing career. Paula Watnick gave me a chance to explore the world of microbiology and taught me the basics of research. Theresa Koehler took me on as a student and developed that basic knowledge to make me the free-thinking scientist that I am today. I am grateful to the members of my advisory, examination, and supervisory committees, Jeffrey Actor, William Margolin, David Engler, Magnus Höök, Heidi Kaplan, and Stephanie Watowich for their suggestions and support throughout the years. Finally, I would like to thank Paul Sumby who has patiently listened to hypotheses, both crazy and reasonable, and has filled the role of supportive husband and science guru throughout my pursuit of a life in science.

Abstract

The Immune Inhibitor A1 protease of *Bacillus anthracis*

Publication No. _____

Kathryn J. Pflughoeft

Supervisory Professor: Theresa M. Koehler, Ph.D.

Bacillus anthracis, an organism ubiquitous in the soil and the causative agent of anthrax, utilizes multiple mechanisms to regulate secreted factors; one example is the activity of secreted proteases. One of the most abundant proteins in the culture supernates of *B. anthracis* is the Immune Inhibitor A1 (InhA1) protease. Here, I demonstrate that InhA1 modulates the abundance of approximately half of the proteins secreted into the culture supernates, including substrates that are known to contribute to the ability of the organism to cause virulence. For example, InhA1 cleaves the anthrax toxin proteins, PA, LF, and EF. InhA1 also targets a number of additional proteases, including Npr599, contributing to a complex proteolytic regulatory cascade with far-reaching affects on the secretome. Using an intra-tracheal mouse model of infection, I found that an *inhA*-null strain is attenuated in relation to the parent strain. The data indicate that reduced virulence of the *inhA* mutant strain may be the result of toxin protein deregulation, decreased association with macrophages, and/or the inability to degrade host antimicrobial peptides.

Given the significant modulation of the secretome by InhA1, it is likely that expression of the protease is tightly regulated. To test this I examined *inhA1* transcript and protein levels in the parent and various isogenic mutant strains and found that InhA1 expression is regulated by several mechanisms. First, the steady state levels of *inhA1* transcript are controlled by the regulatory protein SinR, which inhibits *inhA1* expression. Second, InhA1 abundance is inversely proportional to the SinR-regulated protease camelysin, indicating the post-transcriptional regulation of InhA1 by camelysin. Third, InhA1 activity is dependent on a conserved zinc binding motif, suggesting that zinc availability regulates InhA1 activity. The convergence of these regulatory mechanisms signifies the importance of tight regulation of InhA1 activity, activity that substantially affects how *B. anthracis* interacts with its environment.

Table of Contents

List of Figures

List of Tables

Abbreviations

InhA – Immune Inhibitor A

PA – Protective Antigen

LF – Lethal Factor

EF – Edema Factor

Npr599 – Neutral protease (GBAA0599)

calY – camelysin encoding gene

BSA – Bovine Serum Albumin

NBY – Nutrient Broth Yeast

LB - Luria Broth

DIGE – Differential in Gel Electrophoresis

IPTG - Isopropyl β-D-1-thiogalactopyranoside

Kan - Kanamycin

Spc - Spectinomycin

Erm – Erythromycin

IL8 – Interleukin-8

IL1 – Interleukin-1

TNF-α – Tumor Necrosis Factor alpha

MAPK – Mitogen-Activated Protein Kinase

PAI-1 – Plasminogen Activator Inhibitor -1

kDa – Kilodalton

kb – Kilobase

ANTRX1 – Anthrax Toxin Receptor 1, also known as Tem8

ANTRX2- Anthrax Toxin Receptor 2, also known as CMG2

ECM – Extracellular Matrix

CFU – Colony Forming Unit

ORF – Open Reading Frame

GBAA – Genome of *Bacillus anthracis* Ames ancestor

RT – Room Temperature

Chapter I

Introduction

1.1. History

Bacillus anthracis and the associated anthrax disease have a rich history in infectious diseases research. Anthrax and its symptoms, black lesions and blood, were first described and named 2,500 years ago by Hippocrates. *B. anthracis* was the first bacterium to be linked to a disease by C.J. Davaine nearly 150 years ago, work that was later validated by Robert Koch (129). *B. anthracis* served as the basis for Koch's postulates, and Louis Pasteur used the organism in his early vaccine work (129, 149). The transmission of *B. anthracis* is primarily a problem in developing nations, with the vaccination of livestock in the western world reducing the morbidity and mortality of *B. anthracis* infections (129, 149). The potential use of *B. anthracis* as a biological weapon has spurred additional interest in the molecular and physiological characterization of this organism. Programs studying the weaponization of *B. anthracis* were initiated during World War I and have continued in the subsequent decades. Fears that the organism would be used as an agent of terrorism were realized in 2001 (129).

1.2. Physiology, growth, and lifecycle

B. anthracis is a versatile organism that can adapt to a changing environment by drastically altering its cell morphology. The Gram-positive rod-shaped bacilli forms spores upon nutrient starvation. The vegetative form of the bacterium is a large bacillus 3-10 μm in length and 1-1.5 μm in width (139). Growing bacilli are often found in long chains that can tangle to form knots or clumps in liquid culture (84) (unpublished data). The colony morphology of *B. anthracis* is dependent upon growth condition and can appear either dry with irregular edges or mucoid in the presence of capsule (84). The cell envelope is composed of the membrane, a thick layer of peptidoglycan that constitutes the cell wall, a layer of the cell-wall-associated proteins, Sap and Eag which has been termed the S-layer, and a proteinacious capsule (50). The spore form of the bacterium, which is resistant to extreme temperature, desiccation, and other environmental challenges, appears as a light refractile elongated sphere of 1-2 μm in diameter (139). Spore proteins belong to one of four main structures that are built out from the chromosome-containing core at the center of the spore, the cortex, the coat, and the exosporium (37). As not all species of *Bacillus* possess an exosporium the function of the outermost structure of the spore is not well

defined. The other spore structures are conserved among *Bacillus* species and function to protect the chromosome until nutrients are available allowing for germination and outgrowth to vegetative cells (37).

In the absence of germination signals, *B. anthracis* can retain dormancy as a spore for extended periods of time. Upon germination the vegetative form of the bacterium readily grows and replicates in a wide array of environments. In the laboratory, optimal growth conditions for *B. anthracis* are nutrient rich media with aeration at 37ºC, however the bacterium can grow in media that contains a variety of carbon sources and at temperatures ≤43ºC (84). In the natural environment, the vegetative form of the bacilli can survive in the rhizosphere (126); however the spore appears to be the dominant form in the soil. Low germination frequencies (up to 2%) have been reported for *B. anthracis* spores in soil (72).

While the cell can complete its lifecycle from spore to vegetative cell to spore within the soil or laboratory media, the lifecycle of *B. anthracis* often encompasses both *in vitro* and *in vivo* environments. This cycle begins with dormant spores gaining entry into a host. The spores then germinate, and proliferation of the vegetative cells leads to disease and host death. Upon decay of the host, nutrients are depleted forcing the bacilli to sporulate, returning spores to the soil.

1.3. Taxonomy

Much of what is known regarding the basic physiology of *B. anthracis* has been inferred from studies performed on the archetype species *Bacillus subtilis*. Despite much overlap, detailed research into several conserved pathways has outlined important phenotypic differences between these species (119, 155) (Chapter IV of this work). *B. anthracis* is a member of the *Bacillus cereus* group of closely related organisms, which includes *Bacillus cereus, Bacillus thuringiensis,* and *B. anthracis*. Members of the *B. cereus* group have highly conserved chromosomal gene content and synteny, and are thought to have a common origin (117). The *B. anthracis* genome consists of a 5.2-Mb circular chromosome and two large circular plasmids, pXO1 (181.7-kb, including genes encoding the toxin proteins) and pXO2 (94.8-kb, including capsule biosynthetic genes) (118). Traditionally, one feature that distinguishes *B. anthracis* from other *B. cereus* group

members is the presence of the virulence plasmids pXO1 and pXO2. However, recent findings indicate that at least one strain of *B. cereus* harbors a plasmid with similar gene content to pXO1 (68).

1.4. Anthrax disease and models of infection

B. anthracis is primarily a non-human pathogen, and most anthrax disease occurs in land-grazing animals, however humans are susceptible to the disease. With respect to human cases of anthrax there are three different forms of the disease, each of which are based upon the route of infection, cutaneous (the most common), inhalational (highest lethality rate), and gastrointestinal. For each route of infection the infectious form of the organism is the spore (139). The working model for inhalational anthrax is that the infection can be broken down into three stages: association of spores with phagocytes, spore germination, and dissemination of toxin- and capsule-expressing vegetative cells (139) (Fig. 1-1). Much remains to be determined with regard to disease progression, including the role of immune cells, the timing of germination, and the relative contribution of putative *B. anthracis* virulence factors.

As anthrax is a zoonotic disease many animals are susceptible to infection with *B. anthracis* and have been employed as models to study the progression of anthrax disease. Classically, rabbits and guinea pigs have been used to model human disease and in vaccine development as they have comparable immune systems to that of humans (57). However, mice are often utilized to study infection as they are highly susceptible to infection with *B. anthracis* as well as the effects of anthrax toxin (57). Differences in the infectivity of various mouse strains by *B. anthracis* and routes of infection have been well documented (97) allowing for the efficient use of mice in the study of anthrax disease.

1.5. Virulence factors

B. anthracis produces two classic virulence factors, a poly-D-glutamic acid capsule and a tripartite toxin (139), as well as several putative virulence factors including a number of secreted proteases and the cytolysin anthrolysin O. Similar to the capsule of many other pathogenic bacteria, the *B. anthracis* capsule is anti-phagocytic, prolonging the survival of

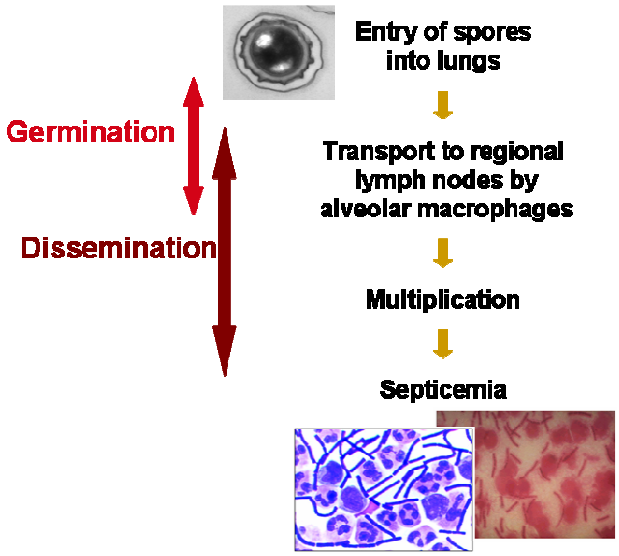

Figure 1–1. Model of the progression of inhalational anthrax. Spores enter the lung where they are transported to the regional lymph nodes by alveolar macrophages. Upon germination, vegetative cells multiply and disseminate throughout the body causing septicemia as depicted in the high numbers of bacilli in the blood and cerebral spinal fluid of the infected host.

bacilli within the host (42). Depolymerization of capsule enhances phagocytosis and killing of *B. anthracis* vegetative cells (130).

The *B. anthracis* tripartite AB toxin consists of two individual A (active or enzymatic) moiety toxin proteins, edema factor (EF) and lethal factor (LF), and the B (binding) moiety protective antigen (PA) (30). PA binds to the host-cell anthrax toxin receptors (ANTXR1 and ANTXR2), and is processed by a host protease, leading to association between host-cell-bound PA and EF and/or LF (6, 9, 66, 153). Upon association of EF and/or LF with PA, the active toxins are translocated into the host cell. Once intracellular, EF and LF interfere with host-cell-signaling through distinct well-defined mechanisms (110). LF inhibits necessary components of host signal transduction pathways by cleaving mitogen-activated protein kinases (MAPKs) (19, 66, 110, 120). EF increases the concentration of intracellular cAMP, reducing the activity of the host-cell-signaling factors Mek 1 / 2 and ERK, and ultimately causing edema at the site of infection (66, 110).

1.6. Contribution of secreted proteases to bacterial virulence

Bacteria secrete proteases as a means to modify their environment, leading to enhanced survival and virulence. With respect to Gram-negative and Gram-positive pathogens the secretion of proteases to serve as virulence factors has been well documented (64). Despite extensive study of secreted proteases in other pathogens little is known regarding the secreted proteases of *B. anthracis*. A classic example of a secreted protease that contributes to virulence is the SpeB protease produced by the human pathogen *Streptococcus pyogenes*. SpeB has a wide range of substrates, including proteins produced by the host, such as IgG and extracellular matrix (ECM) proteins, and proteins produced by the bacterium, including the cell-wall-anchored M protein and the secreted protein C5a peptidase (107, 156).

Additional examples of virulence-enhancing secreted proteases are the HA protease of *Vibrio cholerae*, the SspA, SspB, and Aur, proteases of *Staphylococcus aureus*, and the Rgp protease of *Porphyromonas gingivalis*. The *V. cholerae* HA protease both directly and indirectly effects virulence by processing host proteins and activating cholera toxin (10, 64). In addition to processing bacterial and host proteins, such as ClfB and the heavy chain of human immunoglobulin, the *S. aureus* SspA, SspB, and Aur proteases form a proteolytic

cascade whereby each protease activates the zymogen form of the subsequent protease (134). Such a proteolytic cascade represents a highly regulated mechanism of protein modification that can impact the extent and timing of protease activity. The *P. gingivalis* Rgp protease alters the N-terminus of two filamentous surface proteins involved in the virulence of the organism, the 75-kDa protein and fimbrilin. Following secretion and cleavage of the signal sequence, Rgp processes the fimbrilin and the 75-kDa protein prior to assembly of the mature filaments, such that *rgp* mutant strains are deficient in filament formation (76, 135).

Secreted proteases can also indirectly affect the virulence of a bacterium by modulating the secretory system. The MycP1 protease of *Mycobacterium tuberculosis* cleaves the EspB protein, a necessary component of the ESX-1 secretory system, such that deletion of the protease-encoding gene results in a non-functional secretory apparatus (108). Similarly, some but not all effectors secreted by autotransporters are released from the outer membrane of Gram-negative bacteria by designated proteases. An example of this is the adhesion protein App that is cleaved by the NalP protease of *Neisseria meningitidis,* releasing the active form of App from the cell (34).

1.7. Secreted proteases of *B. anthracis*

Although extracellular proteases have been demonstrated to play substantial roles in the virulence of many pathogens, few of the proteases secreted by *B. anthracis* have been implicated as contributing to the virulence of the organism. The most studied protease secreted by *B. anthracis* is the anthrax toxin component LF. LF is a zinc metalloprotease that has limited targets in the host, cleaving the Mek3/6, Mek 4/7, and Mek 1/2 MAPKs which in turn modulates host signaling pathways (43, 103).

The protease Immune Inhibitor A1 (InhA1) has also been implicated in enhancing *B. anthracis* virulence, through the cleavage of an array of substrates. In work carried out by Popov and co-workers, InhA1 was purified and characterized as a neutral zinc metalloprotease (28). Subsequently, InhA1 was found to cleave ECM proteins, including fibronectin and type I and type IV collagen using *in vitro* protease assays (28). In similar experiments, purified InhA1 was demonstrated to cleave proteins involved in the host coagulation cascade, including fibrinogen, plasmin inhibitors, and prothrombin (28, 79). The

InhA1-mediated cleavage of prothrombin results in the active thrombin protein (79). Moreover, in *ex vivo* experiments examining clot formation, human blood incubated with the *inhA1* mutant strain had a clotting time that was prolonged compared to blood incubated with the parent strain (79). Finally, InhA1 also appears to modulate levels of a host fibrinolysis regulatory protein, Plasminogen Activator Inhibitor (PAI-1), as mice injected with purified InhA1 have elevated PAI-1 transcript and protein levels (26). Taken together these data suggest that InhA1 modulates the coagulation cascade in the host, potentially impacting dissemination of *B. anthracis* in the blood.

Several additional proteases secreted by *B. anthracis* have predicted roles in pathogenesis (3, 28, 114). For example, Neutral Protease (NprB or Npr599) has been posited to contribute to *B. anthracis* virulence, as it cleaves laminin and fibronectin (28). The sheer abundance of Npr599 in culture supernatant alludes to a potentially significant role for the protease in *B. anthracis* survival in the host or environment. Npr599 and InhA1 together account for between 80%-90% of the *B. anthracis* secretome when the organism is grown to stationary phase in Nutrient Broth Yeast extract (NBY) (22). The secreted protein chaperone, HtrA, and the cell-wall hydrolase NlpC/P60, both of which have proteolytic activity, are detected in high levels in the plasma of infected animals (131). In addition to freely secreted proteases, *B. anthracis* also expresses cell-associated proteases, such as camelysin (59). An orthologue of camelysin produced by *B. thuringiensis* was found to cleave the *B. thuringiensis* toxin protein Cyt2Ba (106). Whether camelysin, or indeed any protease other than LF, contributes to the virulence of *B. anthracis* remains to be assessed.

1.8. Regulation of the *B. anthracis* secretome

While knowledge of host signaling molecules that induce *B. anthracis* virulence factor expression is limited, virulence factor expression is regulated by the pleiotropic virulence gene regulator AtxA when cultured in media containing sodium bicarbonate and incubated at elevated CO_2 (51, 84). Under such "toxin-inducing" conditions the most abundant protein in the *B. anthracis* secretome is the anthrax toxin protein PA. Interestingly, while InhA1 and Npr599 are the predominate proteins in the culture supernates in the absence of toxin-inducing conditions, in the presence of toxin-inducing conditions, Npr599

levels are below the level of detection in the supernatant, while InhA1 accounts for between two and five percent of the secretome late in stationary phase of growth (22).

Additional *B. anthracis* proteins that are prominent in the culture supernatant include the S-layer protein Sap and an array of enzymes with proteolytic activity. Sap is a cell-wall-associated protein whose abundance in culture supernates is strain and growth condition dependent (22, 90). *B. anthracis* secretes at least 14 different proteases, the abundance of which are largely growth-condition dependent (22). Many of the proteins secreted *in vitro* are also produced *in vivo* and are immunogenic, reacting with antibodies produced by *B. anthracis*-infected animals (23).

Chapter II

MATERIALS AND METHODS

2.1. Strains and culture conditions. *B. anthracis* strains and plasmids are described in Table 2-1. The virulent Ames strain (pXO1+, pXO2+), attenuated Sterne strain 7702 (pXO1+, pXO2-), and mutants derived from these strains were used in this study, unless otherwise noted. *Escherichia coli* strain TG-1 was used as a host for cloning. *E. coli* strain GM2163 (*dam*$^-$ *dcm*$^-$) was used to generate a source of unmethylated plasmid DNA. *E. coli* strain Rosetta pLysS was used for protein expression. Unless noted otherwise, *B. anthracis* strains were cultured at 37ºC with shaking (200 rpm) in Luria-Bertani (LB) medium with 0.5% glycerol for RNA and protein isolation, or in Nutrient Broth Yeast (NBY) medium for optimal InhA1 protein secretion. *E. coli* strains were cultured in LB at 37ºC with shaking (200 rpm). Antibiotics were added as appropriate: Kanamycin (100µg/ml), Spectinomycin (100µg/ml for *B. anthracis* and 50µg/ml for *E. coli*), Erythromycin (5µg/ml for *B. anthracis* and 150µg/ml for *E. coli*), Carbenicillin (100µg/ml), and Chloramphenicol (34µg/ml).

2.2. DNA isolation and manipulation. Cloning experiments employing *E. coli* were performed using standard protocols (4). Plasmid DNA was extracted from *E. coli* using the Wizard Miniprep kit (Promega, Madison, WI) following the manufacturer's recommendations. Unmethylated plasmid DNA from *E. coli* strain GM2163 was used for electroporation of *B. anthracis* (85). DNA was amplified using PCR using Phusion Polymerase (New England Biolabs, Ipswich, MA) unless otherwise noted. Oligonucleotide primers are described in Table 2-2. PCR products were purified using the Qiagen gel purification kit (Qiagen, Valencia, CA). Restriction enzymes were purchased from New England Biolabs. T4 DNA Ligase was purchased from Promega. Chromosomal DNA was extracted from *B. anthracis* using the Mo Bio genomic isolation kit (Mo Bio Laboratories, Solana Beach, CA).

Table 2-1. Strains and Plasmids used in this study

Strain or Plasmid	Characteristic[a, b]	Source or Reference
Strains		
Ames	Virulent strain, pX01$^+$ and pX02$^+$	Ravel et al 2009
UTA21	*sinR*-null mutant, derivative of Ames	This study
UTA5	UT222 transduced with CP51 propagated on Ames*; inhA1*-null mutant, Spc^r	This study
UTA13	UT324 transduced with CP51 propagated on Ames; *npr599* -null mutant , Kan^r	This study
UTA7	UT282 transduced with CP51 propagated on UTA5; *inhA1 inhA2*-null mutant, Spc^r, Kan^r	This study
7702	Sterne strain, pX01$^+$	Guidi-Rontani et al 2001
UT315	*sinR*-null mutant, derivative of 7702, Spc^r	This study
UT345	*inhA1*-null mutant derivative of 7702	This study
UT356	*calY*-null mutant derivative of 7702, Spc^r	This study
UT365	*sinI*-null mutant derivative of 7702	This study
UT371	*sinI sinR*-null double mutant derivative of 7702	This study
UT222	*inhA1*-null mutant derivative of 7702, Spec^r	This study
UT317	*npr599* -null mutant derivative of 7702, Kan^r	This study
UT368	*inhA1* point mutant H374A derivative of 7702	This study
UT379	*inhA1* point mutant H374D/E375A derivative of 7702	This study
UT381	*inhA1* point mutant E375A derivative of 7702	This study
UT382	*inhA1* point mutant E374A/H378D derivative of 7702	This study
UT385	*inhA1* point mutant H378D derivative of 7702	This study
UT282	*inhA2* -null mutant derivative of 7702, Kan^r	This study
UT284	*inhA1/inhA2*-null mutant derivative of 7702, Kan^r Spc^r	This study
UT306	UT282 derivative, *inhA2* gene integrated into the *plcR* locus, Kan^r Spc^r	This study
UM23c1-2 ΔsecA	*secA*-null derivative of UM23c1-2, Kan^r	Collin Harwood
UT357	UT356 transduced with CP51 propagated on UM23c1-2 *ΔsecA*; *calY*-null mutant, Kan^r, Spc^r	This study
Plasmids		
pUTE583	Vector used for allelic exchange, Erm^r	Chen et al 2004
pHY304	Vector used for markerless deletion, temperature sensitive, Erm^r	Chaffin et al 2005
pET23d	IPTG-inducible expression vector, Ap^r	Novagen
pUTE964	pET28b, SinR N'terminal His-tag	This study
pUTE1011	pET28b, *npr599* minus signal sequence C'terminal His-tag	This study
pUTE973	IPTG-inducible expression vector with hyperspank promoter, Kan^r, Amp^r	This study
pUTE980	pUT973 containing inducible *calY*	This study

[a] null mutants were created by allelic exchange (Spc^r) or markerless mutants

[b] Spc^r - spectinomycin resistant, Kan^r - Kanamycin resistant, Erm^r - Erythromycin resistant

Table 2-2. Primers used in this study

Primers used in this study		
Name	Sequence[a]	Function
KP95	GTCGACCAACGCCAGCTTTTTCGGC	*inhA1* markerless mutation
KP96	GGATCCCAGACTGGCCACCCGCTCC	*inhA1* markerless mutation
KP93	GGATCCGGGTGTACCGAAGTTTGATG	*inhA1* markerless mutation
KP94	GTCGACGTAAGCGGCGTCAGCTGTTTCG	*inhA1* markerless mutation
KP116	GTCGACGCTGGCTTCCATATAGTAAAAG	*calY* allelic exchange
KP117	GGATCCCCTAATTTCTTTTTCAGAC	*calY* allelic exchange
KP118	GGATCCCCAAGAAGCTGGAGAAG	*calY* allelic exchange
KP119	CTCGAGCATAGAGGGAGTTTAATGG	*calY* allelic exchange
KP79	GTCGACGTGTTGTATTTATATAGGTATG	*sinR* allelic exchange
KP80	GGATCCCTTGAATTTACAAAATGGAAG	*sinR* allelic exchange
KP81	GGATCCCGTTTTATACGTTCTCCAATC	*sinR* allelic exchange
KP82	GAATTCGTTTAAACGTTTCGATTTTAC	*sinR* allelic exchange
JR109	GAGAGAGCACTATCACTCACC	*sinR* and *sinIR* markerless mutation
JR110	GGTGCGCAAATTAATAGAAAGAAGTGCTTACAAACC	*sinR* markerless mutation
JR111	CACTTCTTTCTATTAATTTGCGCACCTTTCTATCAATATG	*sinR* markerless mutation
JR112	GCGTACAATGGTGATGTACG	*sinR* markerless mutation
JR107	AGGTATGGGAGTTGCATCAG	*sinI* markerless mutation
JR108	AGGGAGGAATTACATGTTTGTTCTTTTTAACGAAGTTTATG	*sinI* markerless mutation
JR105	CGTTAAAAAGAACAAACATGTAATTCCTCCCTAATTATCAATC	*sinI* markerless mutation
JR106	CAGTTCCTGGTAAAGCTG	*sinI* and *sinIR* markerless mutation
JR114	GGGAGGAATTACATTAATAGAAAGAAGTGCTTACAAACC	*sinIR* markerless mutation
JR113	CTTCTTTCTATTAATGTAATTCCTCCCTAATTATCAATC	*sinIR* markerless mutation
KP138	GCCGTCGACCAGCTGTATTAGGCCTTTCATTC	*inhA1* point mutants
KP139	CTAAATCATGACCATATTCAGCTGCGAATACACCGACCGC	*inhA1* point mutant H374A
KP140	GCGGTCGGTGTATTCGCAGCTGAATATGGTCATGATTTAG	*inhA1* point mutant H374A
KP141	GCCTCTAGAGCATAGTTTCTCCACTCAAC	*inhA1* point mutants
KP162	GCGGTCGGTGTATTCGCAGATGCATATGGTCATGATTTAG	*inhA1* point mutant H374D/E375A
KP163	CTAAATCATGACCATATGCATCTGCGAATACACCGACCGC	*inhA1* point mutant H374D/E375A
KP170	GTATTCGCACATGCATATGGTGATGATTTAGGTTTAC	*inhA1* point mutant E375A and E374A/H378D
KP171	GTAAACCTAAATCATCACCATATGCATGTGCGAATAC	*inhA1* point mutant E375A and E374A/H378D
KP172	CACATGAATATGGTGCTGATTTAGGTTTACCAGATG	*inhA1* point mutant H378D
KP173	CATCTGGTAAACCTAAATCAGCACCATATTCATGTG	*inhA1* point mutant H378D
KP95	GTCGACCAACGCCAGCTTTTTCGGC	*inhA1* markerless mutation
KP96	GGATCCCAGACTGGCCACCCGCTCC	*inhA1* markerless mutation
KP93	GGATCCGGGTGTACCGAAGTTTGATG	*inhA1* markerless mutation
KP94	GTCGACGTAAGCGGCGTCAGCTGTTTCG	*inhA1* markerless mutation
KP71	GGATCCGAAGTAGCAGCAGTTAAGC	*npr599* allelic exchange
KP72	CTGCAGCGTTTGGTGTTTTTTAAG	*npr599* allelic exchange
KP73	GTCGACGGGATATTGCTACACTTGAAGAAG	*npr599* allelic exchange
KP74	GGATCCAACAATATCAGGTTTACTGC	*npr599* allelic exchange
ES27	ATGAGCTCGGGGAAAAGGGTGGATTAGA	*inhA1* allelic exchange
ES28	ATGGATCCGGTGTTCCTGTTGCAGGTTT	*inhA1* allelic exchange
ES29	ATGGATCCGAAGGGACACAATTCAAA	*inhA1* allelic exchange
ES30	ATGGTACCTCGCAATGCCTCGATTAACT	*inhA1* allelic exchange
KP03	GTCGACGCTGGAGTAACGACAAATCCA	*inhA2* allelic exchange
KP08	GGATCCAAGTGGCGCTTTTCTTCTCA	*inhA2* allelic exchange
KP09	GGATCCCAAGTTGTTGGACAGGCAGA	*inhA2* allelic exchange
KP10	CTGCAGGGATAATTCCATCATTGTC	*inhA2* allelic exchange
KP192	biotin-GTGATATACTCGTATGCTAAC	*inhA1* EMSA probe
KP193	GTTTCTTGTTCATCCCTTATTTC	*inhA1* EMSA probe
KP79	biotin-GTGTTGTATTTATATAGGTATG	*calY* EMSA probe
KP117	CCTAATTTCTTTTTCAGAC	*calY* EMSA probe
nprF	biotin-ACCGGAAAGGGGTTTTTCAATATTTG	*npr599* EMSA probe
nprR	GAAAAAGAGTAGTTTCATATTAG	*npr599* EMSA probe
sipWF	biotin-TAACTAATAATTGTAAATTTTCTTATTGC	*sipW* EMSA probe
sipWR	TCTCCGTTGTTTTATATTATTTG	*sipW* EMSA probe
KP111[b]	CCATGGATTCTAAAAATGTGCTGTCTAC	*npr599* expression
KP112	CTCGAGGTTTACGCCAACAGCAC	*npr599* expression
KP168	GGGCTAGCATGATTGGAGAACGTATAAAAC	*sinR* expression
KP169	GGCTCGAGTTATTTTTGATTTTGCTTCC	*sinR* expression
KP183	GGGTCGACCAGCTAGGGGGAATTGATTG	*calY* expression
KP184	GGGCATGCGTGCTTACAAACCGCACTTC	*calY* expression

[a] underline indicates a restriction site

[b] Lysine codon optimized for expression in *E. coli* (CTC to CTG)

2.3. Construction of *B. anthracis* mutants. *B. anthracis* null strains were constructed as allelic exchange mutants or as markerless gene deletion mutants. Allelic exchange mutants, in which specific DNA sequences were replaced with a Ω-spectinomycin or Ω-Kanamycin resistant cassette, were constructed using pUTE583 as described previously (20). Transductants were created as previously described (67). All mutations were verified with PCR and DNA sequencing.

Markerless mutations were created using pHY304, a temperature-sensitive vector harboring an erythromycin-resistance gene (16). DNA fragments corresponding to approximately 1-kb sequences upstream and downstream of the locus to be deleted were cloned in tandem into pHY304. The DNA inserts for the deletion constructs were generated using PCR using EasyA Taq (Stratagene, La Jolla, CA) to amplify upstream and downstream sequences separately, or using overlap extension (SOE) PCR to amplify a single DNA fragment deleted for the gene of interest (70). To obtain a markerless mutant, the specific pHY304 construct was introduced into *B. anthracis* using electroporation (127). The electroporation mixture was plated on LB medium containing erythromycin and incubated at 30ºC for two days to select isolates containing the plasmid. Clones were verified using PCR using Taq Polymerase (NEB, Ipswich, MA), re-streaked on selective medium, and incubated at 30ºC. A single colony was used to inoculate LB broth containing erythromycin and the culture was incubated at 30ºC for 16 h. To obtain an isolate in which the pHY304-derivative had integrated into the chromosome using single cross-over recombination, the culture was passaged at a 1:100 dilution into LB containing erythromycin and cultured at 41ºC (the non-permissive temperature for pHY304) for 10 to 14 h. Following a second passage at a 1:1000 dilution in the same conditions, the culture was streaked onto selective LB plates and incubated at 41ºC for 10 h. To promote excision of the pHY304-derivative from the *B. anthracis* chromosome, a single colony of a clone harboring an integrated plasmid was inoculated into LB without antibiotic, cultured at 30ºC until turbid, and then passaged at a 1:100 dilution multiple times in LB. Starting with passage 3, excision of the pHY304-derivative was assessed by plating serial dilutions of the culture on LB agar and incubating at 30ºC for 16 h. Single colonies were patched to LB agar with and without erythromycin and incubated at 37ºC for 16 h. Erythromycin-sensitive isolates were screened for loss of the plasmid and deletion of specific sequences using PCR

using Taq Polymerase (NEB, Ipswich, MA) and primers corresponding to DNA sequences flanking the locus. Point mutants were created using SOE and pHY304 for gene replacement.

2.4. RNA purification. For transcriptional profiling experiments approximately $1x10^6$ spores were inoculated into 25ml of LB medium and cultures were incubated until mid-exponential (OD_{600} = 0.5-0.6) or early stationary (OD_{600} = 3.5-3.9) growth phase. For qRT-PCR cultures 25ml of NBY was inoculated with vegetative cells at an OD_{600} = 0.07 and were incubated until exponential (OD_{600} = 0.3-0.45), transition (OD_{600} = 1.8-2.5), early stationary (OD_{600} = 3.7-5.0), or stationary (OD_{600} = 4.4-7.4) growth phase. Six-ml samples were taken at exponential phase and 2ml samples were collected at stationary phase. Cells were pelleted at 2,400 x g for 10 min at 4°C. All subsequent centrifugation steps were at 16,000 x g, 4ºC and samples were kept on ice except where noted. All but 500µl of culture supernate was decanted. Cells were resuspended and transferred to a 1.5-ml screwcap tube containing 500µl of 0.1-mm Zirconia/Silica beads (BioSpec Products, Bartlesville, OK) and 500µl of acid phenol warmed to 65ºC (Sigma Aldrich, St. Louis, MO). The cell suspension was subjected to bead beating for 1 min using a Mini BeadBeater (BioSpec Products, Bartlesville, OK). The tube was placed at 65ºC for 5 min, and the bead-beating was repeated. Following centrifugation for 3 min, the aqueous phase was transferred to a new 2-ml tube. Acid phenol (500µl) was added and the tube was held at room temperature (RT) for 5 min followed by vigorous shaking for 15 sec. Following centrifugation for 3 min, the aqueous phase was transferred to a new 2-ml tube, 0.3 volumes of chloroform was added, and the contents were shaken vigorously for 15 sec. The suspension was incubated for 10 min at RT, inverting frequently to avoid separation of phases. Following centrifugation, the aqueous phase was mixed with 250µl of diethylpyrocarbonate-treated water and 500µl of isopropanol. After incubation at room temperature for 10 min, RNA was pelleted using centrifugation for 15 min. Pellets were washed in 75% cold ethanol, air dried, and resuspended in 50µl of diethylpyrocarbonate-treated water. Final concentrations of extracted RNA ranged from 700-3,400ng/µl, as determined using a Nanodrop ND-1000 (Nanodrop Technologies, Wilmington, DE). 20µg of RNA was DNase-treated three times using Turbo DNA-free (Ambion, Austin, Tx) according to the specifications of the supplier,

and the quality and quantity of RNA was assessed using a Bioanalyzer 2100 system (Agilent Technologies, Santa Clara, CA). RNA was stored at -80ºC.

2.5. Transcriptional profiling. A custom Affymetrix (Affymetrix Inc., Santa Clara, CA) microarray containing 16 antisense oligonucleotide probe pairs for each gene in the Ames ancestor genome was used for microarray experiments (111). RNA samples were isolated from three independent cultures of each of the strains analyzed (parent and *sinR* mutant) per time point (exponential and stationary phase), giving 12 samples total. cDNA was created from 5.6µg of each RNA sample using random primers and Superscript III according to the manufacturers protocol (Invitrogen, Carlsbad, CA). Following cDNA synthesis, RNA was removed by NaOH hydrolysis, and the cDNA purified by phenol/chloroform extraction followed by ethanol precipitation. 8µg of each cDNA sample was fragmented using DNase I (Promega), biotin-labeled using the Affymetrix genechip labeling reagent (Affymetrix, Santa Clara, CA) and TDT (Promega), and hybridized to the microarray (one array per cDNA sample). After overnight incubation with rotation (40°C, 60 rpm), the twelve microarrays were washed and scanned using standard Affymetrix protocols. This research was performed in collaboration with Paul Sumby at the Methodist Hospital Research Institute in Houston, TX.

Gene expression estimates were calculated using Gene Chip Operating System (GCOS) v1.4 (Affymetrix, Santa Clara, CA), and data were normalized across samples. The data were transferred from GCOS into EXCEL and analyzed using three independent methods. For manual analysis, EXCEL was used to subtract background (signal intensities of <50), the signal for each gene was averaged across the three replicates per strain per time point, and the fold-change (parent/*sinR* mutant) was determined. Two programs, Arraystar (DNAstar, Madison, WI) and dCHIP (Wing Wong and Cheng Li Labs, Harvard, Cambridge, MA) were used to confirm differential gene expression. For the Arraystar analysis, raw data were imported from EXCEL and fold-change was determined for each gene, with those greater than two-fold being reported. Similarly, for dCHIP analysis, raw data were imported from EXCEL, a background signal of 100 was subtracted, fold-change was determined, and genes with a fold-change of greater than 1.5 were reported. The raw data were deposited at the MIAME compliant Gene Expression Omnibus (GEO) database at the National Center

for Biotechnology Information (http://www.ncbi.nlm.nih.gov/geo) and are accessible through accession number GSE22559.

Changes in gene expression of *sipW* (GBAA1287), *tasA* (GBAA1288), *calY* (GBAA1290), and GBAA_pX02_0023 were confirmed using semi-quantitative RT-PCR. PCR reactions used gene specific primers, cDNA made as described above, RNA controls, or DNA controls (41). The 16S gene amplified from cDNA was used as a loading control. Changes in *inhA1* (GBAA1295) were confirmed using quantitative RT-PCR.

2.6. Quantitative RT-PCR. Specific quantitative assays for *inhA1* and *inhA2* were developed using Beacon Designer, AlleleID (Premier Biosoft), or RealTimeDesign (Biosearch Technologies) software based on the *Bacillus anthracis* Ames strain sequence from NCBI. Real-time qPCR assay information is provided in Table 2-3.

> "cDNA was synthesized in 5µl total volume by the addition of 3 µl/well RT master mix consisting of: 400 nM assay-specific reverse primer, 500µM deoxynucleotides, Superscript II buffer and 1 U/µl Superscript II reverse transcriptase (Invitrogen, Carlsbad, CA), to a 96-well plate (ISC Bioexpress, Kaysville, UT) and followed by a 2µl volume of sample (25 ng/µl). Each sample was assayed in triplicate plus a control without reverse transcriptase to access DNA contamination levels. Each plate also contained an assay-specific sDNA (synthetic amplicon oligo) standard spanning a 5-log template concentration range and a no template PCR control. Each plate was covered with Biofilm A (Bio-Rad, Hercules, CA) and incubated in a PTC-100 thermocycler (Bio-Rad, Hercules, CA) for 30 min at 50°C followed by 72˚C for 10 min. PCR master mix, 15 µl/well, was added directly to the 5µl RT volume. Final concentrations for the PCR were 400 nM forward and reverse primers (IDT, Coralville, IA), 100nM fluorogenic probe (Biosearch Technologies, Novato, CA), 5mM $MgCl_2$, and 200µM deoxynucleotides, PCR buffer, 150nM SuperROX dye (Biosearch Technologies, Novato, CA) and 0.25U JumpStart Taq polymerase per reaction (Invitrogen, Carlsbad, CA). RT master mixes and all RNA samples and DNA oligo standards were pipetted using a Tecan Genesis RSP 100 robotic workstation (Tecan US, Research Triangle Park, NC); PCR master mixes were pipetted utilizing a Biomek 2000 robotic workstation (Beckman, Fullerton, CA). Each assembled plate was covered with optically clear film (Applied Biosystems, Foster City, CA) and run in a 7900 real-time instrument using the following cycling conditions: 95°C, 1 min; followed by 40 cycles of 95°C, 12 sec and 60°C, 30 sec. Data were analyzed using SDS 2.3 (7900) software (Applied Biosystems, Foster City, CA) with FAM reporter and ROX as the reference dye. Synthetic, polyacrylamide gel electrophoresis (PAGE) -purified DNA oligos used as standards (sDNA) encompassed at least the entire 5' – 3' amplicon for the assay (Sigma-Genosys, The Woodlands, TX).

Table 2-3. qRT-PCR primers and probes used in this study

Name	Sequence (and nucleotide in relation to start codon (and strand))	Accession number	PCR Efficiency (%)	Limit of detection (copies)	Length of product (bases)
gyrB F	ACTTGAAGGACTAGAAGCAG (54(+))	NC_003995	98%	218	67
gyrB R	GTCCTTTTCCACTTGTAGATC (121(-))	NC_003995	98%	218	67
gyrB probe	CGAAAACGCCCTGGTATGTATA-BHQ1 (76(+))	NC_003995	98%	218	67
inhA1 F	TATAGCGGTCATGGTGAACCAG (1168(+))	NC_003997	97%	154	95
inhA1 R	GAGAAACTTGTTGGCGTCGTTC (1262(-))	NC_003997	97%	154	95
inhA1 probe	TTTACCTGCCCAGCTTCCGCCGC-BHQ1 (1233(-))	NC_003997	97%	154	95
inhA2 F	ATAGCTTTAAAGATAACTGGGTTG (2036(+))	AE026879	95%	187	78
inhA2 R	GCTTCTGGATGAGAGTCTACA (2111(-))	AE026879	95%	187	78
inhA2 probe	CAAGGAATCCTTCACCTGGATGCACC-BHQ1 (2086(-))	AE026879	95%	187	78

> Each oligo standard was diluted in 100 ng/µl *E. coli* tRNA-H_2O (Roche Diagnostics, Indianapolis, IN) and spanned a 5-log range in 10-fold decrements starting at 0.8 pg/reaction. Due to the inherent inaccuracies in quantifying total RNA using absorbance, the amount of RNA added to an RT-PCR from each sample was more accurately determined by measuring the amount of at least one transcript that was invariant across all samples."

Methods for quantitative RT-PCR were communicated by Gregory Shipley at the University of Texas, Health Science Center, Houston. Final data were normalized to the previously-used housekeeping gene *gyrB* (41). This research was performed in collaboration with Gregory Shipley at the University of Texas, Health Science Center, Houston.

2.7. Coomassie and Western blot analysis. To assess cell-associated and freely-secreted protein levels, 2ml culture samples were centrifuged at 6,000 x g for 5 min. Cell pellets were stored at -20ºC until ready for use, at which time they were thawed on ice and resuspended in 75µl resuspension buffer (50mM Tris, 3mM sodium azide, pH 7.6) and 75µl 2x SDS loading buffer (25% 0.5M Tris pH 6.8, 2.5% SDS, 20% glycerol, 0.05% β-mercaptoethanol, 0.02% Bromo Blue).

Culture supernates were filtered through a 0.22-µM filter (Nalgene, Rochester, NY). To assess proteases in the supernatant, proteins were precipitated using deoxycholate and trichloroacetic acid (21) at 0.01% and 15%, respectively, and incubated on ice for 30 min or stored at -20ºC overnight. Frozen supernatant samples were thawed on ice and precipitated protein was pelleted at 16,000 x g for 20 min at 4ºC. Protein pellets were washed with 1ml of cold acetone at -20 ºC, and incubated on ice for 10 min. Precipitated protein was then pelleted as above. The acetone was removed, and pellets were air-dried for 5 min before resuspending in 50µl of resuspension buffer and 50µl of 2x SDS loading buffer. To assess toxin proteins in the supernatant, culture supernatant samples were filtered and prepared by mixing supernatant in a 1:1 ratio with 2x SDS loading buffer.

Peptides from InhA1, Npr599, and camelysin that were chosen as antigens for antisera production were predicted as surface exposed amino acids by Genscript (Piscataway, NJ). α-InhA1, α-Npr599, and α-camelysin antibodies against peptides LPDKDIKTIDPAFG, EYYDNRNPDWEIGEC, and TLADLQKTDPDLLA, respectively, were generated in rabbits, in collaboration with Genscript (Piscataway, NJ). α-InhA1, α-

Npr599, and α-camelysin antisera was purified using Pierce Nab Spin Columns as per manufacturers instructions (Thermo Scientific, Rockford, IL). α-TasA (raised against purified TasA from *B. subtilis*) was a gift from Adam Driks (Loyola University). Protective Antigen, Lethal Factor, and Edema Factor poly-clonal antibodies were obtained from the John Collier Laboratory (Harvard Medical School). SodA-1 antibodies were obtained from BEI Resources (ATCC, Manassas, VA).

Samples derived from culture supernates and cell pellets were subjected to SDS-PAGE. Gel-imbedded proteins were stained with Coomassie Blue (G-250) or transferred to a nitrocellulose membrane using a semi-dry blotter at 300 mAmps for 20 min using Towbin buffer (3.94g Tris base, 14.4g Glycine, and 20% Methanol) prior to Western hybridization analysis. Membranes were blocked in TBS-T (20mM Tris base, 137mM NaCl, 0.1% Tween 20 [pH 7.6]) with 3% BSA for 1 h at RT prior to exposure to primary antibody for 1 h. α-InhA1, α-Npr599, α-LF, α-EF and α-Camelysin antisera were used at a concentration of 1:1,000 in TBS-T, unless otherwise noted; α-TasA and α-PA antibody was used at 1:5,000; and α-SodA-1 was used in a 1:50,000 dilution in TBS-T. Membranes were rinsed in TBS-T three times for 5 min each, and then exposed to HRP-conjugated goat α-rabbit antibody (Bio-Rad, Hercules, CA) at a concentration of 1:100,000 for 1 h at RT. Membranes were rinsed as above, developed using the Pierce SuperSignal West Dura Extended Duration Substrate (Thermo Scientific, Rockford, IL), and exposed to chemiluminescent light for detection.

2.8. Secretome analysis using 2D gels. *B. anthracis* strains 7702 and UT345 were cultured for optimal InhA1 production in a 30ml volume. Cells were pelleted at 2,400 x g for 10 min at 4ºC. The culture supernatant was concentrated ~50x using a centrifugal concentrator, Centricon-15, with a 30-kDa size exclusion (Millipore, Billerica, MA). Protein concentration was assessed using the Pierce BSA assay (Thermo Fisher Scientific, Rockford, IL) as described by the manufacturer in 20µl volume. Optical density of samples was assessed using a Nanodrop ND-1000 (Nanodrop Technologies, Wilmington, DE). The protein was TCA precipitated (as described above) omitting resuspension of the protein. Protein pellets were shipped to Applied Biomics for analysis using Differential In Gel Electrophoresis (DIGE). DIGE involves the Cy3-labeling of one population of proteins (e.g.

from the parental strain), the Cy5-labeling of a second group of proteins (e.g. from the *inhA1*-null strain), and the mixing and separation of both protein sets on the same gel via 2D-gel electrophoresis to enable quantification of relative protein abundance on a secretome-wide scale. Protein spots were quantified using the software DeCyder 2D version 6.5 (GE Healthcare, Piscataway, NJ). Gel plugs were picked and returned for identification. This research was performed in collaboration with David Engler at the Methodist Hospital Research Institute in Houston, TX.

2.9. Mass Spectrometry. Samples were processed for peptide and protein identification via tandem mass spectrometry and subsequent database search essentially as previously described (60), with some modifications. Briefly, 2D gel spots were subjected to manual in-gel trypsin digestion and peptide recovery, followed by analysis of resulting tryptic peptides using MALDI-MS/MS on a Synapt HDMS mass spectrometer (Waters, Milford, MA) operated in the data-dependent acquisition mode. Protein Lynx Global Server (PLGS v2.4; Waters, Milford, MA) was used as the search engine to search the MS and MS/MS data against an extracted *B. anthracis* Ames ancestor database from NCBI (NCBI release v175.0; containing 11,152 protein entries for *B. anthracis* Ames ancestor).

To assess the purity of our purified InhA1 sample (see below) we used LC/MS^E. The purified InhA1 sample was subjected to in-solution trypsin digestion, and the resulting tryptic peptides were chromatographically separated over a 75µm id C-18 column on a Waters NanoAcquity UPLC (Waters, Milford, MA). Separated peptides were introduced via nanoelectrospray ionization into the Synapt mass spectrometer (Waters, Milford, MA). Peptide analysis was carried out with the mass spectrometer operating in the data-independent (MS^E) mode of operation, taking advantage of the parallel fragmentation capabilities of the Synapt instrument. Peptide identification via database search was carried out as described above using the PLGS software. This research was performed in collaboration with David Engler at the Methodist Hospital Research Institute in Houston, TX.

2.10. Amino-Terminal Sequencing. Proteins were separated using SDS-PAGE and transferred to PVDS membrane using a semi-dry blotter at 300V for 1 h in Towbin buffer.

Protein bands were stained with R-Coomassie blue, destained, and cut from the membrane. The N-terminal sequences of the proteins were sequenced using Applied Biosystems Procise cLC Sequencing system (Model 492cLC, Life Technologies, Carlsbad, CA) in collaboration with Richard G. Cook at the Baylor College of Medicine Protein Chemistry Core facility.

2.11. Purification of recombinant *B. anthracis* SinR. Recombinant SinR protein (rSinR) was purified from *E. coli* using a protocol modified from Kearns *et al*. (80). Briefly, DNA containing the *sinR* coding sequence was amplified using PCR using primers KP168 and KP169. The PCR product was cloned into the *Nhe*I and *Xho*I restriction sites of expression vector pET28b (Novagen, Gibbstown, NJ) to create an inducible gene encoding a thrombin-cleavable amino-terminal His-tagged SinR protein. The plasmid, pUTE964, was transformed into the *E. coli* Rosetta strain expressing pLysS and grown in 600ml of LB broth to an OD_{600} of approximately 0.8. IPTG (1mM final concentration) was added and incubation continued for 3 h. Cells were pelleted using centrifugation (10 min at 1,370 x g), resuspended in 10.8ml of lysis buffer (20mM Tris, 2mM EDTA, pH 8.0), and frozen at -80ºC. Following three cycles of freeze/thaw, cell debris was pelleted at 16,000 x g at 4ºC for 20 min. The supernatant fraction was mixed with 1ml of NTA-Ni Agarose beads (Qiagen) rotating at 4ºC for 1 h, and unbound protein was removed from the beads in five washes (5X bed volume each) with wash buffer (50mM Tris HCl, 500mM NaCl, and 20mM imidazole, pH 8.5). Beads were pelleted at 1,370 x g for 5 min. The NTA-Ni agarose beads and associated protein were resuspended in 1ml of elution buffer (10mM Tris HCl, 10mM $MgCl_2$, 1mM EDTA, 0.3mM DTT, 5% glycerol, 1mM PMSF, pH 8.5), and bound protein was released from the beads using biotinylated thrombin (4.2µl; Novagen, Gibbstown, NJ) in a 16 h reaction rotating at RT. The protein slurry was loaded on a column and rSinR and Thombin were eluted using gravity-flow. Biotinylated thrombin was removed from the rSinR using absorption to streptavidin-agarose beads in a 1 h reaction rotating at RT. Thrombin-bound beads were pelleted at 16,000 x g at 4ºC for 20 min and supernatant containing rSinR was removed. Purified rSinR was dialyzed overnight at 4ºC in 10mM Tris HCl containing 50mM NaCl, 1mM EDTA, 5% glycerol, and 1mM DTT at pH 8.5. Protein purity was assessed following 12% SDS-PAGE and Coomassie Blue staining. Protein concentration was determined using OD_{280} and protein was stored at -80ºC.

2.12. Purification of InhA1. The InhA1 protease was purified from the supernatant of *B. anthracis* strain UM23C1-2 Δ*secA/calY* (UT357) cultured in 1 L of NBY medium, divided into two 2-L bevelled flasks at 37ºC with shaking for 14 hours. The culture was centrifuged at 2,400 x g for 10 min at 4ºC. The resulting culture supernatant was filtered through a 0.22-μM PES filtration devise (Nalgene, Rochester, NY) and concentrated approximately 50-fold using a centrifugal concentrator, Centricon-70, with a 30-kDa size exclusion (Millipore, Billerica, MA) and dialyzed against buffer A containing 50 mM Tris-HCl (pH 7.6), 50 mM NaCl, and 3 mM sodium azide at 4ºC. After passing through a 0.22 μM SFCA filter (Nalgene, Rochester, NY), the protein sample was loaded onto a HiTrap Q HP column (GE Healthcare, Piscataway, NJ) equilibrated with 20 mM Tris-HCl (pH 8) and 50 mM NaCl. The column was washed with the same buffer and proteins were eluted with a linear gradient of 50 mM to 1M NaCl in 20 mM Tris (pH 8) using an AKTA Purifier system (GE Healthcare, Piscataway, NJ). Eluted proteins were analyzed using SDS-PAGE. Gels were stained with Coomassie or proteins were transferred to nitrocellulose for Western hybridization using antibodies specific to InhA1. Fractions determined to contain InhA1 (eluted at 228-304 mM NaCl) were combined and further concentrated to approximately to ~ 1ml at a concentration of 4.6 mg/ml using an Amicon Ultra-15 centrifugation filter (Millipore, Billerica, MA) with a 30kDa cut-off. Purity was assessed using LC/MS^E as described above. This work was performed in collaboration with Hye Jeong Yeo at the University of Houston.

2.13. Purification of rNpr599. npr599 (GBAA0599) was amplified using PCR using KP111 and KP112 and was cloned into the into the *Nco*I and *Xho*I restriction sites of expression vector pET23d (Novagen, Gibbstown, NJ), generating a C-terminal His-tagged protein. The rNpr599 was subsequently expressed and purified from *E. coli* using affinity purification to NTA resin (Qiagen, Valencia, CA). Unbound protein was washed from the resin with 50mM NaH_2PO_4, 300mM NaCl, 50mM Imidazol at pH 8. Bound protein was subsequently eluted with 50mM NaH_2PO_4, 300mM NaCl, 250mM Imidazol at pH 8. The purity of the eluted protein was assessed using Coomassie staining and Western blot analysis with Npr599-specific antibodies.

2.14. *In vitro* protease assays. Purified InhA1 was mixed with substrate (rPA, rEF, rLF, rNpr599, or rSodA-1) in protease buffer (50mM Tris, 100mM NaCl, 1mM $CaCl_2$, 1mM $MgSO_4$, pH 7.8) and incubated at 37ºC for set time points. Reactions were then placed on ice and EDTA added to a final concentration of 50mM to stop the reaction. 2X SDS-buffer was added, samples were boiled for 5 min, separated using SDS-PAGE, and analyzed using Western blot with substrate-specific antibodies. rPA, rLF, and rSodA-1 from *B. anthracis* were obtained from BEI Resources (ATCC, Manassas, VA). rEF was obtained from List Biological Laboratories (List Biological Labaoratories, Campbell, CA). rNpr599 was purified as described above.

2.15. Electrophoretic mobility shift assays. Electrophoretic mobility shift assays (EMSAs) were performed using the Pierce Light Shift EMSA kit (Thermo Fisher Scientific, Rockford, IL). Biotinylated DNA probes used in these studies corresponded to the promoter regions of three genes implicated as SinR targets in microarray experiments, *sipW, calY*, and *inhA1*, *npr599*. Probes were generated using PCR using biotinylated primers (Table 2-2) and purified using the Qiagen gel purification kit. Probe (0.1nM) and 2µg of poly (dI-dC) were added to reaction buffer (10mM Tris, 50mM KCl, 1mM Dithiothreitol, 0.1% NP-40, and 20mM $MgCl_2$, pH 7.5). Five reactions were set-up for each probe tested, with one reaction receiving no rSinR protein, and the remaining four reactions containing increasing concentrations of rSinR protein (0.4, 2.0, 10, and 50nM). Samples were incubated at 37ºC for 35 min and then electrophoresed in a TBE gel containing 5% bis-acrylamide at RT for 1 h at 100V. DNA was transferred from the gels to nitrile membranes using a semi-dry apparatus (280 mA for 13 min). Following cross-linking of the DNA to the membrane using a UV cross-linker (UVC500, GE Healthcare, Piscataway, NJ), membranes were blocked, washed, and developed according to the Pierce Light Shift EMSA kit protocol (Thermo Fisher Scientific, Rockford, IL).

2.16. IPTG-inducible expression of camelysin in *B. anthracis*. Plasmid pdr111Hyperspank (12) containing the IPTG-inducible promoter $P_{hyperspank}$, was modified as follows for use in *B. anthracis*. The *ori1030* from pHT304 (36) was cloned in the *Bam*HI restriction site. The spectinomycin resistance gene was replaced with an Omega cassette

carrying a kanamycin-resistance gene, by digesting the vector with *Eco*RI and *Sac*II, and inserting ΩKan, creating pUTE973 (Table 1). The *calY* gene, carrying its native ribosomal binding site, was amplified from *B. anthracis* genomic DNA with primers KP183 and KP184 (Table 2-2), and cloned into the *Sal*I and *Sph*I restriction sites of pUTE973 such that transcription of the *calY* gene was driven by the IPTG-inducible promoter. The *calY* expression vector was named pUTE980 (Table 2-1). Camelysin and InhA1 levels produced by each strain were assessed using Western blot analysis. Where indicated, densitometry was utilized to quantify the signal intensity of protein bands.

2.17. India ink exclusion assay. Capsule levels were assessed using an india ink exclusion assay as previously described (41). Briefly, cells were cultured in NBY with sodium bicarbonate and 5% CO_2 to the exponential phase of growth and mixed on a microscope slide with india ink. Samples were then examined under 100X microscopy using a Nikon Eclipse TE2000-U microscope (Nikon, Melville, NY). Images were taken using Metamorph (Imaging Series 6.1) software (Molecular Devices, Sunnyvale, CA). Capsule expression is a reflection of the size of the halo of ink particles excluded from the bacilli.

2.18. Heat resistance assays. Suspensions of *B. anthracis* cells were incubated at 65ºC for 90 min. Serial dilutions of cell suspensions were plated on LB plates +/- heat treatment and incubated overnight at 37ºC and colony forming units (CFUs) were enumerated. The percentage of heat resistant spores was determined by the formula: (number of CFUs after heat treatment / number of CFUs before heat treatment) x 100. Heat resistant spores are a reflection of the number of spores that are not undergoing sporulation or germination.

2.19. Macrophage infections. J774A.1 mouse macrophage-like cells were infected at a multiplicity of infection (MOI) of 10 with spores of *B. anthracis* strains 7702 or *inhA* mutant derivatives. Infections took place for 30 minutes and were incubated at 5% CO_2 at 37º C in Difco modified Eagle's medium (DMEM, Invitrogen, Carlsbad, CA) without the addition of fetal bovine serum (FBS, Invitrogen, Carlsbad, CA). Spores that were not attached to, or engulfed by, macrophages were washed out of the wells with 3 PBS rinses (Invitrogen, Carlsbad, CA). A 30 min gentamicin treatment was then applied to kill any germinated

spores that were extracellular to the macrophage. Gentamicin was washed from the cells with PBS and fresh DMEM containing 5% FBS applied. Samples were taken at 0, 3, 6, and 8 h post-infection. At each time-point two cell populations were examined. The first population consisted of all the bacilli in the infection (macrophage-associated and bacilli that were free in the media). The second population consisted of macrophage-associated bacilli only, and was obtained by applying a second gentamicin treatment to kill any germinated spores in the media. After disruption of the macrophage monolayer by cell scraping, serial dilutions were plated on LB plates without antibiotic in duplicate. Plates were incubated overnight at 37ºC with CFUs enumerated the following day. J774A.1 mouse macrophage-like cells were a gift from Jeffrey Actor (University of Texas, Health Science Center, Houston).

2.20. *In vivo* studies. BALB/c mice were infected with a fully virulent strain (Ames) of *B. anthracis* or *inhA* isogenic mutant via intratracheal inoculation, as previously described (97). Briefly, inoculations were made through a small incision in the skin and spores were injected directly into the trachea. Infection was assessed using LD_{50} and mean time-to-death. The LD_{50} (the concentration of bacteria required to kill 50% of infected animals) of the Ames and *inhA* mutant strains was determined by infecting groups of 10 mice with increasing concentrations of spores starting at $1x10^2$. The LD_{50} of the Ames strain was previously determined to be $1x10^3$ (42). For time-to-death experiments, mice were infected with a range of doses (low dose = $1x10^2$ to a high dose = $1x10^4$) and signs of infection were evaluated over time. In all experiments, a negative control group of mice were generated by inoculation with saline. Two independent experiments were carried out, with infections initiated on different days. Experiments were performed in collaboration with Dr. C.R. Lyons (University of New Mexico).

2.21. Minimal inhibitory concentrations. Minimal inhibitory concentrations were determined for various antimicrobial peptides using a radial diffusion assay as previously described (Lisanby et al 2008). Briefly, the Ames strain or *inhA1/2* mutant derivative was seeded within two layers of agarose and dilutions of the peptide of interest were imbedded within wells bored into the agarose. Cells were grown to confluency at 37ºC, and zones of

clearance around the peptides were measured to enable calculation of minimal inhibitory concentrations.

Chapter III

Modulation of the *Bacillus anthracis* secretome by the Immune Inhibitor A1 protease

3.1. Introduction

Cleavage of extracellular substrates by secreted proteases is one method by which bacteria modulate their environment to promote survival and/or proliferation. Secreted proteases of pathogens can inactivate essential host proteins or cleave anti-microbial host factors (108, 156). Proteolysis of extracellular proteins by environmental bacteria can result in peptides that serve as growth substrates or are used in cell-cell communication (1, 122).

Substrate specificity of secreted bacterial proteases can be highly variable. For example, collagenases produced by various *Clostridium* species cleave a single substrate, while the *Streptococcus pyogenes* SpeB protease is active against a large number of proteins (44, 77). Three of the four classes of secreted bacterial proteases are distinguished by the catalytic residue(s) within their active sites. These are the serine, aspartate, and cysteine proteases (64, 123). The fourth class, the metalloproteases, require metal ions for activity. The most common bacterial metalloproteases contain zinc in the active site and harbor a conserved HEXXH zinc-binding sequence (64, 69).

Bacillus anthracis, a soil bacterium that is the etiological agent of anthrax, has a complex "secretome", or population of secreted proteins, that includes many proteases and other degradative enzymes. Published studies employing two-dimensional electrophoresis and mass spectrometry analyses of culture supernates have revealed large differences in the levels of some of these enzymes when *B. anthracis* cells are cultured in different conditions (2, 22, 71, 90). The most notable example is lethal factor (LF), one of the three anthrax toxin proteins. LF, a metalloprotease, and the other (non-proteolytic) toxin proteins, protective antigen (PA) and edema factor (EF) are induced in media containing bicarbonate and incubated in elevated CO_2 (51, 84). During growth in toxin-inducing conditions the toxin proteins accumulate to high levels in the culture supernates but are in relatively low amounts in cells grown under atmospheric conditions. Elevated CO_2 and bicarbonate signals are considered to be an important cue for the bacterium during infection of mammalian host tissues. In contrast to the LF protease, chitin related proteins are abundant in culture supernates of *B. anthracis* grown in air, but less abundant in supernates from cells cultured in toxin inducing conditions (22 52), possibly reflecting a function for these degradative enzymes *B. anthracis* encounters the soil environment.

Among the most abundant proteins identified in *B. anthracis* culture supernatants are the neutral protease Npr599 (also known as NprB) and the zinc metalloprotease Immune Inhibitor A1 (InhA1) (22). Npr599 is highly abundant in supernates of cultures grown in air, however is nearly absent when cultured with CO_2/bicarbonate, whereas high levels of InhA1 are apparent in both growth conditions (22). There have been few reports describing activity of the *B. anthracis* Npr599 protein. Studies of InhA1 function have centered on its potential role as a virulence factor. InhA1 has been reported to cleave extracellular matrix proteins, such as collagen and fibronectin (28), and to modify components of the coagulation cascade including fibrinogen, plasminogen activator inhibitor (PAI-1) and prothrombin (26, 28, 79). A role for InhA1 in thrombosis is apparent from *ex vivo* experiments demonstrating that *B. anthracis*-induced clotting of human blood was delayed in a strain deleted for the InhA1 gene (79). The affects of InhA1 on coagulation would likely impact bacterial dissemination within the host.

Here, I use a proteomic approach to demonstrate that InhA1 activity drastically alters the composition of the *B. anthracis* secretome, including the anthrax toxin proteins. My data indicate that InhA1 functions within a proteolytic regulatory cascade, modulating the abundance of Npr599, and at least nine additional secreted proteases. The potential importance of this proteolytic cascade with respect to *B. anthracis* virulence and survival is discussed.

3.2. Results

3.2.1. InhA1 modulates the *B. anthracis* secretome. Supernate protein preparations from stationary phase cultures of the parent strain 7702 and the isogenic *inhA1*-null mutant UT345 were subjected to SDS-PAGE analysis with Coomassie staining. Despite the comparable growth rates and optical intensities of the cultures, the abundance of protein in the culture supernate of the *inhA1* mutant exceeded that of the supernate from the parent strain culture, as shown in a Coomassie-stained gel (Fig. 3-1A). Proteins associated with bands showing significantly altered densities were identified using MALDI-MS/MS. Proteins exhibiting increased levels in the *inhA1* mutant included those annotated as ABC transporters (GBAA1191 and GBAA2041) a GroEL chaperone (GBAA0267), the S-layer protein Sap (GBAA0885), a sulfatase (GBAA5470), and a serine protease (GBAA3660) (118). In addition, the data indicated that the protease Npr599 (GBAA0599) had an altered molecular weight in the parent and mutant strain samples (Fig. 3-1A), suggesting InhA1-dependent processing of Npr599.

Given the large number of changes apparent in the one-dimensional electrophoretic analysis, differential in-gel electrophoresis (DIGE) experiments were performed to facilitate direct comparison of the parent and *inhA1* mutant supernate protein profiles. Differentially labeled protein preparations were mixed and subjected to two-dimensional SDS-PAGE (Fig. 3-2). Of the 1,340 protein spots identified using DIGE analysis, only 461 spots, approximately one third, fluoresced yellow, indicating that the proteins were present in equal amounts in supernates from both strains. Of the 879 remaining protein spots, 463 were identified as less abundant in the *inhA1* secretome (fluoresced green) and 416 were identified as more abundant (fluoresced red).

I chose 96 spots for MS/MS analysis: 10 exhibiting equal abundance in the two strains and 86 which showed a ≥9-fold change between the parent and mutant strains (17 were less abundant in the mutant and 69 were more abundant in the mutant). Of the 96 spots tested, 51 unique protein identifications were made (Table 3-1 and Fig. 3-2). Multiple proteins were represented as more than one spot, indicating multiple isoforms and/or sizes. Proteases were strongly represented among the altered proteins, suggesting that a proteolytic cascade, whereby one protease regulates the activity of a second protease, which regulates the activity of a third protease, etc., and that the proteolytic cascade was responsible for the

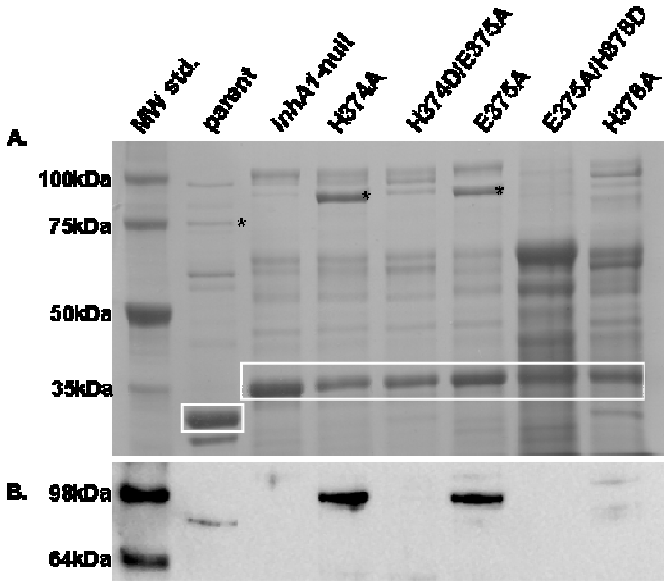

Figure 3-1. Disruption of InhA1 activity through deletion or mutation alters the protein pattern of *B. anthracis*. Parent strain 7702, *inhA1* null mutant UT345, and five 7702-derivatives containing point mutations within the *inhA1* zinc-binding motif (H374A, H374D/E375A, E375A, E375A/H378D, and H378A) were cultured to stationary phase. Supernates were collected and subjected to SDS-PAGE. (A) Coomassie stained gel of secreted proteins. Bands identified as InhA1 in the parent and the H374A and E375A mutant strains are designated with an asterisks. Bands determined to be Npr599 are boxed. (B) Western blot analysis with InhA1 specific antibodies.

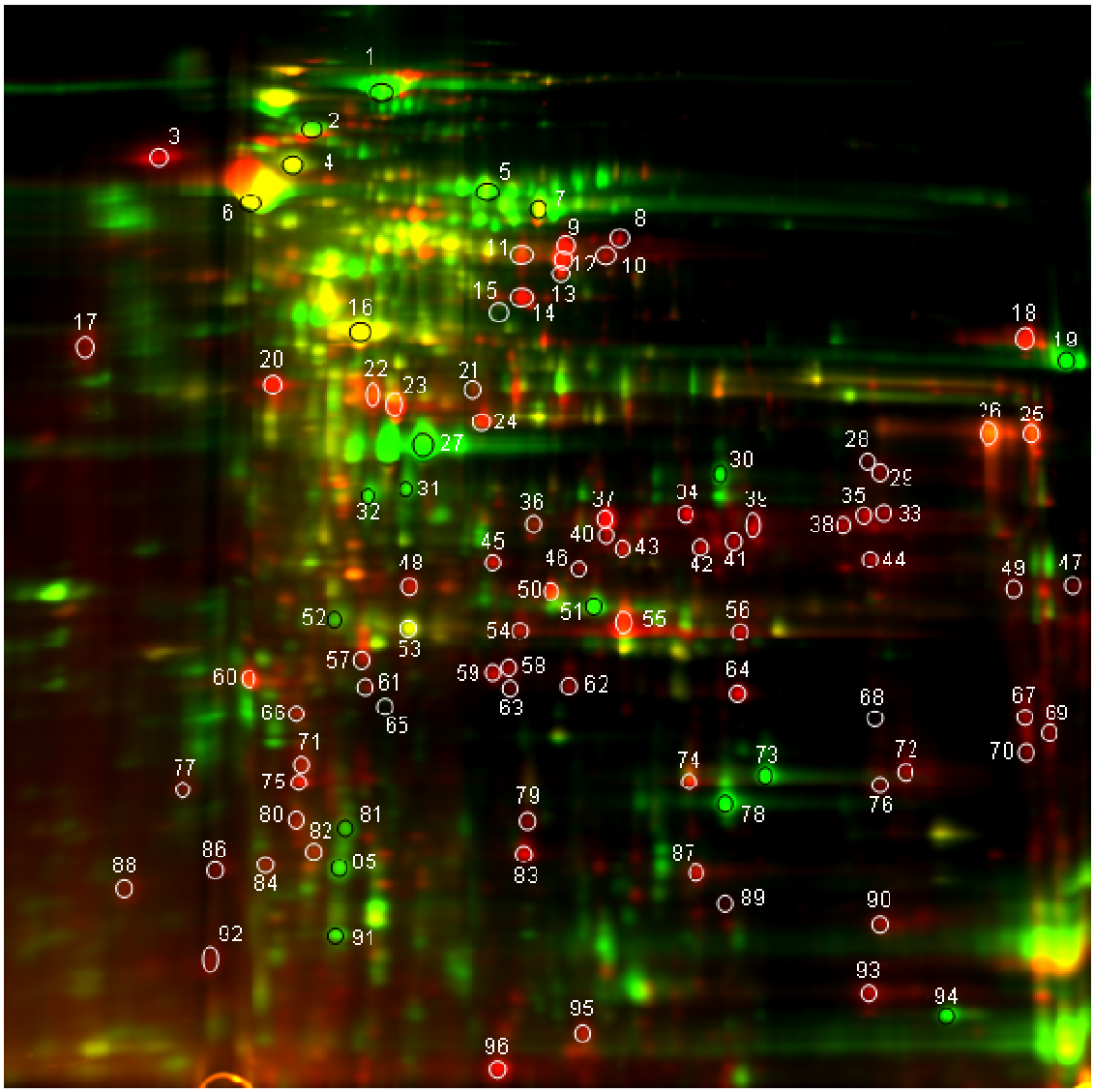

Figure 3-2. Deletion of *inhA1* significantly alters the *B. anthracis* secretome. Cy3-labeled supernatant proteins from parental strain 7702 and Cy5-labeled supernatant proteins from isogenic *inhA1* null mutant strain UT345 were mixed and separated using 2D-gel analysis. Red spots represent proteins more abundant in the mutant strain. Green spots represent proteins less abundant in the mutant strain. Yellow spots represent proteins that are present in equal abundance in the supernatants of the parental and mutant strains. Numbered and circled protein spots were extracted and subjected to mass spec analysis – see Table 3-1.

Table 3-1. Proteins identified from proteomic analysis. Proteins are listed by ascending gene number.

Sample (a)	Gi Accession (b)	GBAA# (c)	Description	Abundance in *inhA1* relative to parent (d)	Predicted signal sequence (e)
8	47500412	GBAA0008	inosine 5 monophosphate dehydrogenase	+	-
92	47500503	GBAA0100	ribosomal protein L7 L12	+	-
6	47500675	GBAA0267	chaperonin GroEL	NC	-
63	47500736	GBAA0322	glutamyl tRNA Gln amidotransferase B subunit	NC	-
60, 77	47500760	GBAA0345	peroxiredoxin	+	-
27	47501025	GBAA0599	neutral protease Npr599	-	+
23, 42, 54, 55, 56	47501025	GBAA0599	neutral protease Npr599	+	+
9, 12	47501113	GBAA0685	conserved hypothetical protein	+	+
62	47501132	GBAA0703	Cytochrome aa3 quinol oxidase subunit II	+	+
18, 33, 35, 38, 39, 41, 44, 47, 95	47501230	GBAA0796	conserved hypothetical protein	+	+
89	47501230	GBAA0796	conserved hypothetical protein	NC	+
81	47501516	GBAA1094	putative wall associated protein	-	+
20	47501516	GBAA1094	putative wall associated protein	+	+
7	50082984	GBAA1191	putative oligopeptide ABC transporter oligopeptide binding protein	NC	+
4	47501617	GBAA1206	Oligoendopeptidase F	NC	-
13, 14	47501872	GBAA1449	peptidase M23 M37 family	+	+
15	47501934	GBAA1511	glutamate dehydrogenase NAD specific	NC	-
85	47501958	GBAA1536	putative nucleoside diphosphate kinase	-	-
65	47502136	GBAA1698	TPR glycosyl transferase domain protein	NC	-
51	47502253	GBAA1817	N acetylmuramoyl L alanine amidase family 3	-	+
87, 90	47551689	GBAA1952	putative cell wall peptidase NlpC P60 family	+	+
39	47502416	GBAA1973	Transcription antiterminator LytR family	+	-
71, 75	47502674	GBAA2230	conserved hypothetical protein	+	+
30, 94	47502823	GBAA2380	alkaline serine protease subtilase family	-	+
19	47503113	GBAA2673	chitosanase	-	+
73, 78	47503268	GBAA2827	putative chitin binding protein	-	+
64	47503268	GBAA2827	putative chitin binding protein	+	+
50	47503384	GBAA2944	Polysaccharide deacetylase	+	+
89	47503408	GBAA2967	conserved domain protein	NC	+
85	47503438	GBAA2996	RocB protein	-	-
20	47503438	GBAA2996	RocB protein	+	-
31	47503629	GBAA3189	manganese ABC transporter manganese binding protein	-	+
81	47503659	GBAA3221	Bifunctional P 450 NADPH P450 reductase 1	-	-
3	47503799	GBAA3367	LPXTG motif cell wall anchor domain protein	+	+

Sample (a)	Gi Accession (b)	GBAA# (c)	Description	Abundance in *inhA1* relative to parent (d)	Predicted signal sequence (e)
25, 26	47503992	GBAA3560	putative glycerophosphoryl diester phosphodiesterase	+	+
1	47504017	GBAA3584	putative microbial collagenase	-	+
45, 46	47551883	GBAA3588	putative lipoprotein	+	+
5	47504077	GBAA3645	putative oligopeptide ABC transporter oligopeptide binding protein	-	+
24	47504093	GBAA3660	serine protease HtrA	+	-
91	47504174	GBAA3737	surface layer N acetylmuramoyl L alanine amidase	-	+
57, 61, 66, 84	47504174	GBAA3737	surface layer N acetylmuramoyl L alanine amidase	+	+
2	47504182	GBAA3744	transketolase	+	-
94	47504280	GBAA3845	conserved domain protein	-	+
67, 69, 70, 72, 74, 76, 79, 83, 93, 96	47504280	GBAA3845	conserved domain protein	+	+
68	47504280	GBAA3845	conserved domain protein	NC	+
58, 59	47504400	GBAA3962	ribosome recycling factor	+	-
22	47504402	GBAA3964	translation elongation factor Ts	+	-
32	47504496	GBAA4055	penicillin binding protein	-	+
65	47504630	GBAA4187	peptide deformylase	NC	-
52	47504637	GBAA4194	putative 2 3 4 5 tetrahydropyridine 2 carboxylate N succinyltransferase	-	-
48	47504637	GBAA4194	putative 2 3 4 5 tetrahydropyridine 2 carboxylate N succinyltransferase	+	-
16	47504830	GBAA4387	leucine dehydrogenase	NC	-
17	47504984	GBAA4539	chaperone protein DnaK	+	-
68	47505149	GBAA4702	ATP dependent protease La 1	NC	-
34, 37, 40, 43	47505198	GBAA4750	D alanyl D alanine carboxypeptidase family protein	+	+
80	47552044	GBAA4890	thiol peroxidase	+	-
36	47505336	GBAA4893	conserved hypothetical protein	+	-
88	47505769	GBAA5312	conserved hypothetical protein	+	-
10, 11, 21, 28, 29, 49	47552107	GBAA5427	putative cell wall endopeptidase NlpC P60 family	+	+
82, 86	47505946	GBAA5481	conserved domain protein	+	+
53	47506179	GBAA5696	superoxide dismutase Mn	NC	-

(a) assigned in figure 3-2.
(b) Ames ancestor strain accession number
(c) Ames ancestor strain associated ORF
(d) NC – No change. +, higher in the *inhA1* mutant. -, lower in the *inhA1* mutant.
(e) presence (+) or absence (-) of a signal sequence predicted using the bioinformatic program Signal P (46)

multiple differences observed in the parent and *inhA1* supernates.

Other proteins of interest that differed in the parent and *inhA1* supernates included a number of cell-envelope-associated proteins, indicating potential processing of cell surface proteins by InhA1 or InhA1-controlled proteases. Notably, putative InhA1 substrates include a chitinase which may be important in the soil niche of *B. anthracis* and enzymes associated with peroxide reduction which may be of significance during infection of mammalian hosts. Some of the *inhA1*-affected proteins are predicted to be cytosolic rather than secreted proteins, as predicted by the presence of a signal secretion sequence. These include certain transcriptional regulators and chaperone proteins. There is considerable overlap of the proteins that have been identified as cytosolic in the secretome analyses of *B. anthracis* (2, 22). While some of these proteins may have been released from the cell as a result of cell lysis others may have been exported through untraditional export mechanisms, resulting in the availability of these proteins as substrates for secreted proteases.

Degradation of the anthrax toxin proteins is dependent upon *inhA1*. The anthrax toxin proteins, PA, LF, and EF, represent the most-well characterized secreted virulence factors of *B. anthracis.* Synthesis of these proteins is greatest when cells are cultured in media with dissolved bicarbonate and in the presence of elevated CO_2 (51, 84). To assess the effect of *inhA1* on the level of the toxin proteins in culture supernates, we cultured the parent and *inhA1* strains in toxin-inducing conditions. Supernates from exponential, transition, and stationary phase cultures were subjected to SDS-PAGE followed by Coomassie staining and Western blot analysis using PA-, LF-, and EF-specific antibodies (Fig. 3-3). Levels of all three toxin proteins in the parent strain culture decreased dramatically following exponential phase. However, the secreted toxin protein levels remained elevated throughout culture of the *inhA1* mutant strain, indicating that degradation of the toxin proteins are dependent upon InhA1. In contrast, the toxin protein levels in supernates of the *npr599*-null mutant were comparable to those of the parent, demonstrating that the Npr599 protease does not affect toxin stability.

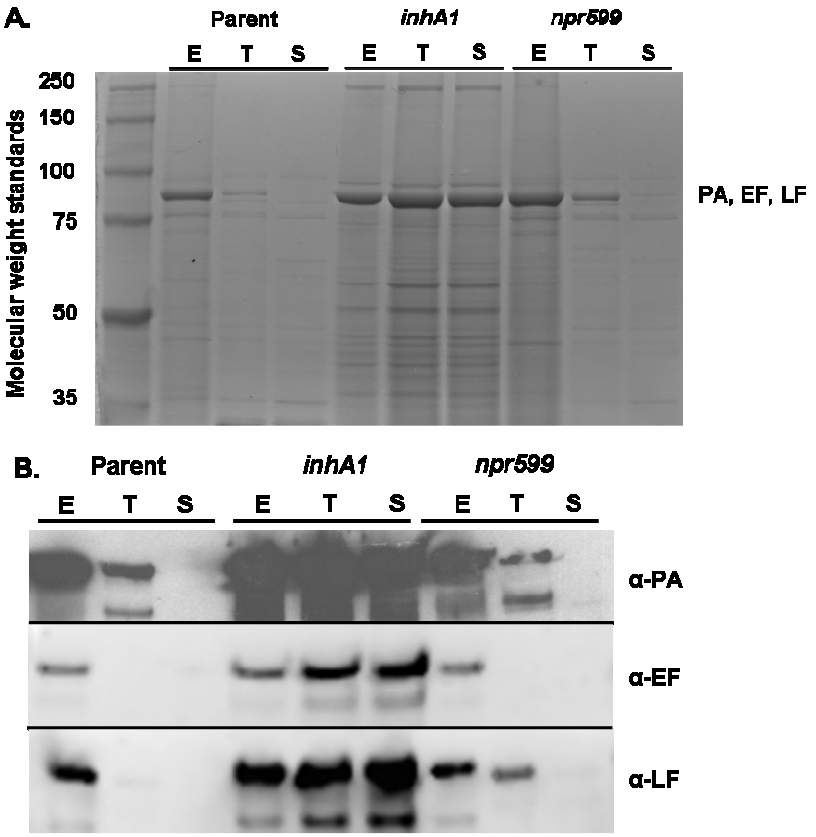

Figure 3-3. Degradation of anthrax toxin proteins is dependent upon *inhA1*. Parental strain 7702, *inhA1* mutant UT345, and *npr599* mutant UT317, were cultured in NBY- CO_2. Secreted proteins were isolated and separated using SDS-PAGE. E, exponential phase. T, transition phase. S, stationary phase. (A) Coomassie blue stained gel of secreted proteins. The three toxin proteins (PA, EF, LF) are of a similar molecular weight at 85-90kDa. (B) Western blot analysis using EF, LF, and PA-specific antibodies.

To further explore the relationship between InhA1 and toxin degradation, InhA1 protein levels in supernates of parent strain cultures were assessed at different growth phases. The abundance of InhA1 increased as cultures transitioned into stationary phase, correlating with diminished PA levels (Fig. 3-4). Taken together, the data support a model in which secretion of InhA1 results in regulation of the anthrax toxin proteins in *B. anthracis* culture supernates.

3.2.5. Capsule is unaffected in *inhA1* mutants. Given the influence of InhA1 on the stability of the secreted anthrax toxin proteins, I tested for the presence of capsule, the other major virulence factor of *B. anthracis*, on cells of *inhA1* and *npr599* mutants. The *B. anthracis* capsule is comprised of poly-D-glutamic acid polymers and is covalently linked to the cell wall. Phase microscopy of india ink preparations of the capsulated Ames strain, an isogenic *inhA1* null mutant (UTA5), and an isogenic *npr599* null mutant (UTA13) revealed no differences in the capsulation of the cells (Fig. 3-5).

3.2.6. InhA1 activity is dependent upon the zinc-binding motif. The predicted amino acid sequence of InhA1 includes the conserved zinc-binding motif HEXXH at amino acids 374-378 (HEYGH), which is characteristic of zinc-metalloproteases (28, 69). To determine if this sequence is associated with InhA1 activity, *inhA1* mutants encoding InhA1 alleles with amino acid substitutions within the zinc-binding motif were constructed. As shown in Figure 3-6, PA degradation did not occur in a culture supernate of a H374A mutant; PA levels were comparable to those observed in the supernate of an *inhA1*-null strain. Moreover, the secretome profile of the H374A mutant was comparable to that of the *inhA*-null strain (Fig. 3-1A). The phenotypes of additional mutants harboring amino acid substitutions in the zinc-binding motif also displayed the *inhA1*-null phenotype (Fig. 3-1A). Interestingly, the H374A and E375A InhA1 proteins migrated more slowly than the native InhA1 protein in SDS-PAGE (Fig 3-1A and 3-1B), suggesting a possible cleavage event is necessary for activity. N-terminal sequencing and mass spectrometry analysis of bands reacting with anti-InhA1 antibody (Fig. 3-1B), confirmed their identity. N-terminal sequencing of the H374A protein confirmed cleavage of the predicted signal peptide,

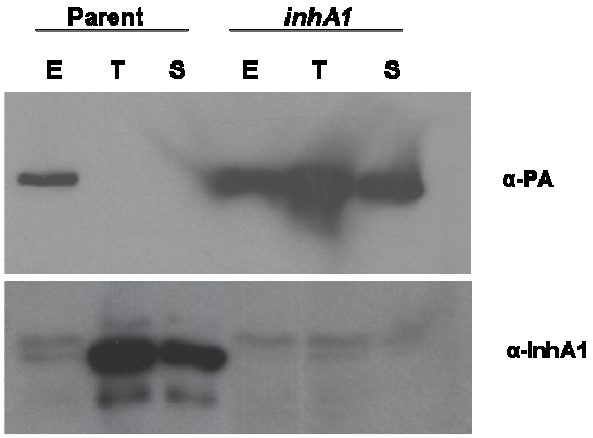

Figure 3-4. Abundance of PA in the supernatant is inversely correlated with the abundance of InhA1. Temporal analysis of PA and InhA1 in *B. anthracis* culture supernatants after culturing in NBY- CO_2 as assessed using Western blot analysis with PA and InhA1-specific antibodies. E, exponential phase. T, transition phase. S, stationary phase.

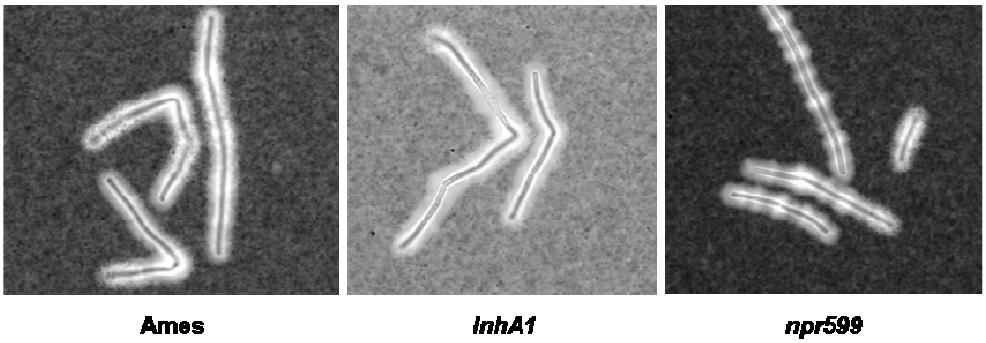

Figure 3-5. Capsule is unaffected by InhA1 or Npr599. Qualitative analysis of capsule produced by the parent (Ames), *inhA1* (UTA5), and *npr599* (UTA13) mutant strains as assessed using India ink exclusion assay.

Figure 3-6. InhA1 activity is dependent on a conserved zinc binding motif. Western blot analysis of PA abundance in the culture supernatant of parental strain 7702, *inhA1* null mutant UT345, and the H_{374}A *inhA1* zinc-binding motif mutant strain UT368. The sequence of the zinc binding motif is shown for each strain. E, exponential phase. T, transition phase. S, stationary phase.

MNKKPFKVLSSIALTAVL GLSFGAGGQSVYA[31], from the full length (795 amino acids) protein. Other mutants, H374D/E375A, E375A/H378D, and H378A did not accumulate in their culture supernates or with in the cell (Fig. 3-1), suggesting that the mutations adversely affected stability of the protease. The instability of the H374D/E375A, E375A/H378D, and H378A mutant strains and the lack of activity of the H374 and E375A mutant strains suggests that the zinc-binding motif and the availability of zinc ions are important in the regulation of InhA1.

3.2.7. Purification of InhA1. Attempts to purify InhA1 from *B. anthracis* Ames cured of pXO1 and pXO2 using methods established previously (28) resulted in impure preparations that contained the camelysin protease and the S-layer protein Sap (data not shown). Camelysin has been implicated in degradation of InhA1 in culture supernates (Chapter IV). To eliminate these problems, I created a *B. anthracis* strain deficient in secretion of these proteins. The recombinant strain, UT357, is deleted for the camelysin gene, *calY,* and carries a mutation in the *secA* gene which prevents Sap secretion but does not affect protease secretion [Colin Harwood, personal communication]. InhA1 was purified from stationary-phase culture supernates of the *calY secA* mutant using anion exchange chromatography. Protein purity was assessed using SDS-PAGE with Coomassie staining, Western hybridization analysis, and mass spectrometry. Repeated purification attempts resulted in preparations containing proteins of non-uniform size (Fig. 3-7). The major proteins with apparent masses of 75- and 42-kD constituted bulk of the protein in the sample. These correspond to the full length and active forms of the protein as reported previously by Chung and coworkers (28). The re-occurring appearance of InhA1 species with specific molecular weights suggests that InhA1 is similar to other secreted proteases in that it processed prior to activation in a reaction that is hypothesized to be auto-proteolytic in nature (64, 157). Results of mass spectrometry analysis of the purified protein sample indicated a pure InhA1 preparation, as all protein fragments observed corresponded to InhA1 amino acid sequences.

3.2.8. InhA1 directly cleaves the *B. anthracis* toxin proteins and neutral protease. Our data from DIGE analysis of parent and *inhA1*-null strains reveal that *inhA1* affects the

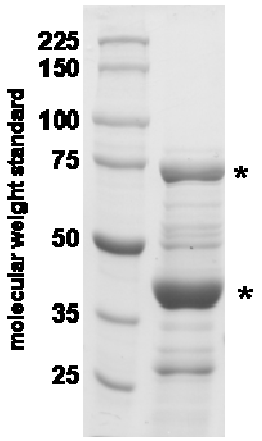

Figure 3-7. Purification of InhA1 from *B. anthracis* culture supernate. Purified InhA1 protein was separated using SDS-PAGE and the gel stained with Coomassie Blue. Bands highlighted with asterisks correspond to the molecular weights of previously identified InhA1 protein isoforms (28).

stability of at least eight other proteases (Table 3-1). Therefore, the global affects of InhA1 on the secretome may be attributed in part to downstream effects of one or more proteases targeted by InhA1. To assess whether InhA1 directly or indirectly cleaves PA, EF, LF, and Npr599 proteins we performed *in vitro* protease assays. Purified InhA1 was incubated with rPA, rLF, rEF, rNpr599, or rSODA-1, a super oxide dismutase of *B. anthracis* utilized as a negative control. Following incubation at 37^{o}C, samples were subjected to Western hybridization using antisera against the potential substrates. The toxin proteins and Npr599 were all degraded by InhA1, but susceptibilities to protease activity varied (Fig. 3-8). Distinct PA fragments with apparent masses of 54 and 43kDa were detected immediately upon contact with InhA1 and PA was fully degraded following extended incubation. In contrast, processing of EF, LF, and Npr599 did not reveal abundant distinct cleavage products, rather the majority of protein became undetectable after prolonged incubation. Equivalent substrate:enzyme ratios and times of incubation did not result in degradation of the SodA-1 protein.

The amino terminal sequences of the distinct PA protein fragments were determined using amino-terminal sequencing. The amino-terminal sequences of the bands indicated in Fig. 3-8A, NRLLNESESS, VHASFFDI, and APIALNAQDD, indicate that InhA1-mediated cleavage of the secreted form of the PA (735-amino acid) protein occurred after residues 5, 308, and 416. It is notable that the resulting protein fragments do not correspond to the cleavage site at residue 167 which is associated with processing required for toxin entry into eukaryotic cells (82, 105).

The amino terminal sequence of the minor cleavage product of EF (Fig. 3-8A), GVEKDRI, indicated InhA1-cleavage of the EF protein between residues 287 and 288. As incubation of rLF and rNpr599 with InhA1 did not result in consistent protease reaction products cleavage sites were not determined for these substrates. Taken together, my data do not reveal a specific amino acid sequence associated with processing by InhA1. Nevertheless, InhA1 directly processes the three toxin proteins and the Npr599 protease with varying degrees of specificity.

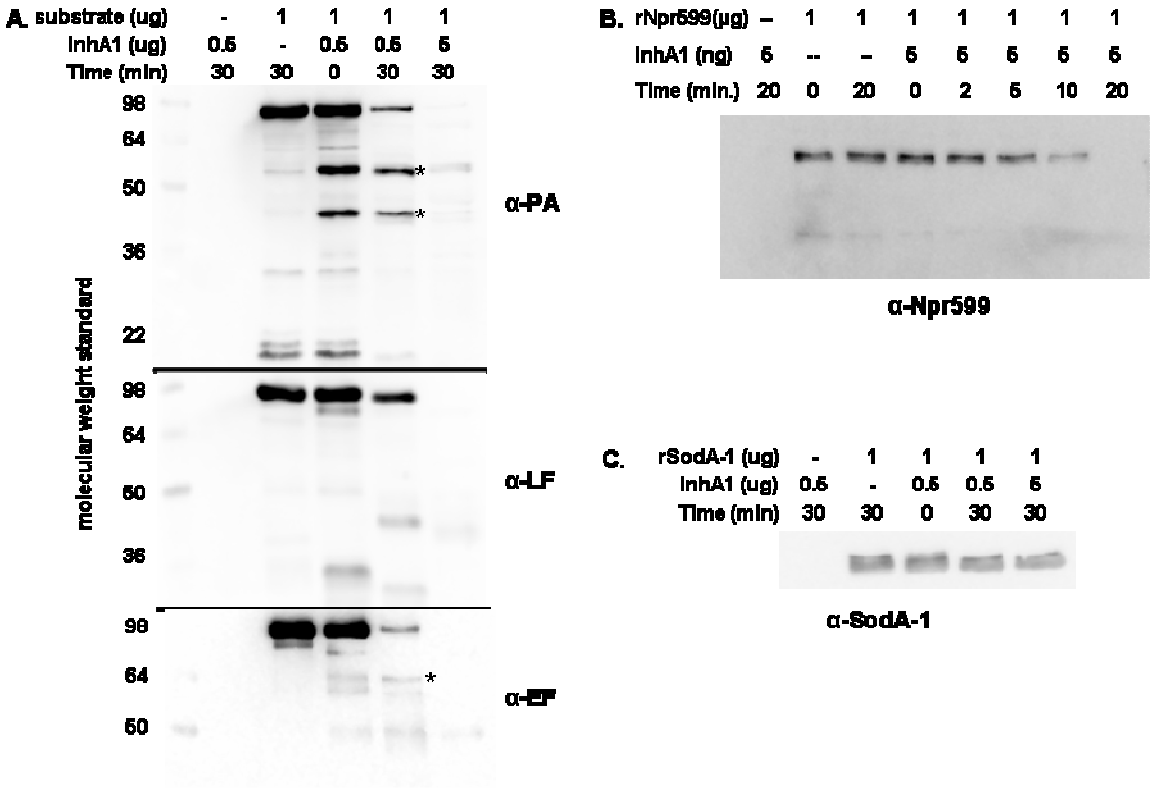

Figure 3-8. InhA1 directly cleaves the anthrax toxin proteins and protease Npr599. Purified InhA1 was incubated with rPA, rLF, rEF, rNpr599, or rSodA-1. Reactions were separated using SDS-PAGE and subjected to Western blot analysis. (A) Western analysis using PA, LF, and EF-specific antibodies. Bands submitted for amino-terminal sequencing are highlighted with asterisks. Amino-terminal sequences identified were VHASFFDI (PA, 54kDa band), NRLLNESESS and APIALNAQDD (PA, 43kDa band), and GVEKDRI (EF band). (B) Western analysis using Npr599-specific antibodies. (C) Western analysis using SodA-1 specific antibodies.

3.3. Discussion

Using DIGE to analyze the secretome of *B. anthracis* it was established that InhA1, either directly or indirectly, modified the abundance of more than half of the proteins found in the culture supernate. While only 96 (of the 1,340 protein spots) of the most abundant protein spots were identified, this analysis uncovered that substrates from multiple functional categories were affected by InhA1, including putative immunomodulatory proteins and proteins involved in nutrient acquisition. The largest functional group identified from the proteomic analysis was proteins with proteolytic activity, including Npr599. While the focus of the study was to assess the contribution of InhA1 in the modulation of the secretome, a number of cell associated proteins were also identified as being InhA1-regulated, which implicates InhA1 in affecting how *B. anthracis* interacts with its environment.

In *B. anthracis*, proteases constitute a considerable fraction of the secretome. InhA1 and Npr599 are the most abundant proteins in the culture supernatant (22). Purified Npr599 has some substrate overlap with InhA1 with respect to host substrates. Like InhA1, Npr599 cleaves ECM proteins collagen and fibronectin, however Npr599 is less active against proteins of the coagulation cascade than InhA1 (28). Cleavage of the ECM components collagen and fibronectin by *B. anthracis* proteases may inhibit colonization of host tissues. Since both InhA1 and Npr599 cleave collagen and fibronectin it is unclear whether *B. anthracis* adherence would be modified as a consequence of Npr599 cleavage by InhA1. Given the abundance of Npr599 in *in vitro* cultures, the inactivation of this protein would be hypothesized to have significant effects on the composition of extracellular proteins, of both host and bacterial origin.

The activity of secreted proteases is regulated post-translationally by several processing events, first by a signal peptidase upon secretion, then often by an auto-cleavage event that precedes activation (64, 147, 157). However, protease activity can also be regulated through a proteolytic cascade, allowing for the various proteases secreted by a bacterium to regulate the activity of other proteases (134); my data suggest that such a cascade is used by *B. anthracis* to regulate the timing of specific protease activity. An early step in the putative regulatory cascade is production of the cell-envelope-associated protease camelysin, which is implicated in degrading InhA1 in the supernatant during early stationary

phase (see Chapter IV). As the cells progress through stationary phase InhA1 increases in abundance (see Chapter IV). Increased InhA1 activity leads to the processing of at least nine other proteases present in *B. anthracis* culture supernatants, including the direct processing of Npr599 and LF. A possible benefit that a protease cascade may confer upon *B. anthracis* is the amplification of the number of extracellular substrates susceptible to proteolysis by active proteases. In addition, each of the proteases available for activation are likely regulated transcriptionally in response to independent environmental or growth phase signals, thereby amplifying the number of input signals into the regulatory cascade. Furthermore, a protease-based regulatory mechanism would allow for the post-translational regulation of the proteins in the secretome, regulation that may be necessary when rapid change of protein activity is necessary. Such regulation could be important in response to changing signals or tissue type as the cell disseminates through the host. The presence of a proteolytic regulatory cascade is not without precedent; such a phenomenon has been described in *Staphylococcus aureus* for the regulation of extracellular proteases SspA, SspB, and Aur. (134).

The activity of the toxin protein PA is regulated in response to physiological conditions in the host (89, 115). PA binds host cell receptors ANTXR1 and ANTXR2 and subsequently forms a heptameric ring on the cell surface creating binding sites for EF and/or LF prior to endocytosis (158). The heptameric form of PA undergoes a change in conformation upon acidification of the endosome, allowing for the translocation of EF and LF into the cytosol (89, 158). In addition, PA undergoes a loss in activity due to prolonged exposure to elevated temperatures (37ºC) (115). Here I report an additional regulatory mechanism that results in differentiated toxin protein accumulation in response to growth phase. InhA1 accumulates in the culture supernates during the transition and stationary phases of growth and cleaves PA within the protease accessible unstructured loops of domain 2 (112). Domain 2 contains critical residues involved in anthrax toxin pore formation and links the receptor binding activity of the C-terminal domain 4 to the EF/LF binding sites within domain-1 (89). Cleavage of PA following resides E308 and L416 by InhA1 would disassociate the receptor and EF/LF binding subunits and may alter the confirmation of the protein allowing for increased protease susceptibility and degradation. Furthermore structural analysis of PA indicates that the InhA1 cleavage sites are likely to

only be accessible when PA is in its monomeric form (89, 112), suggestive of InhA1 acting on PA prior to host cell binding.

Degradation of the toxin proteins by InhA1 may significantly alter virulence. Degradation may reduce development of neutralizing antibodies against these proteins in the infected host. Alternatively, the timing of toxin accumulation may be important during infection, and InhA1 may facilitate this by keeping toxin protein concentration low during certain stages of infection or in a specific tissue or cell type. Interestingly, the accumulation of toxin in the host prior to the patient becoming septic is necessary for full dissemination (96), indicating a need for temporal regulation of the toxin proteins. It should be noted that the processing of toxins in the extracellular milieu is not a mechanism unique to *B. anthracis*. SpeB, a protease secreted by *Streptococcus pyogenes*, limits the concentration of multiple other virulence factors in a growth-phase dependent manner (107), and is hypothesized to be important in reducing the presentation of antigens during upper respiratory tract infection (143). In addition to limiting the abundance or activity of toxins via degradation, proteases secreted by pathogens have also been found to activate toxins, as in the case of the *Vibrio cholerae* protease HA which activates the A subunit of cholera toxin (10). To date I have no evidence of protein activation by InhA1 cleavage.

InhA1 is responsible for the cleavage of a wide array of bacterial and host substrates; however the protease did not alter the concentration of every protein in the culture supernate, indicating that InhA1 does have a level of substrate specificity, albeit a limited one. This was confirmed through my *in vitro* proteolytic assays using purified InhA1, establishing that InhA1 directly cleaves the anthrax toxin proteins and Npr599, but not the superoxide dismutase, SodA-1. The rapid cleavage of PA resulting in distinct products indicates that proteolysis by InhA1 is specific. However, as my purified InhA1 preparation contained multiple forms of InhA1, many of which may have been inactive, it was not possible to determine the specific activity of the protein. It was noted that higher concentrations of InhA1 were necessary to degrade the toxin proteins than Npr599. The seemingly higher affinity of InhA1 for Npr599 may highlight the importance of the protease cascade in *B. anthracis*.

The vast affects on the secretome of *B. anthracis* attributed to InhA1, due to the apparent low substrate cleavage specificity, suggests that the spatial and temporal regulation

of protease activity is crucial to minimize deleterious effects due to InhA1 activity. Spatial regulation of InhA1 activity is in part accomplished through the presence of a secretion signal sequence at the N-terminus of the proenzyme which marks the protein for secretion (147). In its environment the availability of metal ions may limit the activity of InhA1(102). Temporal regulation of InhA1 activity occurs through mechanisms that include: (i) proteolytic inactivation of InhA1 function by other secreted proteases (such as camelysin [see Chapter IV]), and (ii) regulation at the transcript level by the SinI/R regulatory proteins (see Chapter IV).

In addition to a potential role for InhA1 in virulence my data also predict a role for survival in the soil. As the promoter for *inhA1* is active in *B. anthracis* when cultured in the soil (126), it is posited that InhA1 is available to regulate environmentally-significant proteins. Examples of environmentally-significant proteins affected by InhA1 are chitin associated proteins. The abundance of a chitinase and chitin-binding protein were each found to be regulated differentially in the culture supernatant of the parent and *inhA1* mutant strains. Chitinases and chitin-binding proteins are utilized by bacteria to breakdown the cell-wall of fungi or the chitin produced by insects in the soil (151). By modulating proteins in the environment InhA1 may regulate nutrient acquisition and prolong survival of the bacteria or accelerate the progression into sporulation (see Chapter V).

The modulation of the *B. anthracis* secretome by InhA1 may have a multitude of downstream effects, from enhancement of cell survival to increased virulence. Here I have shown that InhA1 can act directly or indirectly to post-translationally regulate extracellular proteins. Modulation of toxin protein levels *in vitro* implicates InhA1 as a post-translational regulator of toxin in the host, potentially directing the timing of toxin protein accumulation. This is the first bacterial protease identified to cleave the anthrax toxin proteins. The post-translational regulation of toxin proteins in response to growth phase adds an additional layer of regulation to toxin production, complementing the well-established regulation of toxin gene transcription by the pleiotropic virulence protein regulator AtxA in response to bicarbonate and elevated CO_2 (51, 84). By maintaining the abundance of proteins in the culture supernate via a proteolytic cascade the number of proteins regulated is amplified, providing the opportunity to fine-tune the composition of proteins in the extra-cellular

milieu through integration of multiple independent extra-cellular signals. Signaling could be direct, in terms of co-factors available in the environment (e.g. metal ion availability), or indirect through a plethora of transcriptional and post-transcriptional regulatory systems.

Chapter IV

The *Bacillus anthracis sin* locus and regulation of secreted proteases

4.1. Introduction

Bacillus species are developmental bacteria that cycle between a dormant spore state and a metabolically active vegetative cell state. Vegetative cells can grow as planktonic cells or in multicellular biofilms. Environmental cues affect cellular and community morphologies via complex regulatory systems that are generally conserved throughout the genus. One such system is the pleiotropic SinI/R regulatory pair. The *sin* locus (sporulation inhibitor) was originally described in *B. subtilis* as a component of the sporulation cascade (55). Subsequent studies revealed that in addition to negatively regulating several genes involved in sporulation, SinR also regulates motility, competency, proteolysis, and biofilm formation genes in *B. subtilis* (7, 24, 25, 62, 78, 83, 88, 94, 100, 152). The SinR protein binds a conserved DNA sequence upstream of the translational start site of target genes to either positively or negatively control transcription. SinI, encoded by a gene adjacent to *sinR*, is a SinR antagonist and binds directly to the SinR protein to inhibit its activity (5). In batch culture, SinR is expressed throughout growth, while SinI expression is limited to stationary phase (54, 133). Thus, SinR-controlled gene expression is relieved when cultures transition from exponential to stationary phase.

While SinI/R function and the *sin* regulon are well established in *B. subtilis*, there are few reports concerning the SinI/R regulatory system in other *Bacillus* species. *B. anthracis*, the etiological agent of anthrax, has a *sinI/R* locus, but is devoid of multiple characteristics associated with SinI/R function in *B. subtilis*. Unlike *B. subtilis*, *B. anthracis* is non-motile, does not produce naturally competent cells, and does not readily produce biofilms (14, 101, 128). Although known and potential virulence factors of *B. anthracis* have been shown to be produced in a growth-phase-dependent manner, there are no reports of control of these factors by SinI/R during growth in batch culture. One study indicates that in *B. thuringiensis*, an insect pathogen closely related to *B. anthracis* (40, 138, 150), the SinI/R system controls expression of the immune inhibitor A1 gene *inhA1*; overexpression of *sinR* in *B. thuringiensis* results in decreased expression of *inhA1*, while overexpression of *sinI* results in elevated *inhA1* transcript levels (58). Immune inhibitor A1 is a secreted metalloprotease that degrades insect antimicrobial peptides and enhances the ability of *B. thuringiensis* to escape from macrophages (116). *B. anthracis* also produces an InhA1 protease that has been implicated as having a role in virulence. The *B. anthracis* protease

may directly affect virulence by cleaving the host proteins von Willebrand Factor and pro-thrombin, proteins associated with the coagulation cascade, as well as several extracellular matrix proteins (26-28, 79, 116). Indirectly, InhA1 may affect virulence by degrading proteins secreted by *B. anthracis*, including the anthrax toxin proteins (see Chapter III). SinI/R control of *B. anthracis inhA1* gene expression has not been reported.

In work described here, the role of the SinI/R system in *B. anthracis* was examined using genome-wide expression microarray and immunoblot analyses to assess transcriptional and post-translational regulation of SinR/I-regulated genes. I show that in addition to homologues of some *B. subtilis* SinR-regulated genes, the *B. anthracis* SinR negatively regulates transcription of genes adjacent to the *sinI/R* locus that are unique to the *B. cereus* group species (*B. anthracis, B. cereus,* and *B. thuringiensis*). My data show that InhA1 protease levels are regulated at the transcriptional level by the SinI/R system and at the post-translational level by a second SinR-regulated protease, camelysin.

4.2. Results

4.2.1. Comparison of *sin* loci. In *B. subtilis*, the *sinI* and *sinR* genes are adjacent to each other on the chromosome and are cotranscribed (133). The *sinI/R* genes of *B. anthracis* are aligned similarly and are likewise hypothesized to be co-transcribed. The amino acid sequences of the SinR proteins are 67% identical, with conserved residues spanning the length of the proteins. Eighteen of 20 conserved residues in the *B. subtilis* SinR helix-turn-helix motif are identical to those of the *B. anthracis* SinR, and the two non-conserved residues represent conservative substitutions. In addition, the region of SinR that is predicted to interact with SinI (92) is moderately conserved; 21 of 29 residues are identical in the SinR proteins of the two species. The *B. subtilis* and *B. anthracis* SinI proteins are conserved to a lesser degree, exhibiting 42% identity and 76% similarity throughout the middle of the proteins, the residues of SinI that interact with SinR (92). The N- and C-termini are not conserved.

There are notable differences between *B. subtilis* and *B. anthracis* with regard to sequences adjacent to *sinI/R* (Fig. 4-1). One target of the *B. subtilis* SinI/R regulatory system, the tricistronic operon comprised of *yqxM*, *sipW*, and *tasA*, is located immediately downstream of the *B. subtilis sin* operon in the opposite orientation. The *yqxM/sipW/tasA* operon is associated with biofilm formation by *B. subtilis* (24). The *yqxM* gene encodes a lipoprotein, while *sipW* encodes a signal peptidase, and *tasA* encodes a biofilm matrix protein. *B. anthracis* lacks the *yqxM* gene and although the tandem *sipW* and *tasA* genes are present, they are separated from *sinI/R* by two open reading frames (ORFs), GBAA1289 and GBAA1290, that are absent in *B. subtilis*. GBAA1289 is annotated as containing a nonsense mutation, and is therefore considered to be a pseudo-gene. ORF1290 has been designated *calY* because the ORF is predicted to encode a protein with an amino acid sequence that is greater than 90% identical to the *calY*-encoded protein, camelysin, of *B. cereus* ((59) and NCBI blast). *B. cereus* camelysin is a protease that is cell-envelope associated (59). Sequences upstream of *sinI/R* also differ between *B. subtilis* and *B. anthracis*. In *B. anthracis, inhA1*, encoding the freely-secreted InhA1 protease, is located upstream of *sinI* and in the opposite orientation (Fig. 4-1). In *B. subtilis*, *yqhG* lies 977-bp upstream of *sinI* in the same orientation; the *inhA1* gene is not present. An orthologue of *yqhG* (GBAA4451), which encodes a conserved hypothetical protein, is present on the chromosome of

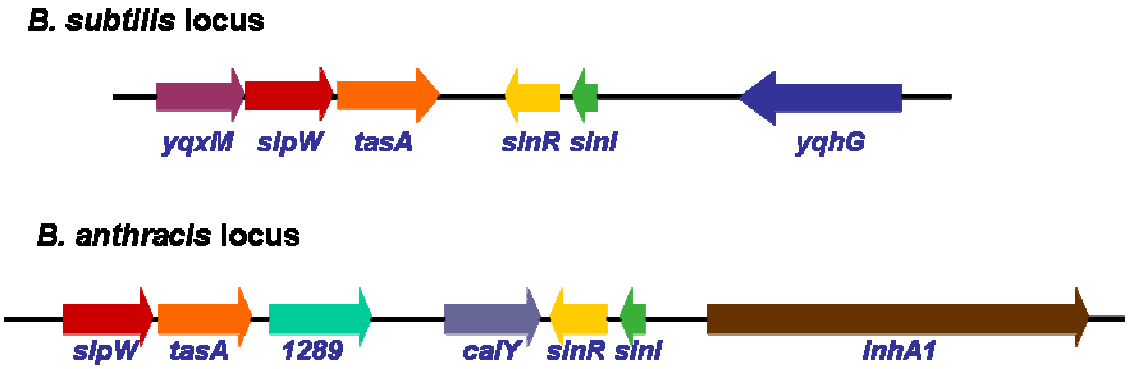

Figure 4-1. Schematic representation of the *sin* loci of *B. subtilis* and *B. anthracis*. Orfs are represented by block arrows facing the direction of transcription. Conserved genes are color coded.

B. anthracis at a distant locus. Analysis of the available genome sequences of species closely related to *B. anthracis*, *B. cereus* and *B. thuringiensis*, indicates that the extended *sin* loci in these species match that of *B. anthracis*.

4.2.2. **Assessment of the SinR regulon in *B. anthracis*.** Differences in *sinI/R*-associated phenotypes of *B. subtilis* and *B. anthracis,* and structural dissimilarities in the *sin* loci, suggest disparities in the SinR regulons of the two species. To determine the SinR regulon of *B. anthracis* genome-wide transcriptional profiling experiments were conducted comparing the fully virulent Ames strain to an isogenic *sinR*-null mutant, UTA21. Transcript levels at exponential and stationary phases of growth were compared (Fig. 4-2A). The data identified that the expression of 41 genes differed between the parent and *sinR* mutant strains. Note that for a gene to be designated as SinR-regulated in my study it required a two-fold or greater difference in regulation between the parent and *sinR* mutant strain as assessed by three independent data analysis programs (Tables 4-1 and 4-2; see chapter 2 section 5). Regulation by SinR was growth phase-dependent in all cases except GBAA1287 (*sipW*), GBAA1288 (*tasA*), GBAA1290 (*calY*), and GBAA1075 (exonuclease/exonuclease phosphotase) (Fig. 4-2A, and Tables 4-1 and 4-2). All genes that displayed differential regulation during exponential growth were negatively regulated by SinR.

The most highly regulated genes were located within the greater *sin* locus. The *calY*, *sipW* and *tasA* gene transcript levels were elevated 140-, 50-, and 58-fold respectively, in the *sinR* mutant strain indicating negative regulation by SinR. Note that probes representing gene GBAA1289, annotated as a pseudo-gene, were not represented in the array. In contrast to the genes 3' of *sinI/R*, expression of the upstream gene *inhA1* was elevated only 2.9-fold in the *sinR* mutant. Moreover, the difference in *inhA1* expression was only observed using RNA from exponential phase cultures, unlike the differences in *calY*, *sipW* and *tasA* expression which were apparent at exponential and stationary phases (Tables 4-1 and 4-2). The three most highly *sinR*-regulated genes outside of the expanded *sin* locus, GBAA1075 (exonuclease/exonuclease phosphotase), GBAA3645 (oligopeptide-binding protein *oppA*), and GBAA5262 (hypothetical exported repetitive protein), were negatively regulated 5-, 6-, and 8-fold, respectively (Tables 4-1 and 4-2).

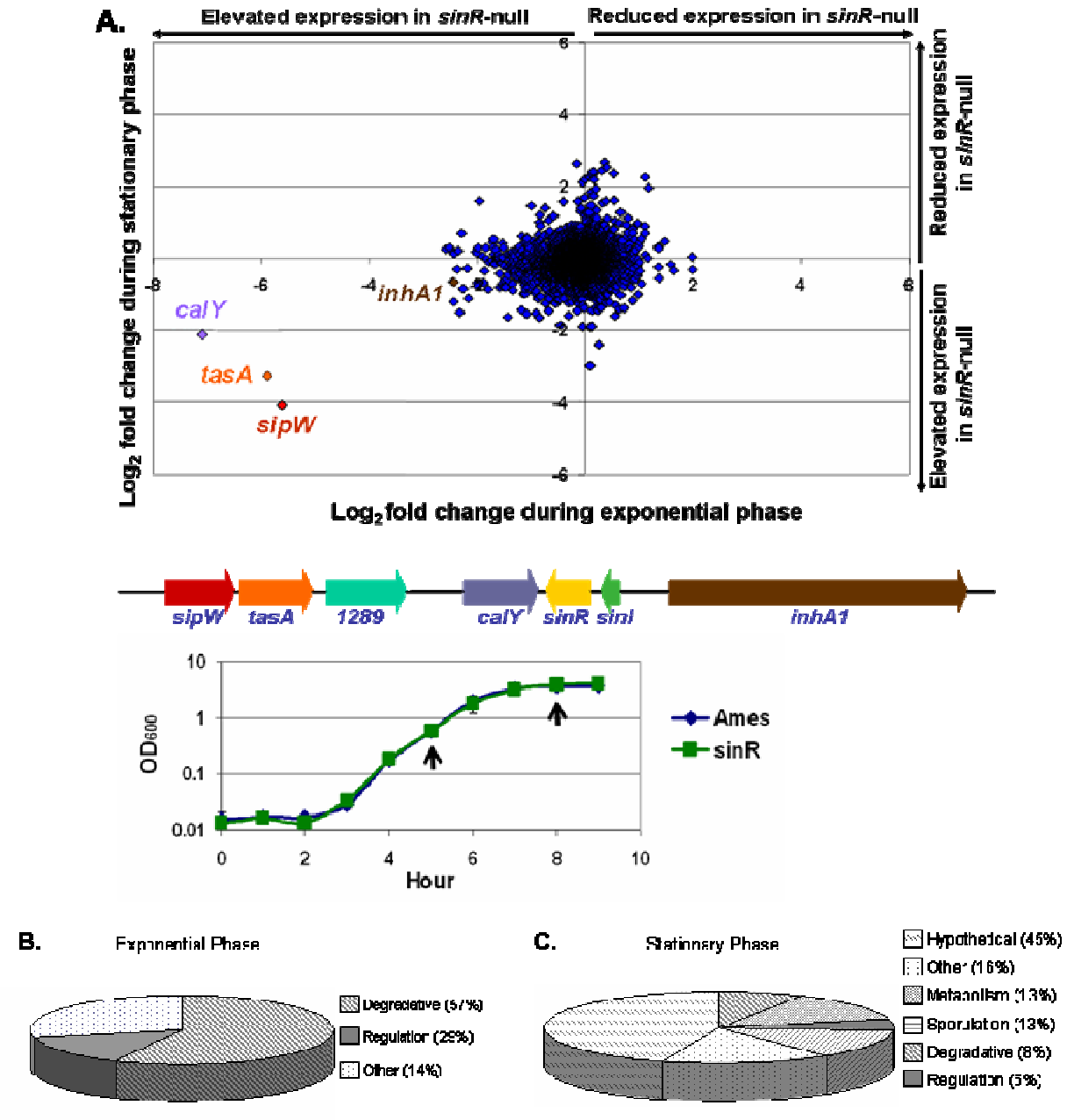

Figure 4-2. SinR-controlled transcriptome of *B. anthracis*. (A.) Scatter plot of ORFs differentially regulated in *sinR* mutant strain (UTA21) relative to the parent strain (Ames) as determined using expression microarray analysis. Data presented as $\log_2$ fold-change. The color of the gene in the schematic below the scatter plot corresponds to the data point. Below the schematic are the average growth of the parent (Ames) and *sinR* mutant strain (UTA21). +/- standard deviation are shown. Arrows highlight the two time points analyzed using expression microarray analysis. (B.) *sinR*-regulated genes during exponential growth phase grouped by annotated function. (C.) *sinR*-regulated genes during stationary growth phase grouped by annotated function.

Table 4-1. SinR-regulated genes in *B. anthracis* during the exponential phase of growth.

Gene (a)	Annotation (b)	d-chip fold-change	Excel fold-change	Array star fold-change	Ba consensus (c)	Bs homologue (d)
GBAA0031	Methyltransferase (EC 2.1.1.-)	2.49	2.21			
GBAA0032	Hypothetical protein with endo excinuclease domain	2.51	2.49			
GBAA0597	Transcriptional activator NprR		3.58	2.48		
GBAA0908	Oligopeptide-binding protein oppA	2.4	2.15			
GBAA0992	RNA polymerase sigma-B factor	2.18	2.21			
GBAA1075	Endonuclease Exonuclease phosphatase family protein	7.99	5	4.77	GTTATAA (-38)	N/A
GBAA1095	Hypothetical protein		2.89	2.1		
GBAA1166	*yajQ*	2.25	2.28			
GBAA1278	Hypothetical protein	2.11	2.1			
GBAA1284	Hypothetical protein	2.26	2.15			
GBAA1287	Signal peptidase I (EC 3.4.21.89) *sipW*	3.8	50	7.55	GTTATAA (-50) GTTATAT (-91)	*sipW*
GBAA1288	*tasA*	9.5	58.82	11.98		*tasA*
GBAA1290	*calY*	63.89	142.86	121.49	ATTCTCT (-63) GTTATAT (-69) GTTATAA (-120)	N/A
GBAA1292	*sinR*	-28.34	-48.43	-21.8	GTTCTTT (-76)	*sinR*
GBAA1295	*inhA1*	1.99	2.92	2.17	GTTATAA (-66)* GTTATAA (-77)*	N/A
GBAA1583	Cell division initiation protein DivIVA	2.33	3.08			
GBAA1959	Hypothetical protein		2.98	2.15		
GBAA2041	Oligopeptide-binding protein *oppA*	2.14	2.65			
GBAA2199	Hypothetical protein		3.64	2.32		
GBAA2399	Zn-dependent hydrolase	4.25	2.85			
GBAA2525	Hypothetical cytosolic protein	2.63	3.14			
GBAA3140	UvrC-like protein		3.95	2.21		
GBAA3146	Hypothetical protein	2.2	2.59			
GBAA3305	Transcriptional repressor *pagR*-like	3.27	3.22	2.04	GTTGTGT (-45) ATTATGT (-61) GTTATGT (-123)	N/A
GBAA3645	Oligopeptide-binding protein *oppA*	5.87	5.95	3.52	ATTATAT (-189)*	*oppA*
GBAA3647	Transcriptional regulator, LytR family	2.65	2.04			
GBAA3829	Phage transcriptional regulator, Cro CI family		5.68	2.34		
GBAA3830	Phage-related protein		3.56	2.39		
GBAA3845	SH3 domain protein 3D domain protein	3.73	2.15			
GBAA4162	GTPase	2.08	2.24			

GBAA4195	Transcriptional regulators, LysR family	3.56	3.31			
GBAA4197	Hypothetical protein	2.55	2.32			
GBAA4342	Hypothetical protein	6.3	5.41			
GBAA_pX01_101	Hypothetical protein	3.71	4			
GBAA_pX01_146	Transcriptional regulator *atxA*	2.44	3.28			
GBAA_pX01_199	GTP pyrophosphokinase (EC 2.7.6.5)	3.04	2.54			

(a) Ames ancestor strain annotated ORF
(b) Ames ancestor strain annotated description
(c) Putative *B. anthracis* SinR binding site of SinR-regulated genes (nucleotides upstream of the ATG). The asterisks indicate an inverted sequence and the number in parentheses notes the base pairs upstream of the translational start.
(d) *B. subtilis* homologue of *B. anthracis* SinR-regulated gene

Table 4-2. SinR-regulated genes in *B. anthracis* during the stationary phase of growth.

Gene (a)	Annotation (b)	d-chip fold-change	Excel fold-change	Array star fold-change	Ba consensus (c)	Bs homologue (d)
GBAA0061	Stage II sporulation protein E (EC 3.1.3.16)	2.60	2.24	2.39	ATTCTTA (-115)	*spoIIE*
GBAA0229	Hypothetical protein	3.74	2.02	3.04	ATTCTCT (-55)	N/A
GBAA0270	Guanine-hypoxanthine permease		-3.83	-2.31		
GBAA0288	*Pure*		-5.42	-2.87		
GBAA0289	*purK*		-2.90	-5.06		
GBAA0290	*purB*		-2.15	-2.78		
GBAA0291	*purC*		-3.29	-4.56		
GBAA0292	*purS*		-3.43	-5.31		
GBAA0293	*purQ*		-2.85	-4.58		
GBAA0294	*Purl*		-2.53	-4.78		
GBAA0295	*purF*		-2.61	-3.59		
GBAA0296	*purM*		-2.18	-6.24		
GBAA0297	*purN*		-2.21	-3.22		
GBAA0573	Hypothetical membrane spanning protein	4.06	3.79	5.29	GTTATTT (-71)	N/A
GBAA0574	Hyptothetical protein	11.37		9.09		
GBAA0977	Hyptothetical protein	3.44	2.05	2.69	GTTATAA (-31)	N/A
GBAA1020	Hyptothetical protein	2.84	2.06			
GBAA1075	Endonuclease Exonuclease phosphatase family protein	3.69	2.85	2.94	GTTATAA (-38)	N/A
GBAA1287	Signal peptidase I (EC 3.4.21.89) *sipW*	10.89	16.95	19.07	GTTATAA (-50) GTTATAT (-91)	*sipW*
GBAA1288	*tasA*	10.17	9.62	13.86		*tasA*
GBAA1290	*calY*	4.29	4.35	8.08	ATTCTCT (-63) GTTATAT (-69) GTTATAA (-120)	N/A
GBAA1292	sinR	-47.78	-50.12	-27.11	GTTCTTT (-76)	*sinR*
GBAA1481	DNA integration recombination inversion protein	3.40	3.76	4.02	ATTCTGT (-106)* GTTGTAT (-153)	*xerD*
GBAA1530	Stage IV sporulation protein A	2.54	2.02			
GBAA1577	Hypothetical protein	2.25	2.26	2.41	GTTCTTT (-200)	N/A
GBAA1578	Hypothetical protein	1.83	2.21			
GBAA1591	*Xpt*		-6.41	-3.00		
GBAA1592	*pbuX*		-5.14	-2.38		
GBAA1756	Cobalt-zinc-cadmium resistance protein *czcD*	1.98	2.21	2.10	GTTCTTT (-253)	*czcD*
GBAA2083	Macrolide glycosyltransferase (EC 2.4.1.-)	3.20	2.39	2.29	ATTATAT (-27)	*yojK*
GBAA2152	Hypothetical protein	2.34	2.27	2.01	GTTATAA (-173)* GTTATAA (-242)	*yvcN*
GBAA2287	polar chromosome segregation	2.35	2.71	2.36	ATTCTTT (-129)	*racA*

GBAA2521	Response regulator aspartate phosphatase inhibitor	2.14		2.15		
GBAA2619	Hypothetical protein		3.14	2.59		
GBAA2770	Hypothetical protein		-2.09	-2.34		
GBAA2771	Hypothetical protein	-2.03	-1.90	-2.24	GTTATTT (-37)*	N/A
GBAA2773	Dihydrolipoamide dehydrogenase (EC 1.8.1.4) *acoL*	-2.24	-2.31	-2.61		*acoL*
GBAA2774	Dihydrolipoamide acetyltransferase component of acetoin dehydrogenase complex (EC 2.3.1.-) *acoC*	-2.24	-2.42	-3.02		*acoC*
GBAA2775	Acetoin dehydrogenase E1 component beta-subunit (EC 1.2.4.-) *acoC*	-2.31	-2.53	-2.96		*acoB*
GBAA2776	Acetoin dehydrogenase E1 component alpha-subunit (EC 1.2.4.-) *acoA*	-2.38	-2.42	-2.30	ATTCTCA (-173)	*acoA*
GBAA2853	Cell division protein *divIC*	3.29	3.04	2.64	ATTGTGT (-21)* GTTATTT (-302)*	*divIC*
GBAA2982	Fructose-bisphosphate aldolase (EC 4.1.2.13)	3.21	2.00			
GBAA3834	Transcriptional regulator glnR, MerR family	-1.99	-2.01	-2.02	ATTGTGA (-218)*	*glnR*
GBAA3844	Hypothetical protein	3.07		3.20		
GBAA4043	RNA polymerase sigma-E factor	2.48	2.76	2.95	GTTATGT (-71)*	*sigE*
GBAA4044	Sporulation sigma-E factor processing peptidase (EC 3.4.23.-)	2.48	2.21	2.18	ATTATGT (-101)	*spoIIGA*
GBAA4202	Hypothetical protein	2.43	2.42	2.36	ATTCTTT (-17)* ATTGTTA (-54) GTTGTAA (-100)	N/A
GBAA4222	Hypothetical cytosolic protein	2.40	2.74	2.58	ATTCTTT (-69)	N/A
GBAA4342	Hypothetical protein	2.46	2.31	2.64	GTTCTGT (-197)	N/A
GBAA4410	Stage III sporulation protein AH	2.92	2.02	2.55		*spoIIIAH*
GBAA4411	Stage III sporulation protein AG	3.30	2.67	2.78		*spoIIIAG*
GBAA4412	Stage III sporulation protein AF		2.03	2.40	GTTATTA (-52)* GTTGTTT (-161)*	
GBAA4572	GTP pyrophosphokinase (EC 2.7.6.5)	2.37	2.47			
GBAA4657	Hypothetical membrane spanning protein	-2.07	-2.21			
GBAA4712	Hypothetical protein	-2.57		-2.20		
GBAA5210	Hypothetical protein	-2.33		-2.01		
GBAA5262	Hypothetical exported repetitive protein	9.65	8.00	6.53	ATTGTAT (-52)	N/A
GBAA5523	Hypothetical protein	2.36	2.42	2.40	ATTATAT (-32)*	N/A
GBAA5524	SpoIIQ		-2.28	-2.06		
GBAA5633	Prespore specific transcriptional activator *rsfA*	2.42	2.56	2.48	ATTGTTA (-70) ATTGTAA (-131)	*rsfA*
GBAA5640	Spore cortex lytic enzyme cwlJ		2.08	2.10		
GBAA_pX02_0017	Hypothetical protein	-4.04	-2.75	-2.29		N/A

GBAA_pX02_0019	Hypothetical protein	-4.57	-3.02	-3.34		N/A
GBAA_pX02_0020	Hypothetical protein	-3.95	-3.00	-2.18		N/A
GBAA_pX02_0021	Hypothetical protein	-4.49	-3.01	-2.42		N/A
GBAA_pX02_0023	Putative Type IV secretion system component	-3.94	-3.35	-2.52		N/A
GBAA_pX02_0024	Hypothetical protein		-2.48	-2.15		N/A
GBAA_pX02_0025	Hypothetical protein	-3.66	-4.78	-2.21		N/A
GBAA_pX02_0026	Hypothetical protein		-1.85	-2.13	GTTGTTT (-24)* ATTCTTT (-87)*	N/A

(a) Ames ancestor strain annotated ORF
(b) Ames ancestor strain annotated description
(c) Putative *B. anthracis* SinR binding site of SinR-regulated genes (nucleotides upstream of the ATG). The asterisks indicate an inverted sequence and the number in parentheses notes the base pairs upstream of the translational start.
(d) *B. subtilis* homologue of *B. anthracis* SinR-regulated gene

The majority of SinR-regulated genes were located on the chromosome, however a putative 26-gene operon on pX02 virulence plasmid, starting with GBAA_pX02_0028, was positively regulated by SinR during stationary phase growth. I note that not all of the genes of the putative operon were found in my analysis. While the genes in the operon are largely annotated as conserved hypotheticals, GBAA_pXO2_0023 is annotated as encoding a type IV secretion system protein (61, 118). *B. subtilis* does not carry homologues of the pXO2 SinR-regulated genes.

The SinR-regulated genes of *B. anthracis* are grouped according to annotated function in figures 4-2B and 4-2C. Only seven genes were identified as SinR-regulated during the exponential phase of growth, with the largest class of genes annotated as encoding proteins with degradative properties, including the secreted protease genes *inhA1* and *calY, sipW,* and the nuclease-encoding gene GBAA1075 (Fig. 4-2B and Table 4-1). Additional genes regulated by SinR during exponential growth phase include a regulatory gene (GBAA3305), and two genes that did not fall into any distinct category (the filamentous biofilm associated gene *tasA* and the ABC transporter gene *oppA*, GBAA3645). In contrast, 38 genes were determined to be SinR-regulated during the stationary growth phase, with the largest class of genes annotated as conserved hypotheticals (Fig. 4-2C). Additional classes of SinR-regulated genes during stationary phase are genes involved in sporulation (five, including *spoIIE* and *spoIIGA*), metabolism (five), degradation (three), and regulation (two) genes (Table 4-2).

The promoter regions of the 41 unique genes identified as being *sinR*-regulated in *B. anthracis* were analyzed for sequence similarity to the deduced SinR consensus sequence from *B. subtilis*, GTTCTYT (Tables 4-1 and 4-2; (24)). In *B. subtilis* the most conserved aspect of the consensus sequence is the spacing of the thymine residues (Fig. 4-3) (24). The promoter regions of SinR-regulated *B. anthracis* genes were searched for the conserved pattern, RTTXTXW, in which R is A or G and W is A or T. *B. anthracis* sequences with similarity to the *B. subtilis* binding site were identified and aligned using the sequence logo program WEBLOGO (Univeristy of CA, Berkley) to determine the putative SinR-binding motif for the SinR protein of *B. anthracis* (Fig. 4-3).

Figure 4-3. Putative SinR binding motif derived from SinR-regulated genes of *B. anthracis*. The putative consensus sequence for SinR binding, derived from sequences upstream of SinR-regulated gene in *B. anthracis* was aligned using the Weblogo program (University of CA, Berkley).

4.2.3. Comparison of the SinR regulons of *B. anthracis* and *B. subtilis*. In *B. subtilis*, the SinR regulon is comprised of at least 35 genes (7, 24, 25, 62, 78, 83, 88, 94, 99, 100, 152). Eighteen of these genes were identified in a transcriptional profiling experiment comparing *sinR*- to *sinI*-null mutants during exponential phase of growth (24). My transcriptional profiling data indicate only limited convergence of SinR-regulated genes from *B. anthracis* and *B. subtilis* (Fig. 4-4). Interestingly, approximately half of the genes controlled by SinR in each species do not have homologues in the other species (e.g. 21 genes that are SinR-regulated in *B. anthracis* have no homologue in *B. subtilis*). Of the 35 genes regulated by SinR in *B. subtilis*, and the 41 genes regulated by SinR in *B. anthracis*, only four genes were common to both regulons (*tasA*, *sipW*, *spoIIE*, and *spoIIG*). Surprisingly, 16 SinR-regulated genes of *B. subtilis* have homologues in *B. anthracis* that did not exhibit differential expression in my transcriptional profiling experiment. Likewise, 17 SinR-regulated genes of *B. anthracis* have homologues in *B. subtilis* that have not been reported as SinR–controlled in that species (Fig. 4-4). As the putative SinR-binding motif in *B. anthracis* is highly similar to the *B. subtilis* SinR-binding consensus sequence (Fig. 4-3), it is unlikely that variation in the binding sequence accounts for the lack of convergence of the two SinR regulons.

4.2.4. Specific binding of rSinR to promoter DNA. To determine if *B. anthracis* SinR binds specifically to promoter regions of target genes, Electrophoretic Mobility Shift Assays (EMSAs) were performed using rSinR purified from *E. coli.* DNA probes corresponded to sequences upstream of the SinR-regulated genes *calY*, *sipW*, and *inhA1*, and a gene unaffected by *sinR*, *npr599* (Tables 4-1 and 4-2). When 10nM or higher rSinR was present in the binding reaction, the gel mobility of the *calY* and *sipW* promoter probes was retarded compared to the free probe (Fig. 4-5). Probes representing the non-SinR-regulated *npr599* promoter and the weakly (2.9-fold) regulated *inhA1* promoter were not shifted, even when the rSinR concentration was increased to 4.2μM (data not shown). The analyses indicate that the *B. anthracis* SinR is a DNA-binding protein that binds specifically to the promoter regions of the highly-regulated target genes *calY* and *sipW*. Given that *inhA1* expression is elevated in a *sinR*-null mutant strain, as determined from the microarray data as well as quantitative RT-PCR (data not shown), I posit that regulation of *inhA1* by SinR is either

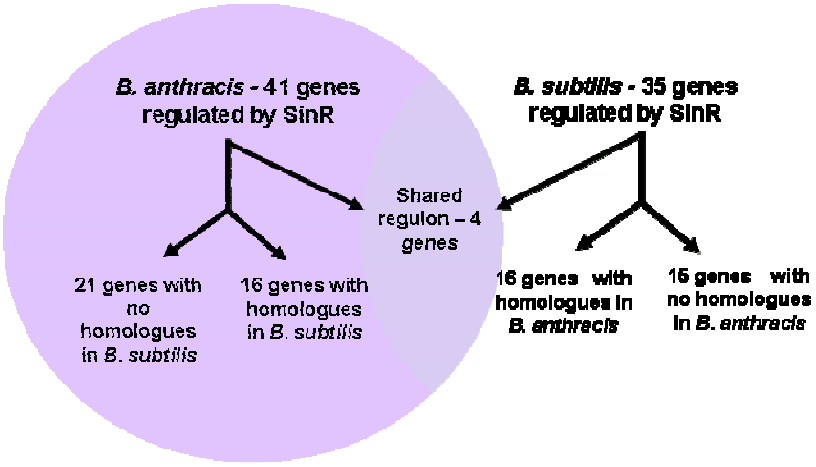

Figure 4-4. Comparison of the SinR regulons of *B. anthracis* and *B. subtilis*. Total SinR-regulated genes are indicated (exponential and stationary growth phases) from *B. anthracis* transcriptional profiling experiments (this study) and from *B. subtilis* literature (7, 24, 25, 62, 78, 83, 88, 94, 99, 100, 152).

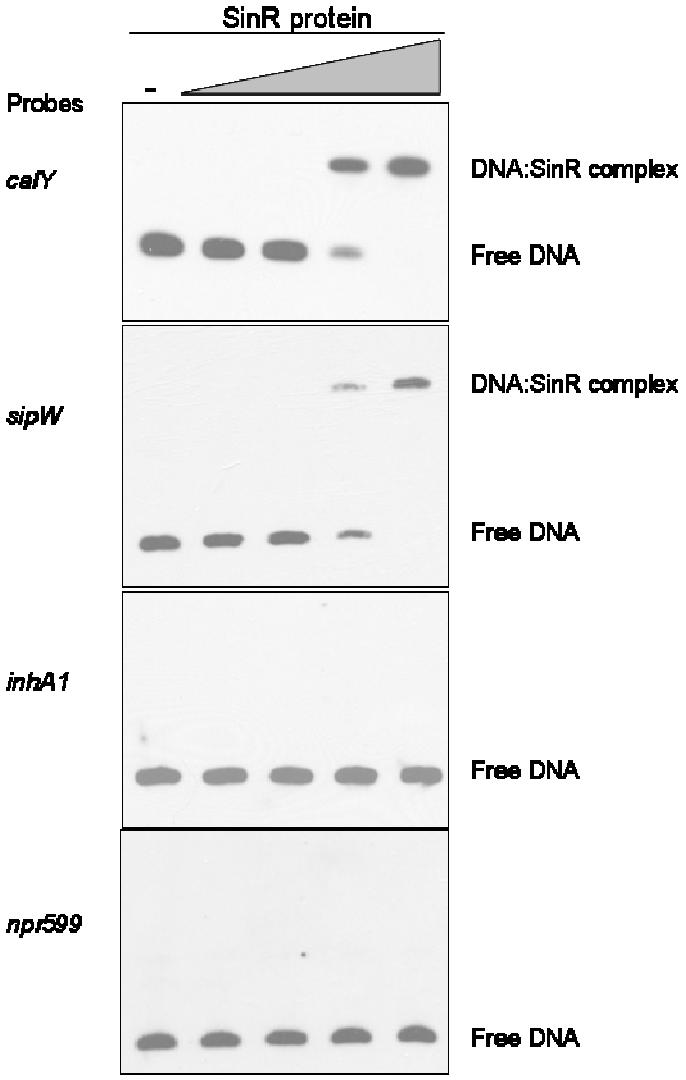

Figure 4-5. SinR specifically binds the promoters of *sinR*-regulated genes *calY* and *sipW*. EMSAs were performed using 0.1nM of probe DNA and increasing concentrations of purified rSinR protein, 0nM, 0.4nM, 2nM, 10nM, and 50nM. *npr599* promoter probe was used as a negative control.

Indirect or the affinity of SinR for the *inhA1* promoter is greatly diminished compared to SinR affinity for the highly-regulated *sipW* and *calY* promoters.

4.2.5. *sin* control of secreted proteases. Regulation of genes encoding the proteases camelysin and InhA1 by SinR is intriguing given that InhA1 has been implicated in *B. anthracis* virulence, and that homologues of camelysin produced by *B. cereus* and *B. thuringiensis* are active against host substrates (22, 23, 26-28, 59, 79, 106). Negative regulation of *inhA1* by SinR is relatively weak (2.9-fold) and InhA has been reported to be an abundant protein in the *B. anthracis* secretome whereas *calY* is repressed 140-fold by SinR and does not appear to be a major component of the *B. anthracis* secretome (22).

I asked if InhA1 and camelysin protein levels reflect the effects of SinR on *inhA1* and *calY* transcription. The parent strain (7702) and *sinR*-, *sinI*-, and *sinI/R*-null mutants were cultured and cell pellets and supernates were collected at exponential ($OD_{600} \approx 1.6$), transition ($OD_{600} \approx 3.1$) and stationary ($OD_{600} \approx 3.1$) phases of growth. Protein samples were assessed for camelysin, InhA1, and TasA (the product of a SinR-controlled gene that is common to *B. subtilis* and *B. anthracis*) using Western hybridization (Fig. 4-6). Consistent with the transcriptional profiling data, the *sinR* mutant produced substantially higher levels of camelysin and TasA compared to the parent strain (Fig. 4-6). Moreover, camelysin and TasA levels in the *sinI* mutant were less abundant compared to the parent strain. These results are consistent with the *B. subtilis* model in which SinR regulates target gene expression and SinI inhibits SinR activity (155). Unlike the results obtained for camelysin and TasA, InhA1 levels did not correlate with the transcriptional profiling data. Steady state levels of InhA1 were detected in the supernate of the parent strain during the stationary phase of growth, but surprisingly, InhA1 protein levels were decreased in the *sinR* mutant and elevated in the *sinI*-null mutant (Fig. 4-6). These experiments were also performed using a different strain background (Ames cured of pXO1 and pXO2) and identical results were obtained (data not shown). Taken together the data are indicative of a gene product under post-transcriptional regulation.

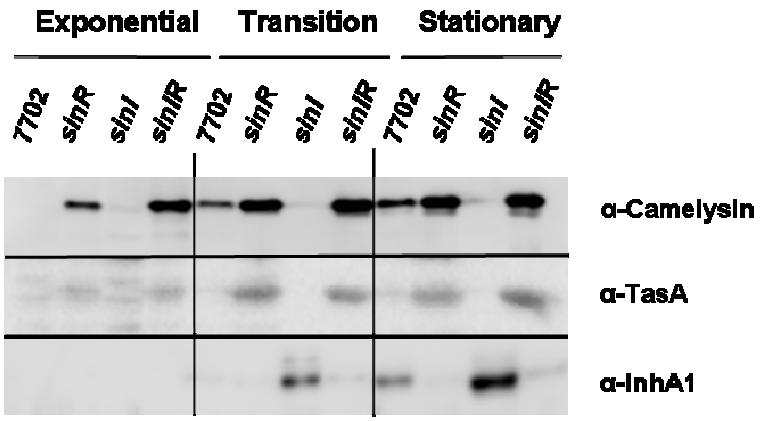

Figure 4-6. Effects of *B. anthracis sinR* and *sinI* on Camelysin, TasA, and InhA1. The parental strain 7702 and *sinR*-, *sinI*-, *sinIR*-mutnant derivatives (UT315, UT365, and UT371, respectively) were cultured in NBY and samples were taken during exponential phase, transition phase, and stationary phase of growth. Cell pellets were sampled to assess camelysin and TasA, and proteins in the culture supernatant were sampled to assess InhA1. Western hybridization experiments were performed with camelysin, TasA, and InhA1 specific antibodies.

Further examination of InhA1 and camelysin levels during culture of the parent strain revealed that InhA1 and camelysin levels are inversely correlated during stationary phase. As camelysin levels decrease, InhA1 levels increase (Fig. 4-7A). To obtain a better understanding of the relationship between camelysin and InhA1, individual isogenic protease mutant strains were created and InhA1 and camelysin levels in the culture supernatant and cell pellet, respectively, were assessed using Western blot analysis. As shown in Fig. 4-7B, in early stationary phase, InhA1 levels were significantly higher in the *calY* mutant strain than in the parent strain, while camelysin levels were unchanged in the absence of *inhA1*. To negate the effects of *sinIR*-mediated control of *calY* on InhA1 levels, the *calY* gene was expressed from an IPTG-inducible promoter in a *calY*-null mutant background. Levels of InhA1 and camelysin produced in the presence of increasing concentrations of IPTG were determined using Western blot analysis (Fig. 4-7C). Again, camelysin and InhA1 protein levels were inversely related, as camelysin levels increased InhA1 levels decreased. Taken together, these results indicate that InhA1 is degraded in supernates of cells in which camelysin synthesis is derepressed.

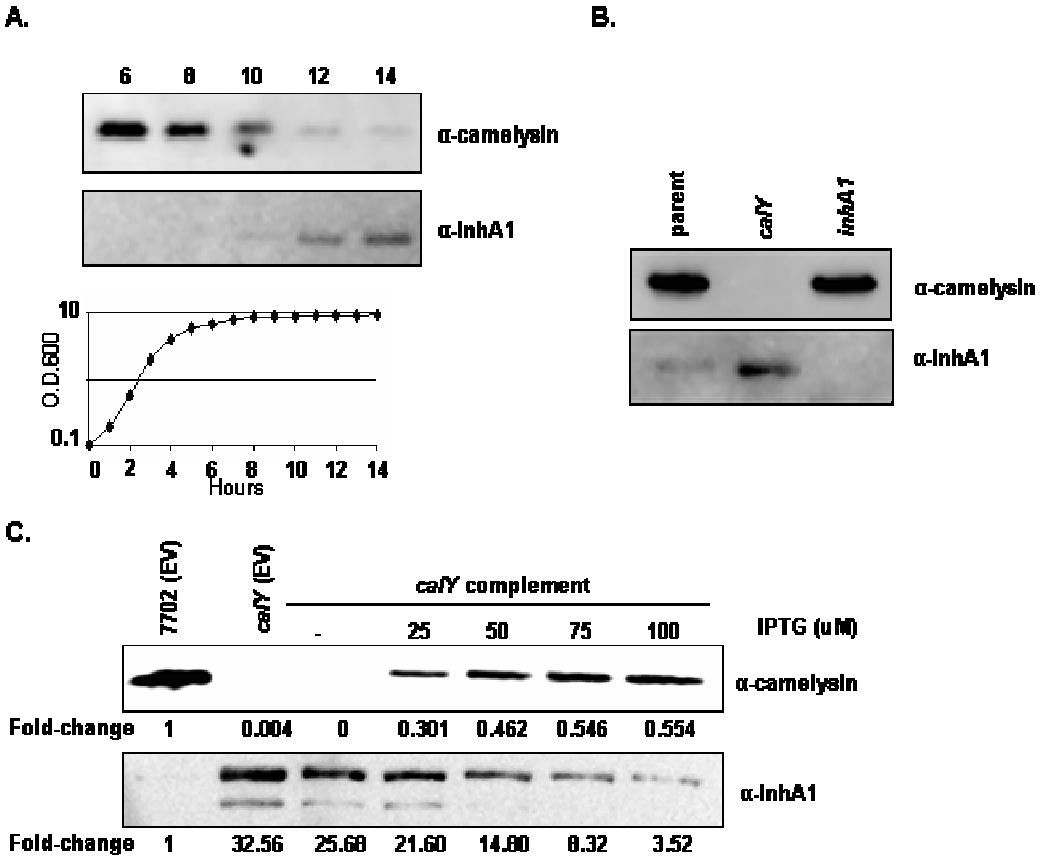

Figure 4-7. camelysin controls the level of InhA1 in culture supernates. (A.) Endogenous InhA1 and camelysin protein levels are inversely related. Parental *B. anthracis* strain 7702 was cultured in NBY and samples were taken every 2 hours, beginning at the transition phase of growth. Shown are Western blots using antibodies against camelysin and InhA1. A corresponding growth curve of 7702 is included as a reference. (B.) InhA1 is up-regulated in a *calY* mutant strain, however camelysin levels are unaffected in an *inhA1* mutant strain. Shown are Western blots of early stationary phase samples from the parent and *inhA1*- and *calY*-mutant derivatives, UT345 and UT356, respectively, using antibodies to InhA1 and camelysin. (C.) Levels of camelysin produced by *B. anthracis* inversely correlate with InhA1 levels in the supernatant. InhA1 and camelysin levels were detected in parent and *calY* mutant strains carrying empty vector (EV; pUTE973) and the *calY* mutant strain carrying the IPTG inducible *calY* (pUTE980). Western blot analysis used antibodies specific to InhA1 or camelysin. The abundance of *calY* and *inhA1* relative to the parent strain, 7702 containing EV, were determined using densitometry analysis, the data are presented as fold-change.

4.3. Discussion

The common physiology of *Bacillus* species reflects their genomic synteny and gene sequence similarity (118, 140). Multiple metabolic and regulatory loci, studied primarily in the archetype species *B. subtilis*, have functional homologues in other *Bacillus* species. For these spore-forming bacteria, shared systems controlling cell development are particularly notable (8, 15, 38, 39, 49, 93, 95, 104, 132, 160). Here I examined function of the *sinIR* locus in *B. anthracis*. The comparable locus in *B. subtilis* was first characterized as part of the extensive sporulation network (55, 137). Subsequent studies revealed that *B. subtilis* SinIR plays a regulatory role in multiple growth-phase–associated phenotypes (24, 56, 62, 94, 99). Results reported here reveal that the *B. anthracis sinIR* locus and the associated regulon exhibit some similarity to those of *B. subtilis*, but also significant differences.

The SinIR regulatory system is comprised of the DNA-binding protein SinR, that controls transcription of target promoters, and the SinR antagonist SinI, which when bound to SinR prevents its association with DNA (5). Given the similarity of the SinR and SinI amino acid sequences and data generated in this study, it is likely that the molecular mechanisms for function of the *B. anthracis* and *B. subtilis* proteins are equivalent. I have shown that *B. anthracis* SinR has specific DNA-binding activity for highly SinIR-regulated promoters, that SinIR-regulated genes of *B. anthracis* possess promoter DNA sequences with similarity to the SinR recognition sequence established in *B. subtilis*, and that a *B. anthracis sinI*-null mutant displays the expected phenotypes for SinR-controlled genes.

Differences in the SinR regulons of *B. anthracis* and *B. subtilis* appear to be primarily due to disparities in target genes encoded by each species. Approximately one half of the genes reported to be SinR-regulated in either *B. anthracis* or *B. subtilis* do not have homologues in the other species. Several SinIR-regulated genes of *B. subtilis* are associated with species-specific phenotypes including biofilm formation, motility, and competency (7, 62, 88, 94). In *B. subtilis*, SinIR negatively controls the biofilm-associated extrapolysaccharide genes (*eps*) and the biofilm structural protein gene *yqxM* (24). *B. anthracis*, which does not readily form biofilms, is missing these *sinIR*-regulated genes. Likewise, *B. anthracis* is non-motile and does not carry a homologue of the *B. subtilis* SinIR-regulated *sigD* gene (88), which encodes a transcriptional regulator of *B. subtilis* motility genes. Two key competency genes, *comS* and *srf*, are SinIR-regulated in *B. subtilis*

(94), but absent in *B. anthracis*. Finally, in *B. subtilis* a *sinR* parologue, *slrR,* has been demonstrated to work in tandem with SinR to regulate select targets (17, 18), however, a *slrR* homologue is not apparent in *B. anthracis*.

In *B. subtilis* and *B. anthracis*, several genes of the SinR regulon encode degradative enzymes, some of which are present in one species but not the other. Among these are the *B. subtilis* gene *aprX*, encoding a serine protease (152) and the *B. anthracis* genes *inhA1* and *calY,* encoding the InhA1 and camelysin secreted metalloproteases, respectively. The *inhA1* and *calY* genes are present in the *B. cereus* group members, *B. anthracis*, *B. thuringiensis*, and *B. cereus*. InhA1 was first identified as a *B. thuringiensis* protease that promotes survival of the bacterium in the hemolymph of infected insects (45, 136). Subsequently it was shown that InhA1 degrades the cecropin and attacin insect antimicrobial peptides (33). Lereclus and coworkers (116) further demonstrated a link between InhA1 and the immune response by showing that InhA1 enhances escape of *B. thuringiensis* from macrophages. It is notable that in *B. thuringiensis*, overexpression of *sinR* results in repression of *inhA1* expression (58), in agreement with the *B. anthracis* data revealing increased *inhA1* expression in a *sinR*-null mutant. Similar to its orthologue in *B. thuringiensis*, InhA1 from *B. anthracis* cleaves a number of host proteins, including proteins involved in the coagulation cascade (including von Willebrand Factor and Pro-Thrombin) as well as extracellular matrix proteins (26-28, 79). In addition InhA1 from *B. anthracis* alters the abundance of over half of proteins in the culture supernatant either directly, as in the case of the anthrax toxin proteins, or indirectly through its activity within a proteolytic regulatory cascade (see Chapter III).

Camelysin, the other SinR-regulated secreted protease of *B. anthracis*, was first described as a casein-lytic protein of *B. cereus* (59). Substrates of *B. cereus* camelysin include host cell matrix proteins such as collagen and actin, as well and proteins of the coagulation cascade (52). A camelysin homologue in *B. thuringiensis* has been reported to activate Cyt2Ba, a protein toxin that exhibits activity against the Dipteran order of insects (106). Function of the *B. anthracis* camelysin has not been described previously.

The degree of SinR-mediated transcriptional control of the *B. anthracis inhA1* and *calY* genes differs considerably. The *calY* gene is the most highly over-expressed in the sinR-null strain compared to the parent and SinR directly binds the gene's promoter region;

while *inhA1* is only weakly regulated by SinR and I was unable to demonstrate binding of SinR to the *inhA1* promoter region. The weak regulation of *inhA1* by SinR is puzzling considering that the *inhA1* promoter region harbors a sequence (GTTATAA) that is similar to the SinR recognition sequence established in *B. subtilis* (GTTCTYT) (24) and to sequences in the promoter regions of the highly-regulated *B. anthracis* genes. In *B. subtilis* and *B. anthracis* the number of putative SinR-binding sites upstream of individual SinR-regulated genes varies from one to four. SinR may have a weak affinity for the *inhA1* promoter region due to the spacing or number (two) of putative binding sites. The highly SinR-regulated promoters examined in my study contain 1-3 putative binding sites (Table 4-1). Alternatively, or in addition, the nucleotide mismatches in the recognition sequence may result in the weak regulation of *inhA1* by SinR. Finally, nucleotides outside of the 7bp putative binding site may also contribute to the strength of SinR binding.

Although SinR has a relatively small affect on *inhA1* transcription, it has a large effect on InhA1 levels in culture supernates. The data suggest that increased InhA1 in cultures of a *sinI*-null mutant is associated with SinR-mediated repression of *calY* transcription. When *B. anthracis* is cultured in rich complex media, InhA1 is one of the most abundant proteins in stationary phase culture supernates, while camelysin levels are relatively low (22). In a *sinR*-null mutant, InhA1 levels are reduced dramatically and camelysin levels are increased. Comparison of InhA1 and camelysin levels revealed an inverse relationship between InhA1 and camelysin, with InhA1 levels increasing as camelysin levels decrease. Moreover, when *calY* expression was artificially induced, a decrease in InhA1 was observed. Taken together, my data support a model in which InhA1 is degraded by camelysin when *calY* gene expression is derepressed.

InhA1 is a major component of the *B. anthracis* secretome that appears to degrade host and bacterial substrates with relatively little specificity (22, 26-28, 79). A system in which InhA1 levels are controlled transcriptionally and post-translationally in response to the growth-phase–associated activity of SinR suggests that limitation of InhA1 abundance is beneficial in certain environments. Interestingly, in *B. thuringiensis inhA1* transcription is controlled by another growth-phase associated regulator, AbrB (58). The weak nucleotide sequence conservation of the reported AbrB recognition site (142, 159) makes it difficult to predict whether the *inhA1* gene is similarly controlled by AbrB in *B. anthracis*.

Nevertheless, involvement of AbrB in addition to SinR in InhA1 expression would provide an interesting link between the protease and well established virulence factors of the bacterium. In *B. anthracis*, AbrB controls transcription of the pleotropic virulence gene regulator *atxA* (127, 142). Future studies addressing the affects of transition state regulators such as SinIR on temporal expression of virulence genes in the context of infection and during *B. anthracis* growth in mammalian hosts and in other environments will further my understanding of target gene function.

The role established here for camelysin in the regulation of InhA1 provides evidence for an early step in the proteolytic regulatory cascade in *B. anthracis* (see Chapter III). Defining the progression of events of the regulatory cascade is necessary to obtain a fundamental understanding of the post-translational regulation of the extracellular proteins of *B. anthracis*. The amplifying nature of a regulatory cascade provides the possibility that regulation by one of the cascade proteases has implications on processes from bacterial development to virulence.

Chapter V

Characterization of the growth and virulence of an *inhA*-null strain of *B. anthracis*

5.1. Introduction

B. anthracis is a spore forming organism and the causative agent of anthrax. Three forms of human anthrax infection have been described, each of which is characterized by the route of infection, cutaneous (the most common), inhalational (highest lethality rate), and gastrointestinal (139). In each case the infectious form of *B. anthracis* is the spore. Upon exposure to nutrients in the host the spore germinates and the vegetative form of *B. anthracis* spreads the disease either locally or systemically (139). While cutaneous anthrax infections occur at higher frequency it is the inhalation form of disease that draws the most attention, in part due to the greater lethality rate associated with inhalational anthrax infections. The working model for the progression of inhalational anthrax can be broken down into the following stages (Fig. 1-1): association of the spore with a phagocyte, spore germination, dissemination of vegetative cells, and the production of virulence factors (19). Without rapid treatment with antibiotics dissemination of the organism commonly results in sepsis, meningoencephalitis, and death (57). It remains contentious whether the spore germinates within the lung, after phagocyte uptake, or upon transport to the regional lymph nodes. An additional dissemination route is emerging as a secondary or alternative to the phagocyte-based model in which spores transverse the epithelial cell membrane prior to dissemination from the lung (125). The anthrax toxin receptors (ANTRX1 and ANTRX2), cell-surface proteins that bind anthrax toxin protein leading to an alteration of host cell signaling pathways induced by specific toxin activities, are expressed by macrophages as well as epithelial cells located at each initial site of *B. anthracis* infection (lung, skin, intestine) (6, 9). Thus, some spores may germinate prior to dissemination resulting in production of toxin at the initial infection site stimulating a change in host cell signaling.

The cellular innate immune response to inhalational anthrax infection includes important roles for dendritic cells and neutrophils, however macrophage are thought to be the key immune cell of the infection process (11, 32). Mouse-derived primary macrophages and dendritic cells infected with *B. anthracis* result in the release of the important pro-inflammatory cytokines IL-1, TNF-α, and IL-8 (11, 29, 113). Furthermore, mice chemically depleted of macrophages show increased susceptibility to *B. anthracis* (32), emphasizing the importance of macrophages in controlling *B. anthracis* infection. Association of *B. anthracis* spores with the macrophage is promoted through an interaction between the host

cell Mac-1 integrin and the *B. anthracis* exosporium protein BclA, an interaction that leads to phagocytosis of the spore (109). Pathogen-induced phagocytosis through macrophage cell-surface integrin binding is a common mechanism of pathogen:macrophage association (65, 75, 144), and it is possible that additional *B. anthracis* surface proteins may also promote this mechanism of entry.

Throughout infection *B. anthracis*, and other pathogens, are exposed to the activity of small cationic peptides, termed antimicrobial peptides (AMPs). AMPs are produced by a variety of cell types, including neutrophils and macrophages. Classically, AMPs are grouped based on structure and fall into three main classes, defensins (α and β), cathelicidins, and histanins (35, 63). Although AMPs such as β-defensin 1 (HBD-1) and the human cathelicidin LL-37 are constitutively expressed in some cell types, the expression of other AMPs can be up-regulated in response to pro-inflammatory cytokines (35, 146). The primary antibacterial mechanism of AMPs is membrane permeation via pore formation (35, 148), leading to bacterial cell lysis. In addition, some AMPs have chemoattractant activity towards immune cells, and are able to activate dendritic cells, induce granulocyte degranulation, and modulate phagocyte activity (35, 63, 148). *B. anthracis* is susceptible to LL-37 and possibly other AMPs (146).

Survival of *B. anthracis* in the host is in part due to the immune evasion activities of anthrax toxin and of several secreted proteases. Studies into the activity of Lethal Factor (LF) indicate that LF disrupts MAPK signaling pathways resulting in cell cycle disruption or apoptosis (103). The secreted protease Immune Inhibitor A1 (InhA1) has also been implicated in enhancing *B. anthracis* virulence, through the cleavage of an array of substrates. *In vitro*, purified InhA1 processes extracellular matrix proteins, including fibronectin and collogen, as well as proteins involved in the coagulation cascade, such as plasmin inhibitors and prothrombin (28, 79). InhA1 also induces the expression of plasminogen activator inhibitor (PAI-1) in mice injected with purified InhA1 (26). This modulation of coagulation proteins in the host results in an increase in the rate of clotting, as demonstrated in human blood incubated with either parent or an *inhA1* mutant strain (79). The effects of InhA1 on host proteins may be particularly pertinent as InhA1 is one of the most abundant proteins secreted by *B. anthracis* in laboratory media, and is immunoreactive with the sera of infected animals (22, 23), suggestive of *in vivo* expression. *B. anthracis*

encodes a homologue of *inhA1*, *inhA2*, whose gene product shares 67.7% amino acid identity to InhA1. In contrast to InhA1, InhA2 has not been detected in secretome analysis of this organism. However, InhA2 is detected by the immunesera of *B. anthracis*-infected animals and therefore is likely produced in the host (53).

Here, I identify that *inhA1* and *inhA2* are transcribed under standard laboratory conditions and, perhaps of greater interest with respect to *B. anthracis* virulence, also under toxin-inducing conditions. The InhA proteins may function both early and late during infection, as evident by an *inhA1/inhA2*-null mutant strain showing decreased association with macrophage-like cells (an early stage of infection), and attenuated lethality in a mouse intra-tracheal model of infection (early and late). I also provide evidence that one mechanism by which the InhA proteases enhance *B. anthracis* virulence is through inhibition of the cathalicidin class of AMPs.

5.2. Results

5.2.1. Homology of InhA1 and InhA2 in *B. anthracis*. Alignment of the predicted amino acid sequences of InhA1 and InhA2 of *B. anthracis* indicate that the two proteins share high levels of homology (Fig. 5-1). Identical regions of sequence between InhA1 and InhA2 include the conserved zinc binding motif HEXXH (Fig. 5-1), a characteristic of zinc metalloproteases (64, 69). Despite high levels of amino acid identity the two InhA proteins are not thought to be functionally redundant as several putative functional domains differ between the proteins (Fig. 5-1). InhA2 but not InhA1 has a predicted lipobox at the amino-terminus of the protein indicating that InhA2 may be a lipoprotein, and as such may be retained at the *B. anthracis* cell surface. In addition, while both InhA1 and InhA2 contain putative integrin-binding motifs, InhA2 contains an arginine-glycine-aspartate (RGD) motif while InhA1 has a conserved substitution in the motif resulting in a KGD sequence. The RGD motif is a binding ligand of an array of distinct integrins, cell surface receptors that can be specific to diverse eukaryotic cell types including macrophages, and binding can alter cell signaling and induce phagocytosis (73, 74, 124, 144). The KGD motif has only been described as a ligand for $\alpha II_b\beta III$ integrins, an integrin specific to platelet cells (124). Thus, the different predicted motifs present in InhA1 and InhA2 indicate that the two proteins may have distinct functions during infection.

5.2.2. Expression analysis of the InhA proteases. InhA1 is highly abundant in the stationary phase secretome of *B. anthracis* grown in laboratory media (22). In addition, InhA1 is present at a higher concentration in germinating spores than in dormant spores (71). InhA2 has not been detected in *in vitro* secretome analyses of *B. anthracis* (2, 28), however antibodies in the sera of infected hosts react with InhA2, indicating that InhA2 is expressed *in vivo* (53, 87). To begin to investigate differences in expression of the two proteins *inhA1* and *inhA2* transcripts levels were assessed using a quantitative RT-PCR approach. Transcript levels were assessed during growth in nutrient rich media at 37°C, both in air and in the presence of sodium bicarbonate with 5% CO_2 (toxin-inducing conditions) (Fig. 5-2). My data showed that *inhA1* transcripts were significantly more abundant than *inhA2* transcripts under each of the conditions tested (Figure 5-2A). In addition, *inhA1* was differentially expressed when cells were grown under atmospheric and toxin-inducing

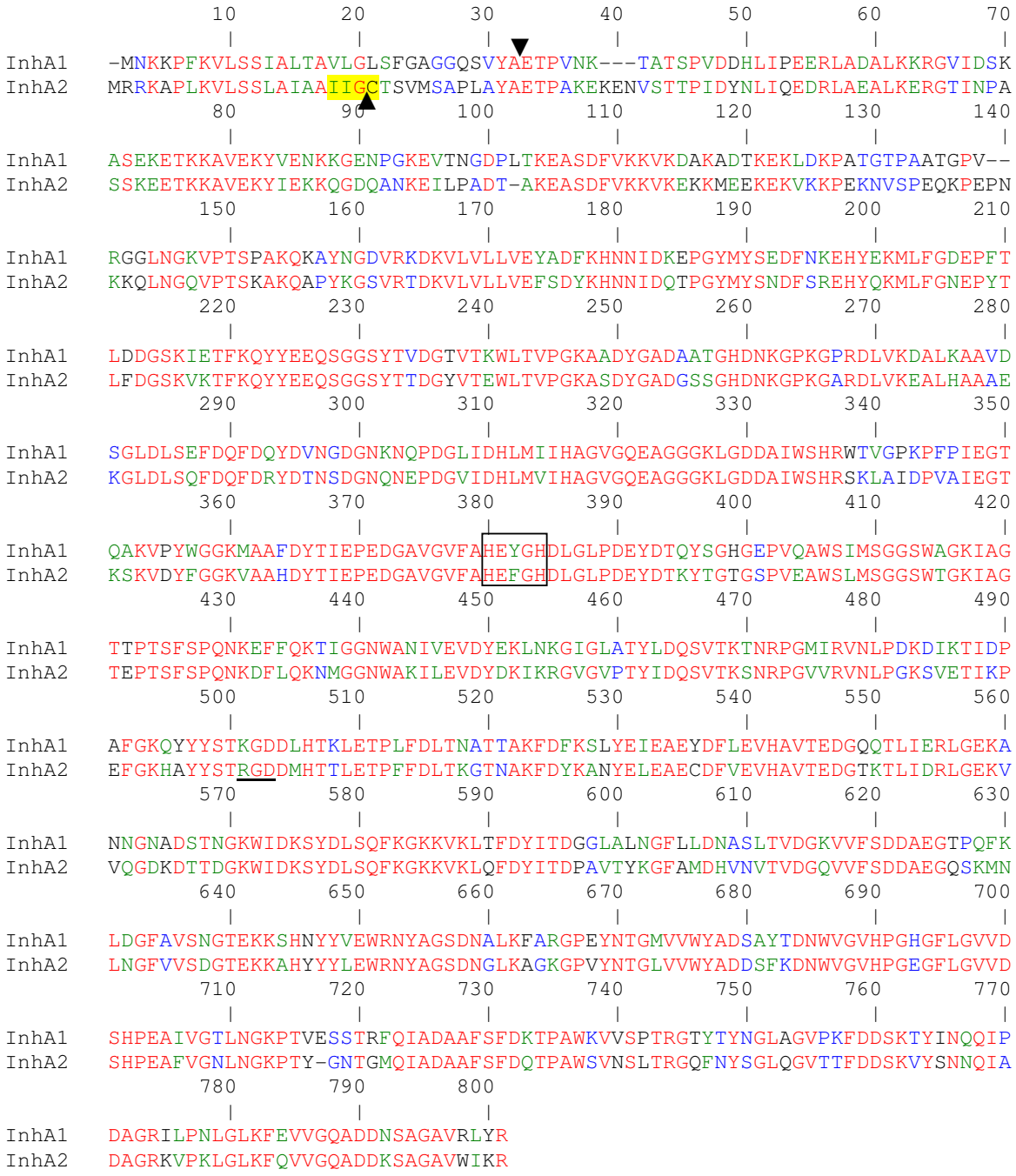

Figure 5-1. Alignment of InhA1 and InhA2 predicted amino acid sequences. Ames ancestor sequences aligned with the ClustalW program (31, 145). Residues of the conserved zinc binding motif are indicated in the boxed sequence. The predicted lipobox of InhA2 is highlighted in yellow and the integrin binding motifs are underlined. Conservation of residues are color coded; red are identical (67.7%), green are strongly similar (16%), blue are weakly similar (8.1%), and black are different (8.2%).

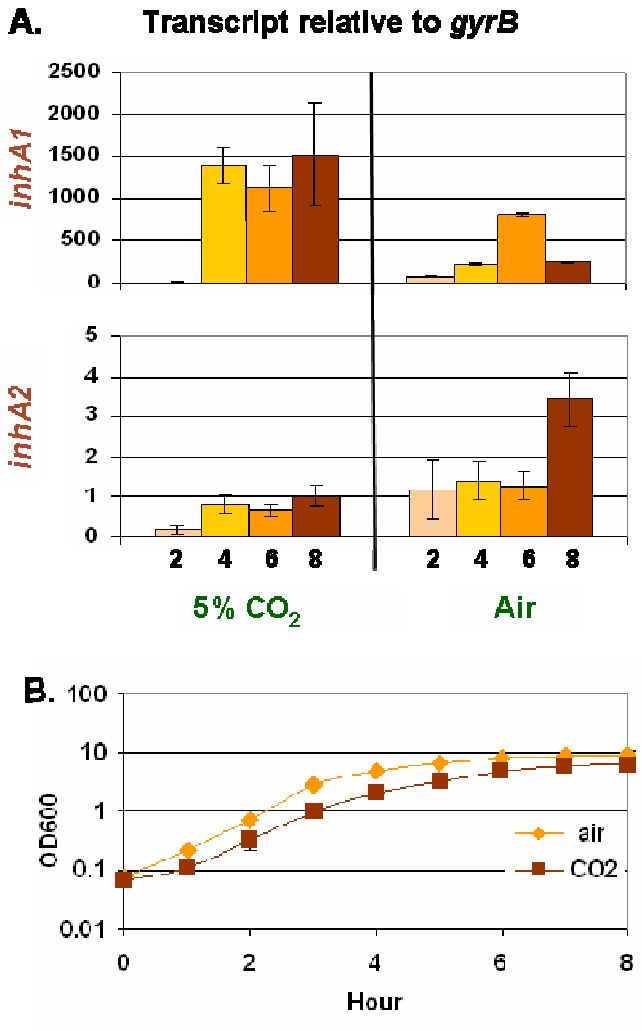

Figure 5-2. Expression of *inhA1* is dramatically higher than *inhA2*. Transcripts were measured from samples taken during growth in air and under toxin-inducing conditions (5% CO_2 and sodium bicarbonate). (A.) Quantitative RT-PCR analysis of *inhA* transcript levels relative to the housekeeping gene *gyrB* from exponential to stationary phases of growth. (B.) Growth of *B. anthracis* in nutrient rich media in air and under toxin-inducing conditions.

conditions. Increased transcript abundance under toxin-inducing conditions is a strong indicator that InhA1 is expressed in the host. While *inhA1* transcript levels correlate with protein expression patterns during growth under toxin-inducing conditions (Fig. 5-2A and 4-4), transcription and steady state protein levels are uncoupled when cells are grown in air. *inhA1* transcript levels peak in early stationary phase of growth (T6; Fig. 5-2A), however, InhA1 does not accumulate in the culture supernatant until late stationary phase (Fig. 4-6A), supporting the hypothesis that InhA1 levels are regulated post-transcriptionally.

5.2.3. Characterization of *inhA* mutant strains. To facilitate analysis of the contribution of InhA1 and/or InhA2 to *B. anthracis* virulence mutant strains lacking in one or both proteases were created. The *inhA* genes were deleted using standard techniques that resulted in replacement of the *inhA* genes with antibiotic resistance cassettes (see chapter 2, section 3). Mutant strain construction was verified using PCR and sequencing.

The growth of the *inhA1*, *inhA2,* and *inhA1/inhA2* mutant strains was assessed in air and under toxin-inducing conditions; each mutant was found to have comparable rates of growth to the parent strain (data not shown). As InhA1 protein levels are elevated in the germinating spore (71), the germination rates of the parent and *inhA* mutant strains were assessed, using heat sensitivity, a characteristic of dormant spores, as a measure of germination (154). Similar germination rates were found for each of the strains tested (data not shown). To further assess the effects of the InhA proteins on the lifecycle of *B. anthracis* the sporulation efficiency of the parent and *inhA* mutant strains were assessed. While each of the mutants readily sporulated in sporulation medium (PA medium, phage assay medium) or nutrient yeast broth (NBY), the *inhA1* mutant strain exhibited a sporulation defect in defined medium (CA medium, Casamino Acids medium) (Fig. 5-3). The difference in sporulation is apparent in micrographs; by 16 hours of growth the parent strain had been engulfed by the mother cell, forming light retractile sporangia (Fig. 5-3), while the *inhA1* mutant strain did not reach the same stage in sporulation until 30 hours (data not shown).

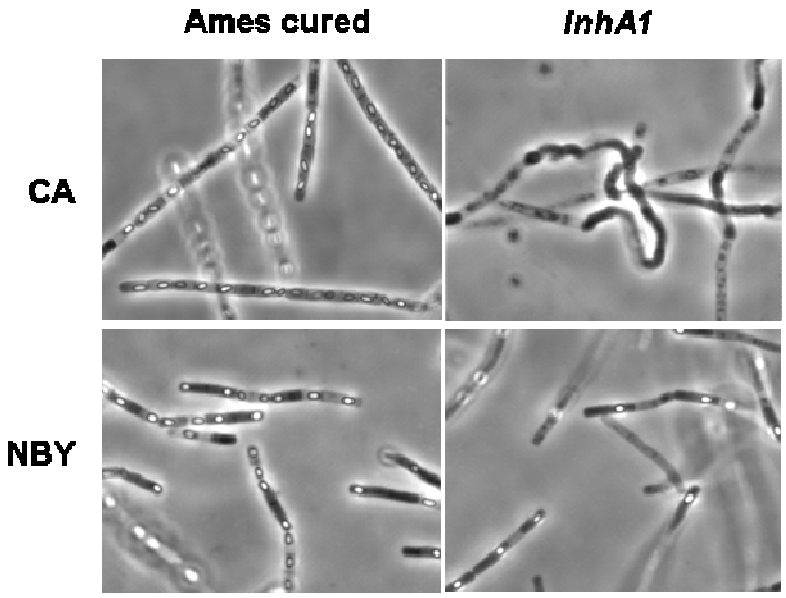

Figure 5-3. InhA1 is necessary for efficient sporulation in defined media. The parent strain (Ames cured of plasmids pXO1 and pXO2), and the *inhA1*-null derivative strain were cultured in nutrient rich (NBY) and defined (CA) media for 16 h. Cell development was assessed using microscopy and the relative presence of light-retractile spores was rated.

Despite extensive efforts to complement the constructed *inhA1* mutant strains I was unsuccessful. The recovery of only small numbers of *E. coli* transformants, each of which harbored mutations within the cloned *inhA1* gene, is consistent with this gene being lethal in *E. coli*. Similar cloning attempts were made using *B. subtilis* as a cloning host but this also resulted in the recovery of colonies with mutated *inhA1* genes. I was able to express an exogenous copy of *inhA1* in an *inhA1*-null strain of *B. anthracis* using an expression vector (pBSmul1) (13). However, while *B. anthracis* cells containing this *inhA1* construct were viable, the cells had a significant growth defect (data not shown). Therefore, the "complemented" strain could not be used in my expression studies nor in subsequent experiments. The *inhA2* gene driven by its native promoter was easily cloned and integrated into the chromosome of *B. anthracis* at the *plcR* locus, a non-functional gene in *B. anthracis*, (generating strain UT306).

5.2.4. InhA proteases contribute to the initial association of *B. anthracis* with macrophages. The contribution of InhA1 and InhA2 early in infection was examined using a macrophage-association model of infection. J774A.1 mouse macrophage-like cells were infected with spores of the *B. anthracis* parent strain 7702, *inhA* single mutant strains, or an *inhA1/inhA2* double mutant strain. Two separate cell populations were examined over time, the total population and the macrophage-associated population. The total population consisted of all the bacteria in the infection (macrophage-associated and free bacteria), while the macrophage-associated population consisted of only those bacilli associated with the macrophages (intracellular and dormant spores), with macrophage-associated cells being differentiated by their resistance to the antibiotic gentamicin. Figure 5-4A is a representative set of data obtained from an infection comparing the parent strain and the *inhA1/inhA2* double mutant strain. The data show that the population of macrophage-associated bacilli remains constant throughout the course of the experiment irrespective of the presence/absence of the *inhA* genes. Thus, the *inhA* genes do not contribute to the ability of *B. anthracis* to remain internalized. This is contrary to similar experiments in *B. thuringiensis*, which is able to escape from the infected macrophage when expressing *inhA1* (116). Interestingly, despite similar trends in the total and macrophage-associated populations for each strain throughout the course of the experiment (Fig. 5-4A), a phenotype

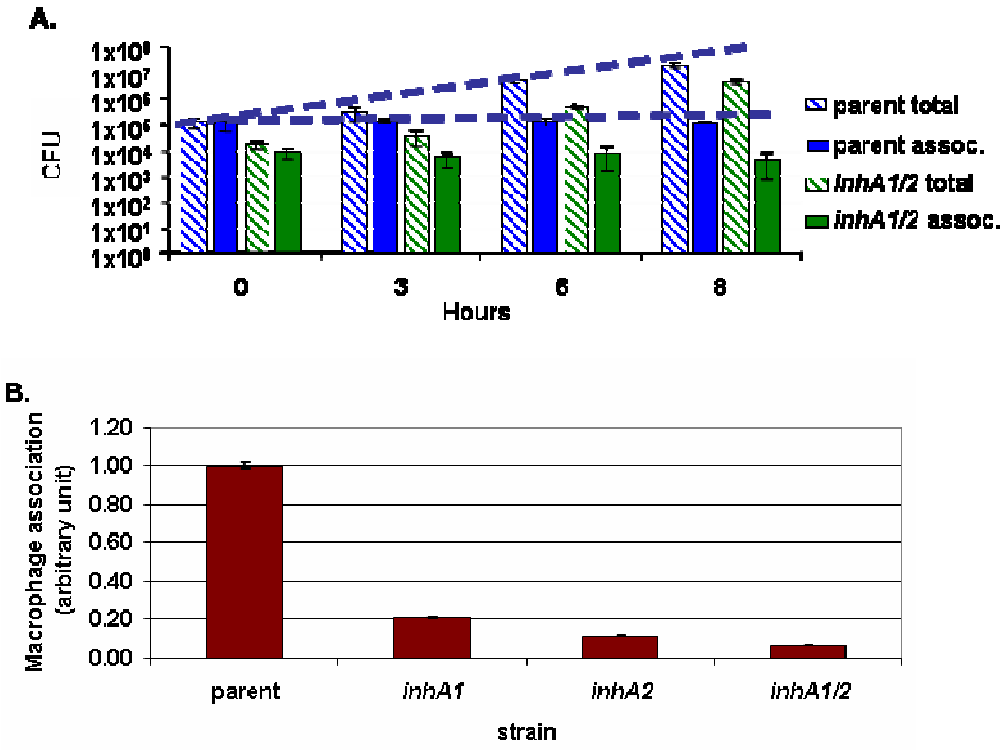

Figure 5-4. *inhA* mutant strains are attenuated in associated with mouse macrophage-like cells. (A.) The parent, 7702, and an *inhA1/2*-mutant derivative, UT284, were incubated with mouse macrophage-like cells and the number of bacilli associated with the macrophages, as well as the total number of bacilli in the well, was assessed over time. Solid bars represent macrophage-associated bacilli and hatched bars represent the total number of bacilli. Trends remain consistent between parent and *inhA1/2* mutant strains. (B.) Initial association of bacilli (T0) with macrophages, normalized to that observed with the parent strain.

consistently found at T_0 was an approximate 10-fold difference in macrophage-association of the parent strain and the *inhA1/inhA2* double mutant strain (Fig. 5-4B). An analysis of the percentage of inoculated spores that were macrophage-associated at T_0 indicated that a similar phenotype was also observed for each of the *inhA* single mutant strains (Fig. 5-4B). The data indicate that both InhA1 and InhA2 contribute to *B. anthracis*:macrophage association.

5.2.5. InhA1 and/or InhA2 protects against the activity of some cathelicidin antimicrobial peptides. The InhA1 orthologue in *B. thuringiensis* degrades the insect antimicrobial peptides cecropins and attacins to promote infection (33). To test whether InhA1 and/or InhA2 play a role in the defense of *B. anthracis* against the cathelicidin class of antimicrobial peptides (AMPs), the resistance of a fully virulent strain (Ames) of *B. anthracis* and an *inhA1/inhA2* isogenic mutant strain were assessed against LL-37 (human), CRAMP (mouse), protogrin 1 (pig), and cecropin A (insect) AMPs using a radial diffusion assay. From the data I infer that InhA1 and/or InhA2 promote the resistance of *B. anthracis* to CRAMP and Cecropin A, but not to LL-37 or Protogrin 1 (Table 5-1). Differences in protection afforded by the InhA proteins to various AMPs may be due to the fold of the mature AMP and the ability of the InhA proteases to access cleavage sites within the folded peptide. It remains to be tested whether other representative human AMPs can be cleaved and inactivated by the InhA proteins.

5.2.6. An *inhA1/inhA2* double mutant strain is attenuated in a murine inhalational model of infection. To assess the contribution of InhA1 and/or InhA2 to *B. anthracis* virulence I used an intra-tracheal mouse model of infection (97). BALB/c mice were infected with a fully virulent strain (Ames) of *B. anthracis* or an *inhA1/inhA2* isogenic mutant. Infection was assessed using LD_{50} and mean time-to-death. Survival curves identified that the *inhA1/inhA2* mutant strain was significantly less virulent than the parent strain (Fig. 5-5). While survival differences between the mice infected with the two strains were reduced at higher inoculums, the mutant strain never-the-less was consistently

Table 5-1. Minimal inhibitory concentrations of members of the cathalocidin class of antimicrobial peptides against the parent and *inhA1/2* (UTA7) strains using a radial diffusion assay.

	LL-37	CRAMP	Protogrin 1	Cecropin A
Ames	0.685 μM	0.899 μM	0.033 μM	3.440 μM
ΔinhA1inhA2	0.625 μM	0.203 μM	0.041 μM	1.070 μM

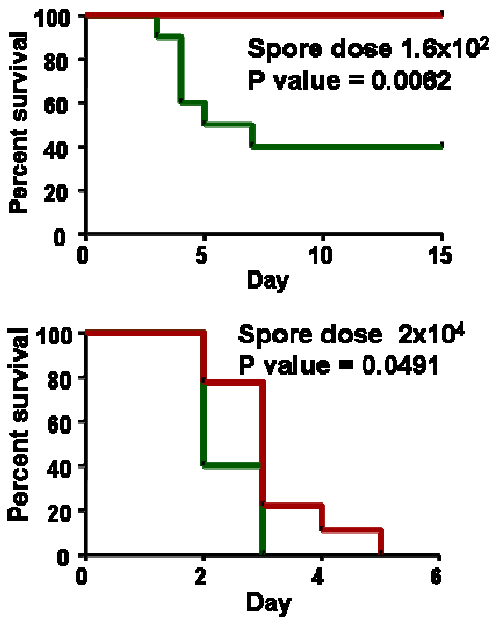

Figure 5-5. InhA proteins contribute to *B. anthracis* virulence in a mouse model of infection. Mice were infected with one of two doses of the parent (Ames; green) or the *inhA1/2* mutant strain (UTA7; red). N=10 for each strain in each experiment. Survival curves generated using GraphPad Prism are representative of data collected from 2 experiments. Statistical significance was determined using logrank test.

attenuated. The trend of decreased virulence in the mutant strain was also apparent from the LD_{50} data (Table 5-2). The data are consistent with InhA1 and/or InhA2 contributing to the virulence of *B. anthracis*.

Table 5-2. Lethal $Dose_{50}$ of the parent (Ames) and *inhA1/2* (UTA7) using a mouse intra-tracheal model of infection, n=10 for each experiment.

Strain	**Experiment 1**	**Experiment 2**
Parent	**330**	**560**
ΔinhA1 / inhA2	**2243**	**1100**

5.3. Discussion

The progression or stages of anthrax disease coincide with the progression of bacterial development in the host, from dormant spore in the alveolar space of the lung to the vegetative cell actively secreting virulence factors in blood and tissue. My data indicate that the InhA proteins may contribute to multiple stages of infection. InhA1 and InhA2 contribute to association with macrophage-like cells, an event early in infection. By enhancing the *B. anthracis*-macrophage association, the InhA proteins may advance the efficiency of the initial dissemination from the lung, augmenting the ability of the bacterium to cause disease. Given that *B. anthracis* is likely exposed to the membrane-disrupting activity of antimicrobial peptides throughout infection, produced by epithelial, myeloid precursors, and other cell types (63, 91, 121), the protective activity of the InhA proteins against AMPs may contribute to bacterial survival both early and late in the infection process. Due to the general activity attributed to InhA1 it is conceivable that InhA1 protects against a wide array of AMPs that are produced throughout infection, the effectiveness of which should be assessed in future experiments.

InhA1 activity has also been proposed late in infection (during dissemination) as the protease modulates important factors of the coagulation cascade (26, 28, 79). In addition to directly affecting virulence through interaction with host proteins InhA1 may affect virulence through the processing of bacterial substrates. InhA1 significantly modulates the secretome of *B. anthracis*, directly cleaving the anthrax toxin proteins, thereby affecting the timing of toxin accumulation. While anthrax toxin significantly influences the ability of *B. anthracis* to survive in the host (66), the affect of over expressing toxin in specific host tissues has not been assessed and may detrimentally impact the progression of the infection. As a member of a proteolytic cascade InhA1 affects the activity of numerous *B. anthracis* proteases, including Npr599, greatly inflating the effects of InhA1 on proteins secreted by *B. anthracis*. Taken together these processing events may affect multiple stages of infection. The *inhA* double mutant strain is attenuated in the mouse intra-tracheal model of infection; however the degree of influence of each of the aforementioned activities on infectivity has not been determined. That said it is likely that the decreased association of the *inhA* mutant strains with macrophages would directly impede the progression of disease and result in the attenuated phenotype of the *inhA* mutant strain. The vast difference in *inhA1* and *inhA2*

transcript levels *in vitro* suggest that the attenuated phenotype in the mouse can, at least in part, be attributed to the deletion of the *inhA1*. However, transcript levels have not been assessed *in vivo* and given that both proteins are expressed in the host, as assessed antibodies in the sera of infected animals (23, 53), the difference in *inhA1* and *inhA2* steady state transcript levels may be reduced in the host.

InhA1, and to a lesser extent InhA2, have been implicated in numerous processes, suggestive of roles in survival and virulence. The InhA proteins are classified as zinc metalloproteases, however it may be more pragmatic to think of InhA1 and InhA2 as multifunctional proteins with proteolytic activity. While the proteolytic activity of InhA1 has been clearly defined (see chapter III and (27, 28)), the presence of a putative integrin binding motif within the primary amino acid sequence is suggestive of further protein functions. If the KGD residues within the InhA1 sequence are surface exposed, InhA1 could bind the platelet glycoprotein II_bIII_a ($\alpha II_b\beta III$ integrin) (124) inhibiting clot formation and furthering the involvement of InhA1 in the coagulation cascade during the infection process. A similar activity has been suggested for the *S. pyogenes* integrin-binding protease SpeB (141). Unlike InhA1, proteolytic activity has not been confirmed for InhA2 in *B. anthracis* or other related species, however InhA2 does act synergistically with the *B. thuringiensis* toxin proteins to cause virulence through an undefined mechanism (47, 48). Here I show that a strain of *B. anthracis* with an *inhA2* deletion is deficient in macrophage-association. I propose that InhA2 uses the unique lipobox as well and the predicted RGD motif to bind phagocyte integrins, such as CD11b/CD18 and induce bacterial:macrophage association, as is the case of the filamentous hemagglutinin protein in *Bordetella pertussis* (65). As multifunctional proteins, InhA1 and InhA2 appear to be important contributors to the lifecycle of *B. anthracis*.

In addition to the postulated role of the InhA proteins in the host, a role for InhA1 in survival outside of the host can be posited from the sporulation defect of the *inhA1* mutant strain in defined medium, a limiting environment. As sporulation is a survival mechanism there are several possible scenarios that may explain the delay in sporulation of the *inhA1* mutant strain and the possible role of InhA1 in sporulation. In the absence of InhA1 a toxic substrate may build in abundance, slowing the progression into sporulation. Alternatively, InhA1 may be degrading extraneous substrates in the environment, thereby providing for

additional nutrients. While the posited limited nutrients in the *inhA1* mutant strain would affect the fitness of the organism, it is counterintuitive that this would delay sporulation. Finally, cleavage by InhA1 may lead to the activation of a protein necessary for the sporulation process. Given the number of secreted proteins that are either directly or indirectly altered by InhA1, including a number of transporters, metabolic enzymes, and environmentally significant proteins (e.g. chitin associated), and that sporulation is merely delayed and not aborted, suggests that InhA1 is the primary, but not sole protease, that is necessary for a cleavage event that allows for progression into sporulation. An additional role for InhA1 in the environment may be the inhibition of the architecture necessary for biofilm formation. The soil bacterium and archetype of the *Bacillus* species *B. subtilis* actively produces biofilms, a process that is regulated by the SinIR proteins (24, 80). In *B. anthracis inhA1* is located just upstream of *sinIR* and is regulated the by SinR (Chapter IV). The expression and subsequent activity of InhA1 may partially be responsible for the limited ability of *B. anthracis* to produce biofilms. Further research into the involvement of proteases in the *B. anthracis* lifecycle (spore to vegetative cell to spore) is necessary.

Chapter VI

Discussion

Bacteria secrete an array of proteins that enhance the virulence and/or survival of the organism. Regulation of secreted protein abundance is key to ensure appropriate timing of protein activity. Here I provide evidence that expression of the secreted *Bacillus anthracis* protease InhA1 is regulated at both the transcriptional and post-translational levels. InhA1 accumulation in culture supernate has major effects on the composition and abundance of other secreted proteins of *B. anthracis*, including each of the three anthrax toxin proteins and the protease Npr599. The potential contribution of InhA1 to *B. anthracis* virulence is indicated from the attenuated virulence of an *inhA* mutant strain in a mouse inhalational model of infection.

In chapter III I assessed how InhA1, directly or indirectly, modulates the secretome of *B. anthracis*. Data from a proteomic analysis indicated that InhA1 affects the abundance of more than half of the proteins in the culture supernatant. The identities of 96 proteins represented in the Differential in Gel Electrophoresis (DIGE) analysis were determined. The focus of the study was on proteins affected by InhA1 activity, hence proteins that were more abundant in the *inhA1* mutant background were primarily chosen for identification. Proteins from numerous functional classes were determined to be InhA1-regulated, including proteins involved in peroxide reduction, chitin degradation and proteins with proteolytic activity.

Importantly, the DIGE analysis indicates the possible existence of a proteolytic regulatory cascade in *B. anthracis*, in which a given protease activates or disrupts the activity of another protease, which in turn activates or disrupts additional proteases. This is suggestive from the fact that the steady state protein levels of eight proteases (including Npr599, the most abundant supernatant protein) were altered following *inhA1* mutation. InhA1 directly cleaves Npr599, as determined using *in vitro* protease cleavage assays with purified proteases, and may also directly cleave other proteases in the cascade. The abundance of only two proteases was unaffected by *inhA1* mutation. Thus, the data suggest that if a proteolytic regulatory cascade is utilized by *B. anthracis* then InhA1 acts in a key position within the cascade to directly or indirectly affect the abundance and/or activity of a substantial number of proteolytic enzymes. The general activity attributed to InhA1 would suggest that InhA1 acts late in the cascade and may abort the activity of the other proteases in the cascade. An alternative to the cascade model is the possibility that InhA1 acts in a

protease complex in which the proteases act in tandem and enhance the activity of other proteases. The models could be differentiated by assaying for an increase in the specific activity of each protease in the absence of cleavage of the proteases using *in vitro* assays. The events in either model should be further elucidated.

While InhA1 cleaves an array of substrates it does, however, retain some level of substrate specificity. This is evident from the fact that not all proteins in the DIGE analysis had altered abundance, as well as from *in vitro* protease assays using purified InhA1 protein which showed that InhA1 does not cleave the *B. anthracis* superoxide dismutase protein, SODA-1. To date the specific cleavage recognition sequence or structure has not been determined. The broad spectrum of substrates susceptible to InhA1, as described here and in published literature (27, 28), indicates that the protease acts as what has been termed a "general protease". General proteases commonly cleave both bacterial and host / environmental proteins. While the InhA1-mediated cleavage of proteins during the environmental stage of the *B. anthracis* lifecycle (spore to vegetative cell to spore) has yet to be assessed, a function of such activity could be to utilize degradation products as an energy source.

My DIGE analysis indicated that InhA1 affects the accumulation of the majority of proteins secreted by *B. anthracis* when cultured under atmospheric conditions. Subsequently, I determined that InhA1 has an equally significant role when strains were cultured with 5% CO_2 with sodium bicarbonate, conditions that are inductive for toxin production (51, 84). Elevated CO_2 and bicarbonate signals are considered to be an important cue for the bacterium during infection of mammalian host tissues. During the exponential phase of growth under toxin-inducing conditions the most abundant proteins in the culture supernatant are the anthrax toxin proteins (PA, EF, and LF), with these proteins being depleted as the cell progresses into stationary phase (85). The toxin protein expression pattern is drastically altered in the *inhA1* mutant strain, with the toxin proteins remaining abundant throughout stationary phase, indicating that toxin protein degradation is dependent upon InhA1. The timing of toxin protein degradation corresponds to InhA1 protein expression, as under toxin-inducing conditions InhA1 is found in the culture supernatant from transition through stationary phases of growth. Results from *in vitro*

protease assays showed that regulation of toxin protein abundance by InhA1 was direct, with the protease degrading all three of the toxin proteins.

One model for toxin protein activity dictates that the monomeric form of PA binds host cell receptors prior to cleavage by the host protease, furin, heptamer formation, and binding of the EF and/or LF proteins (30). InhA1 preferentially cleaves after two amino acids (308 and 416) within unstructured loops of domain 2 of PA (89, 112). Importantly, InhA1 cleaves PA at sites separate from the furin cleavage site (82, 105). Domain 2 of PA not only functions as a linker region between the EF/LF binding site of domain 1 and the receptor binding site of domain 4 but also contains an unstructured loop that inserts into the host cell membrane prior to the translocation of EF and/or LF (89). Cleavage by InhA1 may disassociate the binding activities of PA as well as alter the confirmation of PA increasing the susceptibility of PA to proteolytic activity. Structural analyses of PA in monomeric and heptameric states suggest that the InhA1 cleavage sites may only be accessible in the PA monomeric form (89, 112).

Given the dramatic alteration of the *B. anthracis* secretome by InhA1, the expression of this protease was hypothesized to be tightly regulated. In chapters IV and V the expression and regulation of the *inhA1* transcript and protein levels were discussed. The expression of the InhA1 protein under toxin-inducing conditions correlates with transcript levels of *inhA1* which are elevated late in exponential phase and throughout stationary phase. However, when cultured under atmospheric conditions the steady state levels of *inhA1* transcript peak as the cells enter stationary phase while protein levels are not readily detectible until late in stationary phase. Taken together, the divergent transcript and protein data indicate that one or more post-transcriptional regulatory event(s) regulate InhA1 expression.

Using whole-genome expression microarrays I determined that the regulatory protein SinR regulates the transcript levels of 41 genes in *B. anthracis*, including negative regulation of *inhA1* transcript levels. The SinI/R regulatory proteins are conserved among *Bacillus* species. In *B. subtilus*, SinR is a DNA-binding protein that regulates transcription of target genes during exponential growth, while SinI is an antagonist of SinR that inhibits SinR activity upon transition into stationary phase (5, 133). To test whether the *B. anthracis* SinR protein also possessed DNA-binding activity I performed electrophoretic mobility shift

assays. Recombinant SinR protein from *B. anthracis* bound specifically to the promoter regions of two highly SinR-regulated genes (*calY* and *sipW*) but not to the promoter regions of the negative control gene *npr599* or *inhA1*. Thus, it appears that SinR only weakly binds the putative binding motif upstream of *inhA1* or that the regulation of *inhA1* transcript levels by SinR is indirect.

Post-transcriptionally, InhA1 is subjected to multiple mechanisms of regulation. The activity of InhA1 is likely dependent on a processing event, an event that is hypothesized to be auto-proteolytic in nature. In addition, InhA1 levels are inversely proportional to the levels of the secreted protease camelysin. Similar to *inhA1,* the camelysin-encoding gene, *calY,* is only found in the genomes of pathogenic members of the *Bacillus* genus, and is regulated by SinI/R. Under atmospheric conditions camelysin is detected from the transition to stationary phases of growth. As the cell progresses through stationary phase camelysin levels are depleted. My data are consistent with camelysin reducing the abundance of InhA1 in the culture supernatant under atmospheric conditions, limiting detectible levels of InhA1 to a late stage of stationary phase growth. The regulation of these proteolytic enzymes has yet to be addressed under toxin-inducing conditions.

I have presented evidence for a model in which a series of regulatory steps are used to control the activity of InhA1 (Fig. 6-1). InhA1 is regulated transcriptionally and post-translationally by the Sin proteins during growth under atmospheric conditions. Transcription of the *inhA1* gene is inhibited by SinR during exponential phase. Upon transition to stationary phase, inhibition of SinR by SinI alleviates repression and *inhA1* is expressed. Following translation and secretion, InhA1 is degraded in the culture supernatant by the SinR-regulated protease camelysin, reducing InhA1 activity in the culture supernatant. As the cells progress through stationary phase camelysin levels decrease allowing for an accumulation of InhA1 and subsequent InhA1 activity. The possible existence of the proteolytic cascade outlined in chapter III implies that similar regulatory mechanisms are responsible for maintaining control of other proteases secreted by *B. anthracis*.

Employing multiple levels of regulation of secreted proteins is to the organism's advantage, enabling modulation of protein levels in response to a greater number of signals than is achievable through a single level of regulation. The ability to post-translationally

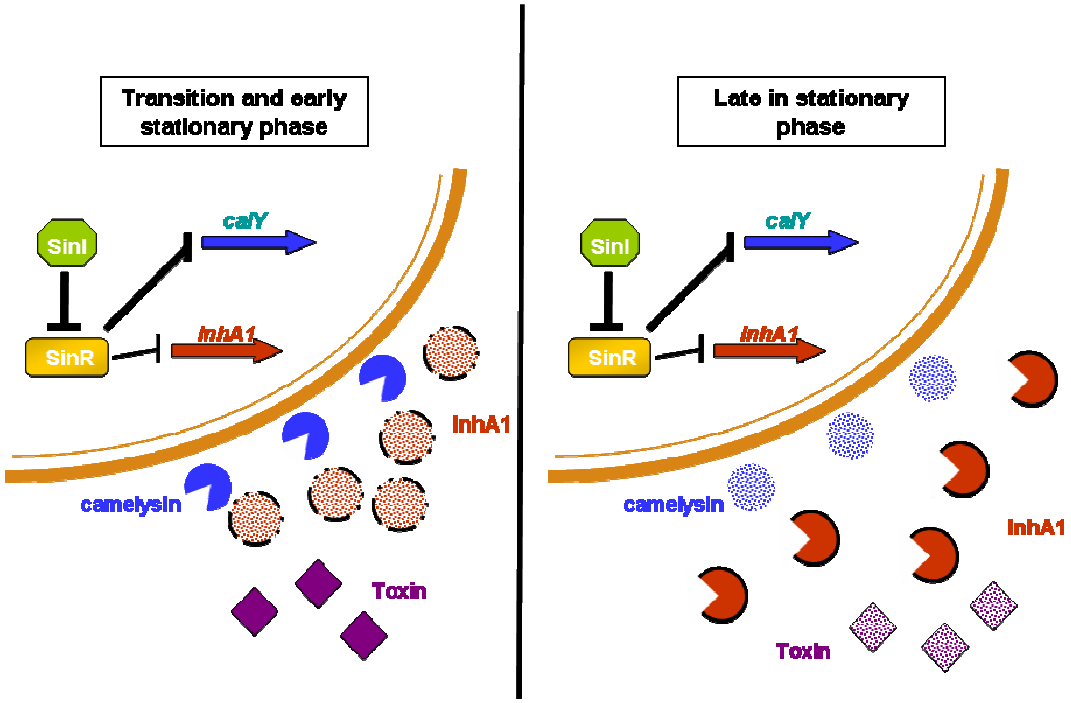

Figure 6-1. Model of the regulation of InhA1. SinI/R regulate expression of *inhA1* and *calY*, limiting gene expression to transition and stationary phases of growth. Post-translationally, InhA1 levels in the culture supernatant are inhibited by Camelysin via proteolysis, resulting in an accumulation of InhA1 substrates, represented here by the Toxin proteins. As the cells progress through stationary phase camelysin levels decrease allowing for an accumulation of InhA1 and subsequent InhA1 activity. Solid shapes signify active proteins, while spottled shapes signify cleaved (inactive) proteins.

regulate proteins via proteolysis provides for a level of negative regulation once a gene is transcribed and translated, of particular importance when rapid turn-over of protein activity is necessary. This may be the case in the host; the beneficial nature of elevated toxin levels may be limited to certain time points in infection or at niches in the host, making InhA1 activity critical for progression of disease.

The timing of InhA1 expression, and subsequent activity, may be critical during infection. The progression of anthrax disease can be correlated with bacterial development and expression of virulence factors in the host. The established model for the progression of inhalational anthrax is that once spores enter the lung they are transported to the regional lymph nodes by phagocytes, at which point the spores germinate. The vegetative cells disseminate throughout the host ultimately resulting in septic shock and death (139). The characterized virulence factors produced by *B. anthracis,* the anthrax toxin proteins and the poly γ-D-glutamic acid capsule, are produced during dissemination (86, 96, 98). The involvement of the InhA proteins in *B. anthracis* virulence was addressed in chapter V using *inhA1, inhA2* (a homologue of *inhA1*), and *inhA1/inhA2* mutant strains. The *inhA1/inhA2* mutant strain was attenuated in an intra-tracheal mouse model of infection, indicating that InhA1 and/or InhA2 contribute to the infection process. As only the double mutant strain was assessed in the mouse, the phenotype of the single mutants will need to be assessed in future experiments to determine if the affect of the InhA proteins is due to a single protein or if the affect is cumulative.

Given that InhA1 regulates the timing of the steady state levels of the anthrax toxin proteins in culture supernatant, it would be interesting to assess the regulation of toxin protein levels *in vivo*. Changes in PA accumulation in the blood of infected animals in response to secreted InhA1 could be measured using an ELISA assay (98) and utilized as a marker to monitor InhA1 activity in the host. An extension of the current study would be to map the temporal expression of each of the proteases that constitute the putative *B. anthracis* proteolytic cascade, including InhA1, in the host. In addition to furthering our understanding of the regulation of the secreted proteins of *B. anthracis*, such research would provide insight into which, if any, of the proteases may make attractive therapeutic targets.

In addition to the putative role of InhA1 in regulating toxin protein levels in the host, the attenuated virulence of the *inhA1/inhA2* mutant strain may be due to these proteins

contributing to an early stage of infection, the association of *B. anthracis* with macrophages. As macrophages are thought to be necessary to transport spores from the site of infection to regional lymph nodes (19), a defect in association with the macrophage may lead to attenuated virulence. In a macrophage-association model utilizing unencapulated strains of *B. anthracis* I determined that each of the single *inhA* mutants as well as the double mutant exhibited a defect in association. As the capsule of *B. anthracis* is anti-phagocytic in nature (81) and may mask the affects of the InhA proteins an unencapsulated strain background was used in this study. The strong phenotype in the *inhA2* mutant strain was surprising considering that *inhA2* steady state transcript levels are >1000-fold lower than that of *inhA1* under toxin-inducing conditions, conditions that are thought to mimic physiologic conditions in the host. However, these data, along with published reports that antibodies to InhA2 are present in the sera of the infected host (53, 87), indicate that *inhA2* transcript levels may be elevated in the animal, and therefore both *inhA1* and *inhA2* transcript levels should be assessed *in vivo*. The contribution of InhA1 and InhA2 in host-cell-association appears to be additive. Despite the two single mutant strains having similar phenotypes, the two proteins may not be functional homologues as assessed by differences in functional motifs predicted from the primary amino acid sequence of the two proteins.

Bioinformatic analysis of the InhA1 and InhA2 predicted amino acid sequences revealed that the zinc-binding motif (HEXXH) is conserved in both proteins. InhA2 contains two putative motifs that are absent in InhA1 that may differentiate the activities of the two proteins. InhA2 encodes a lipobox motif, a motif that promotes tethering of proteins to the bacterial cell membrane, and an RGD or integrin binding motif, which could facilitate interactions between *B. anthracis* and host cell integrins. Considering the differences in the predicted amino acid sequences of the homologues it is conceivable that the InhA proteins differentially contribute to *B. anthracis*-macrophage association. InhA1 may process surface exposed proteins enhancing the ability of the target protein to associate with the macrophage or prolong bacterial survival using its demonstrated proteolytic activity against both host and bacterial substrates ((28) and chapter III); while InhA2 may be cell surface-associated and as such facilitate interactions with host cell integrins to aid in host cell association. As these activities would result in a similar phenotype in the macrophage-association assay the proteins would appear, incorrectly, to be functionally redundant. The

activity of the InhA proteins could be differentiated experimentally, for example by assessing integrin binding by the two proteins.

From the data presented in this work I posit that the secreted proteases of *B. anthracis* form a global regulatory mechanism used to modulate the abundance of extracellular proteins. Given that several of these proteases are present only in the pathogenic members of the *Bacillus* genus, that proteases are highly abundant in *B. anthracis* cultures, and that an *inhA1/inhA2* double mutant strain is attenuated in a mouse model of infection, these data all point to the secreted proteases playing key roles in the lifecycle of *B. anthracis*. By regulating extracellular protein activity *B. anthracis* may better adapt to the changing environment, enhancing the survival and/or virulence of the pathogen.

References

1. **Albrecht, R., C. Perissol, F. Ruaudel, J. L. Petit, and G. Terrom.** 2010. Functional changes in culturable microbial communities during a co-composting process: carbon source utilization and co-metabolism. Waste Manag **30:**764-70.
2. **Antelmann, H., R. C. Williams, M. Miethke, A. Wipat, D. Albrecht, C. R. Harwood, and M. Hecker.** 2005. The extracellular and cytoplasmic proteomes of the non-virulent Bacillus anthracis strain UM23C1-2. Proteomics **5:**3684-95.
3. **Aronson, A. I., C. Bell, and B. Fulroth.** 2005. Plasmid-encoded regulator of extracellular proteases in Bacillus anthracis. J Bacteriol **187:**3133-8.
4. **Ausubel, F. M. (ed.).** 1993. Current protocols in molecular biology. Greene Publishing Associates and Wiley-Interscience, New York, NY.
5. **Bai, U., I. Mandic-Mulec, and I. Smith.** 1993. SinI modulates the activity of SinR, a developmental switch protein of Bacillus subtilis, by protein-protein interaction. Genes Dev **7:**139-48.
6. **Banks, D. J., M. Barnajian, F. J. Maldonado-Arocho, A. M. Sanchez, and K. A. Bradley.** 2005. Anthrax toxin receptor 2 mediates Bacillus anthracis killing of macrophages following spore challenge. Cell Microbiol **7:**1173-85.
7. **Barilla, D., T. Caramori, and A. Galizzi.** 1994. Coupling of flagellin gene transcription to flagellar assembly in Bacillus subtilis. J Bacteriol **176:**4558-64.
8. **Bergman, N. H., E. C. Anderson, E. E. Swenson, M. M. Niemeyer, A. D. Miyoshi, and P. C. Hanna.** 2006. Transcriptional profiling of the Bacillus anthracis life cycle in vitro and an implied model for regulation of spore formation. J Bacteriol **188:**6092-100.
9. **Bonuccelli, G., F. Sotgia, P. G. Frank, T. M. Williams, C. J. de Almeida, H. B. Tanowitz, P. E. Scherer, K. A. Hotchkiss, B. I. Terman, B. Rollman, A. Alileche, J. Brojatsch, and M. P. Lisanti.** 2005. ATR/TEM8 is highly expressed in epithelial cells lining Bacillus anthracis' three sites of entry: implications for the pathogenesis of anthrax infection. Am J Physiol Cell Physiol **288:**C1402-10.
10. **Booth, B. A., M. Boesman-Finkelstein, and R. A. Finkelstein.** 1984. Vibrio cholerae hemagglutinin/protease nicks cholera enterotoxin. Infect Immun **45:**558-60.

11. **Brittingham, K. C., G. Ruthel, R. G. Panchal, C. L. Fuller, W. J. Ribot, T. A. Hoover, H. A. Young, A. O. Anderson, and S. Bavari.** 2005. Dendritic cells endocytose Bacillus anthracis spores: implications for anthrax pathogenesis. J Immunol **174:**5545-52.
12. **Britton, R. A., P. Eichenberger, J. E. Gonzalez-Pastor, P. Fawcett, R. Monson, R. Losick, and A. D. Grossman.** 2002. Genome-wide analysis of the stationary-phase sigma factor (sigma-H) regulon of Bacillus subtilis. J Bacteriol **184:**4881-90.
13. **Brockmeier, U., M. Wendorff, and T. Eggert.** 2006. Versatile expression and secretion vectors for Bacillus subtilis. Curr Microbiol **52:**143-8.
14. **Brown, E. R., W. B. Cherry, M. D. Moody, and M. A. Gordon.** 1955. The induction of motility in Bacillus anthracis by means of bacteriophage lysates: significance for the relationship of Bacillus anthracis to Bacillus cereus. J Bacteriol **69:**590-602.
15. **Brunsing, R. L., C. La Clair, S. Tang, C. Chiang, L. E. Hancock, M. Perego, and J. A. Hoch.** 2005. Characterization of sporulation histidine kinases of Bacillus anthracis. J Bacteriol **187:**6972-81.
16. **Chaffin, D. O., L. M. Mentele, and C. E. Rubens.** 2005. Sialylation of group B streptococcal capsular polysaccharide is mediated by cpsK and is required for optimal capsule polymerization and expression. J Bacteriol **187:**4615-26.
17. **Chai, Y., R. Kolter, and R. Losick.** 2009. Paralogous antirepressors acting on the master regulator for biofilm formation in Bacillus subtilis. Mol Microbiol **74:**876-87.
18. **Chai, Y., T. Norman, R. Kolter, and R. Losick.** 2010. An epigenetic switch governing daughter cell separation in Bacillus subtilis. Genes Dev **24:**754-65.
19. **Chakrabarty, K., W. Wu, J. L. Booth, E. S. Duggan, K. M. Coggeshall, and J. P. Metcalf.** 2006. Bacillus anthracis spores stimulate cytokine and chemokine innate immune responses in human alveolar macrophages through multiple mitogen-activated protein kinase pathways. Infect Immun **74:**4430-8.
20. **Chen, Y., F. C. Tenover, and T. M. Koehler.** 2004. Beta-lactamase gene expression in a penicillin-resistant Bacillus anthracis strain. Antimicrob Agents Chemother **48:**4873-7.

21. **Chevallet, M., H. Diemer, A. Van Dorssealer, C. Villiers, and T. Rabilloud.** 2007. Toward a better analysis of secreted proteins: the example of the myeloid cells secretome. Proteomics **7:**1757-70.

22. **Chitlaru, T., O. Gat, Y. Gozlan, N. Ariel, and A. Shafferman.** 2006. Differential proteomic analysis of the Bacillus anthracis secretome: distinct plasmid and chromosome CO2-dependent cross talk mechanisms modulate extracellular proteolytic activities. J Bacteriol **188:**3551-71.

23. **Chitlaru, T., O. Gat, H. Grosfeld, I. Inbar, Y. Gozlan, and A. Shafferman.** 2007. Identification of in vivo-expressed immunogenic proteins by serological proteome analysis of the Bacillus anthracis secretome. Infect Immun **75:**2841-52.

24. **Chu, F., D. B. Kearns, S. S. Branda, R. Kolter, and R. Losick.** 2006. Targets of the master regulator of biofilm formation in Bacillus subtilis. Mol Microbiol **59:**1216-28.

25. **Chu, F., D. B. Kearns, A. McLoon, Y. Chai, R. Kolter, and R. Losick.** 2008. A novel regulatory protein governing biofilm formation in Bacillus subtilis. Mol Microbiol **68:**1117-27.

26. **Chung, M. C., S. C. Jorgensen, T. G. Popova, J. H. Tonry, C. L. Bailey, and S. G. Popov.** 2009. Activation of plasminogen activator inhibitor implicates protease InhA in the acute-phase response to Bacillus anthracis infection. J Med Microbiol **58:**737-44.

27. **Chung, M. C., T. G. Popova, S. C. Jorgensen, L. Dong, V. Chandhoke, C. L. Bailey, and S. G. Popov.** 2008. Degradation of circulating von Willebrand factor and its regulator ADAMTS13 implicates secreted Bacillus anthracis metalloproteases in anthrax consumptive coagulopathy. J Biol Chem **283:**9531-42.

28. **Chung, M. C., T. G. Popova, B. A. Millis, D. V. Mukherjee, W. Zhou, L. A. Liotta, E. F. Petricoin, V. Chandhoke, C. Bailey, and S. G. Popov.** 2006. Secreted neutral metalloproteases of bacillus anthracis as candidate pathogenic factors. J Biol Chem.

29. **Cleret, A., A. Quesnel-Hellmann, J. Mathieu, D. Vidal, and J. N. Tournier.** 2006. Resident CD11c+ Lung Cells Are Impaired by Anthrax Toxins after Spore Infection. J Infect Dis **194:**86-94.

30. **Collier, R. J., and J. A. Young.** 2003. Anthrax toxin. Annu Rev Cell Dev Biol **19:**45-70.

31. **Combet, C., C. Blanchet, C. Geourjon, and G. Deleage.** 2000. NPS@: network protein sequence analysis. Trends Biochem Sci **25:**147-50.

32. **Cote, C. K., N. Van Rooijen, and S. L. Welkos.** 2006. Roles of macrophages and neutrophils in the early host response to Bacillus anthracis spores in a mouse model of infection. Infect Immun **74:**469-80.

33. **Dalhammar, G., and H. Steiner.** 1984. Characterization of inhibitor A, a protease from Bacillus thuringiensis which degrades attacins and cecropins, two classes of antibacterial proteins in insects. Eur J Biochem **139:**247-52.

34. **Dautin, N., and H. D. Bernstein.** 2007. Protein secretion in gram-negative bacteria via the autotransporter pathway. Annu Rev Microbiol **61:**89-112.

35. **De Smet, K., and R. Contreras.** 2005. Human antimicrobial peptides: defensins, cathelicidins and histatins. Biotechnol Lett **27:**1337-47.

36. **de Souza, M. T., M. M. Lecadet, and D. Lereclus.** 1993. Full expression of the cryIIIA toxin gene of Bacillus thuringiensis requires a distant upstream DNA sequence affecting transcription. J Bacteriol **175:**2952-60.

37. **Driks, A.** 2009. The Bacillus anthracis spore. Mol Aspects Med **30:**368-73.

38. **Driks, A.** 2002. Maximum shields: the assembly and function of the bacterial spore coat. Trends Microbiol **10:**251-4.

39. **Driks, A.** 2002. Overview: Development in bacteria: spore formation in Bacillus subtilis. Cell Mol Life Sci **59:**389-91.

40. **Drobniewski, F. A.** 1993. Bacillus cereus and related species. Clin Microbiol Rev **6:**324-38.

41. **Drysdale, M., A. Bourgogne, S. G. Hilsenbeck, and T. M. Koehler.** 2004. atxA controls Bacillus anthracis capsule synthesis via acpA and a newly discovered regulator, acpB. J Bacteriol **186:**307-15.

42. **Drysdale, M., S. Heninger, J. Hutt, Y. Chen, C. R. Lyons, and T. M. Koehler.** 2005. Capsule synthesis by Bacillus anthracis is required for dissemination in murine inhalation anthrax. Embo J **24:**221-7.

43. **Duesbery, N. S., C. P. Webb, S. H. Leppla, V. M. Gordon, K. R. Klimpel, T. D. Copeland, N. G. Ahn, M. K. Oskarsson, K. Fukasawa, K. D. Paull, and G. F. Vande Woude.** 1998. Proteolytic inactivation of MAP-kinase-kinase by anthrax lethal factor. Science **280:**734-7.

44. **Eckhard, U., E. Schonauer, P. Ducka, P. Briza, D. Nuss, and H. Brandstetter.** 2009. Biochemical characterization of the catalytic domains of three different Clostridial collagenases. Biol Chem **390:**11-8.

45. **Edlund, T., I. Siden, and H. G. Boman.** 1976. Evidence for two immune inhibitors from Bacillus thuringiensis interfering with the humoral defense system of saturniid pupae. Infect Immun **14:**934-41.

46. **Emanuelsson, O., S. Brunak, G. von Heijne, and H. Nielsen.** 2007. Locating proteins in the cell using TargetP, SignalP and related tools. Nat Protoc **2:**953-71.

47. **Fedhila, S., M. Gohar, L. Slamti, P. Nel, and D. Lereclus.** 2003. The Bacillus thuringiensis PlcR-regulated gene inhA2 is necessary, but not sufficient, for virulence. J Bacteriol **185:**2820-5.

48. **Fedhila, S., P. Nel, and D. Lereclus.** 2002. The InhA2 metalloprotease of Bacillus thuringiensis strain 407 is required for pathogenicity in insects infected via the oral route. J Bacteriol **184:**3296-304.

49. **Fisher, N., and P. Hanna.** 2005. Characterization of Bacillus anthracis germinant receptors in vitro. J Bacteriol **187:**8055-62.

50. **Fouet, A.** 2009. The surface of Bacillus anthracis. Mol Aspects Med **30:**374-85.

51. **Fouet, A., and M. Mock.** 2006. Regulatory networks for virulence and persistence of Bacillus anthracis. Curr Opin Microbiol **9:**160-6.

52. **Fricke, B., K. Drossler, I. Willhardt, A. Schierhorn, S. Menge, and P. Rucknagel.** 2001. The cell envelope-bound metalloprotease (camelysin) from Bacillus cereus is a possible pathogenic factor. Biochim Biophys Acta **1537:**132-46.

53. **Gat, O., H. Grosfeld, N. Ariel, I. Inbar, G. Zaide, Y. Broder, A. Zvi, T. Chitlaru, Z. Altboum, D. Stein, S. Cohen, and A. Shafferman.** 2006. Search for Bacillus anthracis Potential Vaccine Candidates by a Functional Genomic-Serologic Screen. Infect Immun **74:**3987-4001.

54. **Gaur, N. K., K. Cabane, and I. Smith.** 1988. Structure and expression of the Bacillus subtilis sin operon. J Bacteriol **170:**1046-53.

55. **Gaur, N. K., E. Dubnau, and I. Smith.** 1986. Characterization of a cloned Bacillus subtilis gene that inhibits sporulation in multiple copies. J Bacteriol **168:**860-9.

56. **Gaur, N. K., J. Oppenheim, and I. Smith.** 1991. The Bacillus subtilis sin gene, a regulator of alternate developmental processes, codes for a DNA-binding protein. J Bacteriol **173:**678-86.

57. **Goossens, P. L.** 2009. Animal models of human anthrax: the Quest for the Holy Grail. Mol Aspects Med **30:**467-80.

58. **Grandvalet, C., M. Gominet, and D. Lereclus.** 2001. Identification of genes involved in the activation of the Bacillus thuringiensis inhA metalloprotease gene at the onset of sporulation. Microbiology **147:**1805-13.

59. **Grass, G., A. Schierhorn, E. Sorkau, H. Muller, P. Rucknagel, D. H. Nies, and B. Fricke.** 2004. Camelysin is a novel surface metalloproteinase from Bacillus cereus. Infect Immun **72:**219-28.

60. **Greenlee, K. J., D. B. Corry, D. A. Engler, R. K. Matsunami, P. Tessier, R. G. Cook, Z. Werb, and F. Kheradmand.** 2006. Proteomic identification of in vivo substrates for matrix metalloproteinases 2 and 9 reveals a mechanism for resolution of inflammation. J Immunol **177:**7312-21.

61. **Grynberg, M., Z. Li, E. Szczurek, and A. Godzik.** 2007. Putative type IV secretion genes in Bacillus anthracis. Trends Microbiol **15:**191-5.

62. **Guillen, N., Y. Weinrauch, and D. A. Dubnau.** 1989. Cloning and characterization of the regulatory Bacillus subtilis competence genes comA and comB. J Bacteriol **171:**5354-61.

63. **Hancock, R. E., and G. Diamond.** 2000. The role of cationic antimicrobial peptides in innate host defences. Trends Microbiol **8:**402-10.

64. **Hase, C. C., and R. A. Finkelstein.** 1993. Bacterial extracellular zinc-containing metalloproteases. Microbiol Rev **57:**823-37.

65. **Hellwig, S. M., W. L. Hazenbos, J. G. van de Winkel, and F. R. Mooi.** 1999. Evidence for an intracellular niche for Bordetella pertussis in broncho-alveolar lavage cells of mice. FEMS Immunol Med Microbiol **26:**203-7.

66. **Heninger, S., M. Drysdale, J. Lovchik, J. Hutt, M. F. Lipscomb, T. M. Koehler, and C. R. Lyons.** 2006. Toxin-Deficient Mutants of Bacillus anthracis Are Lethal in a Murine Model for Pulmonary Anthrax. Infect Immun **74:**6067-74.

67. **Hoffmaster, A. R., and T. M. Koehler.** 1997. The anthrax toxin activator gene atxA is associated with CO2-enhanced non-toxin gene expression in Bacillus anthracis. Infect Immun **65:**3091-9.

68. **Hoffmaster, A. R., J. Ravel, D. A. Rasko, G. D. Chapman, M. D. Chute, C. K. Marston, B. K. De, C. T. Sacchi, C. Fitzgerald, L. W. Mayer, M. C. Maiden, F. G. Priest, M. Barker, L. Jiang, R. Z. Cer, J. Rilstone, S. N. Peterson, R. S. Weyant, D. R. Galloway, T. D. Read, T. Popovic, and C. M. Fraser.** 2004. Identification of anthrax toxin genes in a Bacillus cereus associated with an illness resembling inhalation anthrax. Proc Natl Acad Sci U S A **101:**8449-54.

69. **Hooper, N. M.** 1994. Families of zinc metalloproteases. FEBS Lett **354:**1-6.

70. **Horton, R. M., H. D. Hunt, S. N. Ho, J. K. Pullen, and L. R. Pease.** 1989. Engineering hybrid genes without the use of restriction enzymes: gene splicing by overlap extension. Gene **77:**61-8.

71. **Huang, C. M., K. W. Foster, T. S. DeSilva, K. R. Van Kampen, C. A. Elmets, and D. C. Tang.** 2004. Identification of Bacillus anthracis proteins associated with germination and early outgrowth by proteomic profiling of anthrax spores. Proteomics **4:**2653-61.

72. **Hugh-Jones, M., and J. Blackburn.** 2009. The ecology of Bacillus anthracis. Mol Aspects Med **30:**356-67.

73. **Hynes, R. O.** 2004. The emergence of integrins: a personal and historical perspective. Matrix Biol **23:**333-40.

74. **Hynes, R. O.** 2002. Integrins: bidirectional, allosteric signaling machines. Cell **110:**673-87.

75. **Ishibashi, Y., S. Claus, and D. A. Relman.** 1994. Bordetella pertussis filamentous hemagglutinin interacts with a leukocyte signal transduction complex and stimulates bacterial adherence to monocyte CR3 (CD11b/CD18). J Exp Med **180:**1225-33.

76. **Kadowaki, T., K. Nakayama, F. Yoshimura, K. Okamoto, N. Abe, and K. Yamamoto.** 1998. Arg-gingipain acts as a major processing enzyme for various cell surface proteins in Porphyromonas gingivalis. J Biol Chem **273:**29072-6.

77. **Kagawa, T. F., J. C. Cooney, H. M. Baker, S. McSweeney, M. Liu, S. Gubba, J. M. Musser, and E. N. Baker.** 2000. Crystal structure of the zymogen form of the group A Streptococcus virulence factor SpeB: an integrin-binding cysteine protease. Proc Natl Acad Sci U S A **97:**2235-40.

78. **Kallio, P. T., J. E. Fagelson, J. A. Hoch, and M. A. Strauch.** 1991. The transition state regulator Hpr of Bacillus subtilis is a DNA-binding protein. J Biol Chem **266:**13411-7.

79. **Kastrup, C. J., J. Q. Boedicker, A. P. Pomerantsev, M. Moayeri, Y. Bian, R. R. Pompano, T. R. Kline, P. Sylvestre, F. Shen, S. H. Leppla, W. J. Tang, and R. F. Ismagilov.** 2008. Spatial localization of bacteria controls coagulation of human blood by 'quorum acting'. Nat Chem Biol **4:**742-50.

80. **Kearns, D. B., F. Chu, S. S. Branda, R. Kolter, and R. Losick.** 2005. A master regulator for biofilm formation by Bacillus subtilis. Mol Microbiol **55:**739-49.

81. **Keppie, J., P. W. Harris-Smith, and H. Smith.** 1963. The Chemical Basis of the Virulence of Bacillus Anthracis. Ix. Its Aggressins and Their Mode of Action. Br J Exp Pathol **44:**446-53.

82. **Klimpel, K. R., S. S. Molloy, G. Thomas, and S. H. Leppla.** 1992. Anthrax toxin protective antigen is activated by a cell surface protease with the sequence specificity and catalytic properties of furin. Proc Natl Acad Sci U S A **89:**10277-81.

83. **Kodgire, P., M. Dixit, and K. K. Rao.** 2006. ScoC and SinR negatively regulate epr by corepression in Bacillus subtilis. J Bacteriol **188:**6425-8.

84. **Koehler, T. M.** 2009. Bacillus anthracis physiology and genetics. Mol Aspects Med **30:**386-96.

85. **Koehler, T. M., Z. Dai, and M. Kaufman-Yarbray.** 1994. Regulation of the Bacillus anthracis protective antigen gene: CO2 and a trans-acting element activate transcription from one of two promoters. J Bacteriol **176:**586-95.

86. **Kozel, T. R., W. J. Murphy, S. Brandt, B. R. Blazar, J. A. Lovchik, P. Thorkildson, A. Percival, and C. R. Lyons.** 2004. mAbs to Bacillus anthracis

capsular antigen for immunoprotection in anthrax and detection of antigenemia. Proc Natl Acad Sci U S A **101:**5042-7.

87. **Kudva, I. T., R. W. Griffin, J. M. Garren, S. B. Calderwood, and M. John.** 2005. Identification of a protein subset of the anthrax spore immunome in humans immunized with the anthrax vaccine adsorbed preparation. Infect Immun **73:**5685-96.

88. **Kuroda, A., and J. Sekiguchi.** 1993. High-level transcription of the major Bacillus subtilis autolysin operon depends on expression of the sigma D gene and is affected by a sin (flaD) mutation. J Bacteriol **175:**795-801.

89. **Lacy, D. B., D. J. Wigelsworth, R. A. Melnyk, S. C. Harrison, and R. J. Collier.** 2004. Structure of heptameric protective antigen bound to an anthrax toxin receptor: a role for receptor in pH-dependent pore formation. Proc Natl Acad Sci U S A **101:**13147-51.

90. **Lamonica, J. M., M. Wagner, M. Eschenbrenner, L. E. Williams, T. L. Miller, G. Patra, and V. G. DelVecchio.** 2005. Comparative secretome analyses of three Bacillus anthracis strains with variant plasmid contents. Infect Immun **73:**3646-58.

91. **Levy, O.** 2000. Antimicrobial proteins and peptides of blood: templates for novel antimicrobial agents. Blood **96:**2664-72.

92. **Lewis, R. J., J. A. Brannigan, W. A. Offen, I. Smith, and A. J. Wilkinson.** 1998. An evolutionary link between sporulation and prophage induction in the structure of a repressor:anti-repressor complex. J Mol Biol **283:**907-12.

93. **Liu, H., N. H. Bergman, B. Thomason, S. Shallom, A. Hazen, J. Crossno, D. A. Rasko, J. Ravel, T. D. Read, S. N. Peterson, J. Yates, 3rd, and P. C. Hanna.** 2004. Formation and composition of the Bacillus anthracis endospore. J Bacteriol **186:**164-78.

94. **Liu, L., M. M. Nakano, O. H. Lee, and P. Zuber.** 1996. Plasmid-amplified comS enhances genetic competence and suppresses sinR in Bacillus subtilis. J Bacteriol **178:**5144-52.

95. **Lopez, D., and R. Kolter.** Extracellular signals that define distinct and coexisting cell fates in Bacillus subtilis. FEMS Microbiol Rev **34:**134-49.

96. **Loving, C. L., T. Khurana, M. Osorio, G. M. Lee, V. K. Kelly, S. Stibitz, and T. J. Merkel.** 2009. Role of anthrax toxins in dissemination, disease progression, and induction of protective adaptive immunity in the mouse aerosol challenge model. Infect Immun **77:**255-65.

97. **Lyons, C. R., J. Lovchik, J. Hutt, M. F. Lipscomb, E. Wang, S. Heninger, L. Berliba, and K. Garrison.** 2004. Murine model of pulmonary anthrax: kinetics of dissemination, histopathology, and mouse strain susceptibility. Infect Immun **72:**4801-9.

98. **Mabry, R., K. Brasky, R. Geiger, R. Carrion, Jr., G. B. Hubbard, S. Leppla, J. L. Patterson, G. Georgiou, and B. L. Iverson.** 2006. Detection of anthrax toxin in the serum of animals infected with Bacillus anthracis by using engineered immunoassays. Clin Vaccine Immunol **13:**671-7.

99. **Mandic-Mulec, I., L. Doukhan, and I. Smith.** 1995. The Bacillus subtilis SinR protein is a repressor of the key sporulation gene spo0A. J Bacteriol **177:**4619-27.

100. **Mandic-Mulec, I., N. Gaur, U. Bai, and I. Smith.** 1992. Sin, a stage-specific repressor of cellular differentiation. J Bacteriol **174:**3561-9.

101. **Miron´czuk A.M., Á. T. K., and O.P. Kuipers.** 2008. Induction of natural competence in Bacillus cereus ATCC14579. Microbial Biotechnology **1:**226–235.

102. **Miyoshi, S., and S. Shinoda.** 2000. Microbial metalloproteases and pathogenesis. Microbes Infect **2:**91-8.

103. **Moayeri, M., and S. H. Leppla.** 2009. Cellular and systemic effects of anthrax lethal toxin and edema toxin. Mol Aspects Med **30:**439-55.

104. **Moir, A., B. M. Corfe, and J. Behravan.** 2002. Spore germination. Cell Mol Life Sci **59:**403-9.

105. **Molloy, S. S., P. A. Bresnahan, S. H. Leppla, K. R. Klimpel, and G. Thomas.** 1992. Human furin is a calcium-dependent serine endoprotease that recognizes the sequence Arg-X-X-Arg and efficiently cleaves anthrax toxin protective antigen. J Biol Chem **267:**16396-402.

106. **Nisnevitch, M., S. Cohen, E. Ben-Dov, A. Zaritsky, Y. Sofer, and R. Cahan.** 2006. Cyt2Ba of Bacillus thuringiensis israelensis: activation by putative endogenous protease. Biochem Biophys Res Commun **344:**99-105.

107. **Nooh, M. M., R. K. Aziz, M. Kotb, A. Eroshkin, W. J. Chuang, T. Proft, and R. Kansal.** 2006. Streptococcal mitogenic exotoxin, SmeZ, is the most susceptible M1T1 streptococcal superantigen to degradation by the streptococcal cysteine protease, SpeB. J Biol Chem **281:**35281-8.

108. **Ohol, Y. M., D. H. Goetz, K. Chan, M. U. Shiloh, C. S. Craik, and J. S. Cox.** 2010. Mycobacterium tuberculosis MycP1 protease plays a dual role in regulation of ESX-1 secretion and virulence. Cell Host Microbe **7:**210-20.

109. **Oliva, C., C. L. Turnbough, Jr., and J. F. Kearney.** 2009. CD14-Mac-1 interactions in Bacillus anthracis spore internalization by macrophages. Proc Natl Acad Sci U S A **106:**13957-62.

110. **Paccani, S. R., F. Tonello, R. Ghittoni, M. Natale, L. Muraro, M. M. D'Elios, W. J. Tang, C. Montecucco, and C. T. Baldari.** 2005. Anthrax toxins suppress T lymphocyte activation by disrupting antigen receptor signaling. J Exp Med **201:**325-31.

111. **Perez, N., J. Trevino, Z. Liu, S. C. Ho, P. Babitzke, and P. Sumby.** 2009. A genome-wide analysis of small regulatory RNAs in the human pathogen group A Streptococcus. PLoS One **4:**e7668.

112. **Petosa, C., R. J. Collier, K. R. Klimpel, S. H. Leppla, and R. C. Liddington.** 1997. Crystal structure of the anthrax toxin protective antigen. Nature **385:**833-8.

113. **Pickering, A. K., M. Osorio, G. M. Lee, V. K. Grippe, M. Bray, and T. J. Merkel.** 2004. Cytokine response to infection with Bacillus anthracis spores. Infect Immun **72:**6382-9.

114. **Popov, S. G., T. G. Popova, S. Hopkins, R. S. Weinstein, R. MacAfee, K. J. Fryxell, V. Chandhoke, C. Bailey, and K. Alibek.** 2005. Effective antiprotease-antibiotic treatment of experimental anthrax. BMC Infect Dis **5:**25.

115. **Radha, C., P. Salotra, R. Bhat, and R. Bhatnagar.** 1996. Thermostabilization of protective antigen--the binding component of anthrax lethal toxin. J Biotechnol **50:**235-42.

116. **Ramarao, N., and D. Lereclus.** 2005. The InhA1 metalloprotease allows spores of the B. cereus group to escape macrophages. Cell Microbiol **7:**1357-64.

117. **Rasko, D. A., M. R. Altherr, C. S. Han, and J. Ravel.** 2005. Genomics of the Bacillus cereus group of organisms. FEMS Microbiol Rev **29:**303-29.

118. **Ravel, J., L. Jiang, S. T. Stanley, M. R. Wilson, R. S. Decker, T. D. Read, P. Worsham, P. S. Keim, S. L. Salzberg, C. M. Fraser-Liggett, and D. A. Rasko.** 2009. The complete genome sequence of Bacillus anthracis Ames "Ancestor". J Bacteriol **191:**445-6.

119. **Read, T. D., S. N. Peterson, N. Tourasse, L. W. Baillie, I. T. Paulsen, K. E. Nelson, H. Tettelin, D. E. Fouts, J. A. Eisen, S. R. Gill, E. K. Holtzapple, O. A. Okstad, E. Helgason, J. Rilstone, M. Wu, J. F. Kolonay, M. J. Beanan, R. J. Dodson, L. M. Brinkac, M. Gwinn, R. T. DeBoy, R. Madpu, S. C. Daugherty, A. S. Durkin, D. H. Haft, W. C. Nelson, J. D. Peterson, M. Pop, H. M. Khouri, D. Radune, J. L. Benton, Y. Mahamoud, L. Jiang, I. R. Hance, J. F. Weidman, K. J. Berry, R. D. Plaut, A. M. Wolf, K. L. Watkins, W. C. Nierman, A. Hazen, R. Cline, C. Redmond, J. E. Thwaite, O. White, S. L. Salzberg, B. Thomason, A. M. Friedlander, T. M. Koehler, P. C. Hanna, A. B. Kolsto, and C. M. Fraser.** 2003. The genome sequence of Bacillus anthracis Ames and comparison to closely related bacteria. Nature **423:**81-6.

120. **Ribot, W. J., R. G. Panchal, K. C. Brittingham, G. Ruthel, T. A. Kenny, D. Lane, B. Curry, T. A. Hoover, A. M. Friedlander, and S. Bavari.** 2006. Anthrax lethal toxin impairs innate immune functions of alveolar macrophages and facilitates Bacillus anthracis survival. Infect Immun **74:**5029-34.

121. **Rogan, M. P., P. Geraghty, C. M. Greene, S. J. O'Neill, C. C. Taggart, and N. G. McElvaney.** 2006. Antimicrobial proteins and polypeptides in pulmonary innate defence. Respir Res **7:**29.

122. **Rolbetzki, A., M. Ammon, V. Jakovljevic, A. Konovalova, and L. Sogaard-Andersen.** 2008. Regulated secretion of a protease activates intercellular signaling during fruiting body formation in M. xanthus. Dev Cell **15:**627-34.

123. **Rudenskaya, G. N., and D. V. Pupov.** 2008. Cysteine proteinases of microorganisms and viruses. Biochemistry (Mosc) **73:**1-13.

124. **Ruoslahti, E.** 1996. RGD and other recognition sequences for integrins. Annu Rev Cell Dev Biol **12:**697-715.

125. **Russell, B. H., R. Vasan, D. R. Keene, T. M. Koehler, and Y. Xu.** 2008. Potential dissemination of Bacillus anthracis utilizing human lung epithelial cells. Cell Microbiol **10:**945-57.

126. **Saile, E., and T. M. Koehler.** 2006. Bacillus anthracis multiplication, persistence, and genetic exchange in the rhizosphere of grass plants. Appl Environ Microbiol **72:**3168-74.

127. **Saile, E., and T. M. Koehler.** 2002. Control of anthrax toxin gene expression by the transition state regulator abrB. J Bacteriol **184:**370-80.

128. **Schuch, R., and V. A. Fischetti.** 2009. The secret life of the anthrax agent Bacillus anthracis: bacteriophage-mediated ecological adaptations. PLoS One **4:**e6532.

129. **Schwartz, M.** 2009. Dr. Jekyll and Mr. Hyde: a short history of anthrax. Mol Aspects Med **30:**347-55.

130. **Scorpio, A., D. J. Chabot, W. A. Day, K. O'Brien D, N. J. Vietri, Y. Itoh, M. Mohamadzadeh, and A. M. Friedlander.** 2006. Poly-{gamma}-glutamate capsule-degrading enzyme treatment enhances phagocytosis and killing of encapsulated Bacillus anthracis. Antimicrob Agents Chemother.

131. **Sela-Abramovich, S., T. Chitlaru, O. Gat, H. Grosfeld, O. Cohen, and A. Shafferman.** 2009. Novel and unique diagnostic biomarkers for Bacillus anthracis infection. Appl Environ Microbiol **75:**6157-67.

132. **Setlow, P.** 2003. Spore germination. Curr Opin Microbiol **6:**550-6.

133. **Shafikhani, S. H., I. Mandic-Mulec, M. A. Strauch, I. Smith, and T. Leighton.** 2002. Postexponential regulation of sin operon expression in Bacillus subtilis. J Bacteriol **184:**564-71.

134. **Shaw, L., E. Golonka, J. Potempa, and S. J. Foster.** 2004. The role and regulation of the extracellular proteases of Staphylococcus aureus. Microbiology **150:**217-28.

135. **Shoji, M., M. Naito, H. Yukitake, K. Sato, E. Sakai, N. Ohara, and K. Nakayama.** 2004. The major structural components of two cell surface filaments of Porphyromonas gingivalis are matured through lipoprotein precursors. Mol Microbiol **52:**1513-25.

136. **Siden, I., G. Dalhammar, B. Telander, H. G. Boman, and H. Somerville.** 1979. Virulence factors in Bacillus thuringiensis: purification and properties of a protein inhibitor of immunity in insects. J Gen Microbiol **114:**45-52.

137. **Smith, I., I. Mandic-Mulec, and N. Gaur.** 1991. The role of negative control in sporulation. Res Microbiol **142:**831-9.

138. **Sneath, P. H. A.** 1986. Endospore-forming Gram-positive rods and cocci, p. 1104-1139. *In* J. G. Holt (ed.), Bergey's Manual of Systematic Bacteriology. The Williams & Wilkins Co, Baltimore, MD.

139. **Spencer, R. C.** 2003. Bacillus anthracis. J Clin Pathol **56:**182-7.

140. **Srivatsan, A., Y. Han, J. Peng, A. K. Tehranchi, R. Gibbs, J. D. Wang, and R. Chen.** 2008. High-precision, whole-genome sequencing of laboratory strains facilitates genetic studies. PLoS Genet **4:**e1000139.

141. **Stockbauer, K. E., L. Magoun, M. Liu, E. H. Burns, Jr., S. Gubba, S. Renish, X. Pan, S. C. Bodary, E. Baker, J. Coburn, J. M. Leong, and J. M. Musser.** 1999. A natural variant of the cysteine protease virulence factor of group A Streptococcus with an arginine-glycine-aspartic acid (RGD) motif preferentially binds human integrins alphavbeta3 and alphaIIbbeta3. Proc Natl Acad Sci U S A **96:**242-7.

142. **Strauch, M. A., P. Ballar, A. J. Rowshan, and K. L. Zoller.** 2005. The DNA-binding specificity of the Bacillus anthracis AbrB protein. Microbiology **151:**1751-9.

143. **Sumby, P., A. R. Whitney, E. A. Graviss, F. R. DeLeo, and J. M. Musser.** 2006. Genome-wide analysis of group a streptococci reveals a mutation that modulates global phenotype and disease specificity. PLoS Pathog **2:**e5.

144. **Sussmuth, S. D., A. Muscholl-Silberhorn, R. Wirth, M. Susa, R. Marre, and E. Rozdzinski.** 2000. Aggregation substance promotes adherence, phagocytosis, and intracellular survival of Enterococcus faecalis within human macrophages and suppresses respiratory burst. Infect Immun **68:**4900-6.

145. **Thompson, J. D., D. G. Higgins, and T. J. Gibson.** 1994. CLUSTAL W: improving the sensitivity of progressive multiple sequence alignment through sequence weighting, position-specific gap penalties and weight matrix choice. Nucleic Acids Res **22:**4673-80.

146. **Thwaite, J. E., S. Hibbs, R. W. Titball, and T. P. Atkins.** 2006. Proteolytic Degradation of Human Antimicrobial Peptide LL-37 by Bacillus anthracis May Contribute to Virulence. Antimicrob Agents Chemother **50:**2316-22.

147. **Tjalsma, H., A. Bolhuis, J. D. Jongbloed, S. Bron, and J. M. van Dijl.** 2000. Signal peptide-dependent protein transport in Bacillus subtilis: a genome-based survey of the secretome. Microbiol Mol Biol Rev **64:**515-47.

148. **Tosi, M. F.** 2005. Innate immune responses to infection. J Allergy Clin Immunol **116:**241-9; quiz 250.

149. **Turnbull, P. C.** 1991. Anthrax vaccines: past, present and future. Vaccine **9:**533-9.

150. **Turnbull, P. C.** 1999. Definitive identification of Bacillus anthracis--a review. J Appl Microbiol **87:**237-40.

151. **Vaaje-Kolstad, G., S. J. Horn, D. M. van Aalten, B. Synstad, and V. G. Eijsink.** 2005. The non-catalytic chitin-binding protein CBP21 from Serratia marcescens is essential for chitin degradation. J Biol Chem **280:**28492-7.

152. **Valbuzzi, A., E. Ferrari, and A. M. Albertini.** 1999. A novel member of the subtilisin-like protease family from Bacillus subtilis. Microbiology **145 (Pt 11):**3121-7.

153. **van der Goot, G., and J. A. Young.** 2009. Receptors of anthrax toxin and cell entry. Mol Aspects Med **30:**406-12.

154. **Vary, J. C., and H. O. Halvorson.** 1965. Kinetics of Germination of Bacillus Spores. J Bacteriol **89:**1340-7.

155. **Voigt, C. A., D. M. Wolf, and A. P. Arkin.** 2005. The Bacillus subtilis sin operon: an evolvable network motif. Genetics **169:**1187-202.

156. **von Pawel-Rammingen, U., and L. Bjorck.** 2003. IdeS and SpeB: immunoglobulin-degrading cysteine proteinases of Streptococcus pyogenes. Curr Opin Microbiol **6:**50-5.

157. **Wandersman, C.** 1989. Secretion, processing and activation of bacterial extracellular proteases. Mol Microbiol **3:**1825-31.

158. **Wimalasena, D. S., J. C. Cramer, B. E. Janowiak, S. J. Juris, R. A. Melnyk, D. E. Anderson, K. L. Kirk, R. J. Collier, and J. G. Bann.** 2007. Effect of 2-

fluorohistidine labeling of the anthrax protective antigen on stability, pore formation, and translocation. Biochemistry **46:**14928-36.

159. **Xu, K., and M. A. Strauch.** 1996. In vitro selection of optimal AbrB-binding sites: comparison to known in vivo sites indicates flexibility in AbrB binding and recognition of three-dimensional DNA structures. Mol Microbiol **19:**145-58.

160. **Zaman, M. S., A. Goyal, G. P. Dubey, P. K. Gupta, H. Chandra, T. K. Das, M. Ganguli, and Y. Singh.** 2005. Imaging and analysis of Bacillus anthracis spore germination. Microsc Res Tech **66:**307-11.

Vita

Kathryn J. Pflughoeft was born in Winona, Minnesota August 30, 1977. After graduating from Niwot High School in Niwot, CO in 1996 she began her college career at the University of Colorado in Boulder. She later transferred to the University of North Carolina in Greensboro where she earned a Bachelors of Arts degree with a concentration in Anthropology in 2000. She then moved to Boston, MA where she worked as a research assistant in the laboratory of Dr. Paula I. Watnick (New England Medical Center), studying osmoadaptation in *Vibrio cholerae*. Kathryn continued her career in research in the laboratory of Dr. D. Scott Samuels (University of Montana in Missoula), studying carbohydrate utilization and stress response in *Borrelia bourgdorferi*. After moving to Houston, TX in 2004 she entered the Ph.D. program at the University of Texas, Health Science Center, Houston.